THE UNIVERSITY OF CHICAGO

A NOVEL B-1B PRECURSOR STAGE IN THE PERITONEAL CAVITY

A DISSERTATION SUBMITTED TO

THE FACULTY OF THE DIVISION OF THE BIOLOGICAL SCIENCES

AND THE PRITZKER SCHOOL OF MEDICINE

IN CANDIDACY FOR THE DEGREE OF

DOCTOR OF PHILOSOPHY

COMMITTEE ON IMMUNOLOGY

BY

STEVEN ANDREW ERICKSON

CHICAGO, ILLINOIS

AUGUST 2020

TABLE OF CONTENTS

LIST OF FIGURES

LIST OF TABLES

ACKNOWLEDGEMENTS

The successful completion of graduate training oftentimes requires a village of supporters. In my case, the requirement was more on the scale of a mid-sized county or municipality. I have many people to extend thanks toward as I reflect on all that has occurred over the last six years.

To my parents Kathy and Mike, thank you for shaping who I have become today. To my brothers Peter and Kevin, both much better engineers in their fields than I will ever become in mine, thank you for leading the way. To my partner Hailey, who might be atop the podium for most difficult graduate tenures if I cannot claim it for myself, thank you for your endless support and love.

To my thesis committee of Patrick Wilson, Erin Adams and Alexander Chervonsky, thank you for doing the right thing. To my colleagues in lab, especially Shan Kasal and Christoph Drees, it has been a pleasure working with you. To my fellow graduate students, in particular the matriculants of 2014, thank you for the camaraderie and support. To Tatyana Golovkina, you are a friend and a mentor. I will not forget your kindness. To Linda Degenstein, none of this work was possible without your expertise. Thank you.

My graduate training was one marked by peaks and valleys more reminiscent of my Pacific Northwest roots than of the Midwest. It is easy to get lost in the darkness. A guiding principle for me, expressed perhaps most poignantly by a fairly well-known philosopher of years past, is as follows: Man can do what he wills, but he cannot will what he wills.

ABSTRACT

B cells participate in constitutive immunological processes to maintain host health and homeostasis. B cells in the mucosa produce a homeostatic barrier of local antibodies, while others take on innate-like phenotypes and patrol bodily cavities, producing homeostatic IgM. There are several unknown aspects of homeostatic B cell function and ontogeny. I primarily employed genetic approaches to address questions about the function of mucosal antibody and of the cellular origins of mucosal antibodies. I developed robust Cas9-based gene editing methods for the targeted introduction of rearranged immunoglobuins to their corresponding loci and to disrupt the immunoglobulin A locus. My system, called "Speed-Ig," is a rapid Cas9-based method for generating Ig knock-in mouse lines with high on-target integration rates at both heavy and light chain alleles. With standardized target sites and promoter regions, Speed-Ig mice can be used for comparative studies of B cell biology and vaccine optimization in vivo. I used Speed-Ig to create panels of mice with Ig pairs derived from IgA^+ plasma cells, control follicular B-2 cells, or from the innate-like cell lineages B-1a and B-1b to understand the cellular ontogeny of mucosal antibody producing cells and innate-like subsets. IgA^+ plasma cells appeared to derive from normal follicular B-2 precursors. Surprisingly, B-1b and B-2 Ig pairs drove both B-1b and B-2 phenotypes, suggesting a previously unknown lineage relationship between these subsets. I then confirmed the B-1b/B-2 relationship with transcription factor reporter lines and through adoptive cell transfer experiments.

1. INTRODUCTION

1.1 B cells and the humoral immune system

The mammalian immune system is a complex defense network of specialized components evolved to maintain organismal health. The humoral immune component represents a soluble defense mechanism against noxious stimuli, including pathogenic and toxic entities. Humoral immunity may be divided into innate and adaptive arms. The innate arm, comprised of germline encoded soluble factors such as complement proteins, collectins, ficolins, and pentraxins, provide non-specific defense against disseminated or blood-borne pathogens.[1–3] Conservation of some innate humoral effector molecules extends across the animal kingdom, suggesting important functions of soluble immunity.[2] In parallel with innate factors, mammalian humoral immune responses also include a layer of adaptive, antigen-specific antibodies. Antibodies are soluble, secreted splice variants of the B cell receptor (BCR), the antigen receptor of B lymphocytes. Each BCR and antibody is a dimer of dimers: covalently linked heavy and light immunoglobulin pairs dimerize to produce a bivalent complex.

During lymphopoiesis, B cells somatically rearrange immunoglobulin (Ig) gene segments, producing clonally unique BCRs.[4,5] Although the number of gene segments varies across species, the combinatorial diversity of these rearrangements alone can give rise to millions of unique combinations in mice. On top of this, junctional diversity, including the trimming or addition of nucleotides to each junction between rearranged gene segments, pushes the theoretical diversity of Ig pairs to into the billions. The resulting breadth of antigen recognition contained in the total B cell population is staggering. Upon pathogen encounter, B cells with specificity to pathogen-associated antigens activate, and in processes described below, export vast quantities of specific antibody. Adaptive humoral responses are indeed critical for host protection against many

pathogenic challenges, especially during subsequent encounters with the same pathogen. Although antibody-independent functions of B cells exist and will be elaborated on below, the major effector function is thought to be the adaptive production of antibodies in response to antigenic challenge.

The protective effect of an adaptive blood-borne protective agent has been known since the 1890s. By transferring blood from animals immunized with a pathogen-associated antigen, von Behring and Kitasato could protect a recipient animal from morbidity following antigen exposure.[6] Thereafter it was found that the proteinaceous, cell-free extract of immunized blood held the protective factor, specifically in the gamma globulin fraction following electrophoresis.[7–9] It was not until 1947 that gamma globulins, or antibodies, were found to emanate from plasma cells (PCs), a cell type which had been discovered before the turn of the 19th century. Over the ensuing decades, many important features of antibody responses have been elucidated. It is of particular importance to highlight here the pathway a B cell takes in order to become an antibody-secreting cell.

1.2 B cell activation and differentiation into antibody-secreting cells

The standard model for B cell activation and differentiation into an antibody-secreting PC involves several steps. Since B cells can recognize antigens in native states, it is thought a B cell localized within secondary lymphoid tissue encounters a cognate antigen present in the extracellular milieu or bound to the surface of a neighboring cell. The B cell, once stimulated through the BCR, initiates a signaling cascade that forces a binary fate choice. Two initial possibilities exist for the activated clone—participation in humoral immunity or clonal death—dictated by the presence or absence of non-BCR signaling cascades. Growth factors such as APRIL, BAFF, and various cytokines might be present in the microenvironment surrounding the

activated cell, facilitating progression to an antibody-secreting fate.[10] If the activated B cell does not receive any of these signals, the cell will not upregulate key metabolic pathways necessary to sustain proliferation, and some cells will eventually undergo apoptosis[11–13]. This is the phenomenon of anergy, and is thought to contribute to peripheral tolerance of B cells.[14] If instead the activated cell receives growth and/or differentiative signaling, the cells will survive and polarize to one of several cell fates. Some cells immediately produce antibody, which is thought to provide the earliest adaptive response possible, although it is likely of low affinity and therefore not as efficient as fully matured humoral immunity. Other cells will enter into the germinal center (GC) to undergo affinity maturation to generate a stronger, more specific humoral response. The GC is a temporary aggregation of follicular dendritic cells, specialized follicular helper T cells (T_{FH}), and B cells.[15] Here, GC B cells will oscillate between two identified stages, named after their relative locations within the GC. In the light zone (LZ), GC B cells present BCR-captured antigens to T_{FH}. In conditions of limited antigen availability, the amount of antigen presented by the B cell depends on BCR affinity. If the T_{FH} recognizes cognate peptide-MHCII complexes on the B cell, the T_{FH} provides CD40L signaling, instructing the B cell to traffic back to the dark zone (DZ).[16,17] In the DZ, GC B cells successively divide and somatically mutate BCR genes; the iterative presentation and division/mutation cycles of GC B cells allows for selective improvements of the BCR/antibody toward a target antigen.

Naïve B cells express both IgM and IgD, isotypes that are tuned for cell activation but have limited effector functions as secreted antibodies. Under the right conditions, activated B cells are induced to switch isotypes in a process termed class-switch recombination (CSR).[18] By exchanging the default IgM/IgD isotype for IgG, IgE, or IgA, CSR allows antibodies to take on different effector functions specialized to different immune challenges.[19] Although somatic

mutation and CSR both require the same enzyme, Activation-induced cytidine deaminase (AID, encoded by *Aidc* in mice), CSR is likely instructed prior to B cell GC entrance.[20] Isotype choice is taken from the local environment via cytokine signals received by the activated B cell.[18]. Upon departure from the GC, emigrating B cells will take on a PC phenotype, distribute systemically, and secrete large quantities of antibody. IgG^+ PCs, arising after classical antigen challenge, home primarily to the bone marrow. IgA^+ PCs, on the other hand, possess chemokine receptors and integrins that facilitate biased trafficking to mucosal tissue, including the intestinal lamina propria.[21] The instructions for IgA CSR and gut homing both come from the local tissue environment of mesenteric lymph nodes (mLNs) and Peyer's Patches (PPs), where IgA^+ PC precursors are thought to be first induced.[22] The large numbers of mucosal-resident IgA^+ PCs, and the vast quantity of IgA produced at mucosal sites, both suggest an important biological function for IgA (Fig.1).

1.3 Mucosal antibodies

Although most early antibody studies were serological, it became appreciated in the 1960s that mucosal surfaces and nonvascular secretions contained special antibodies.[23,24] In mammals and avians, the primary mucosal antibody isotype is IgA. Similarly specialized mucosal antibody isotypes have also been described in amphibians and teleosts.[25,26] The antibodies found in mucosal secretions were structurally distinct from serum antibodies, and were posited to have functions adapted to the harsh extraorganismal environment.[23]

IgA is typically secreted as a dimer with both Fc regions covalently linked to a Joining chain (J chain), a small polypeptide.[27,28] The J chain is recognized by the polymeric Ig receptor (pIgR) on the basolateral side of intestinal epithelial cells.[29] The occupation of pIgR by IgA triggers transcytosis and deposition of IgA into the intestinal lumen[30]. As the molecule is secreted, part of

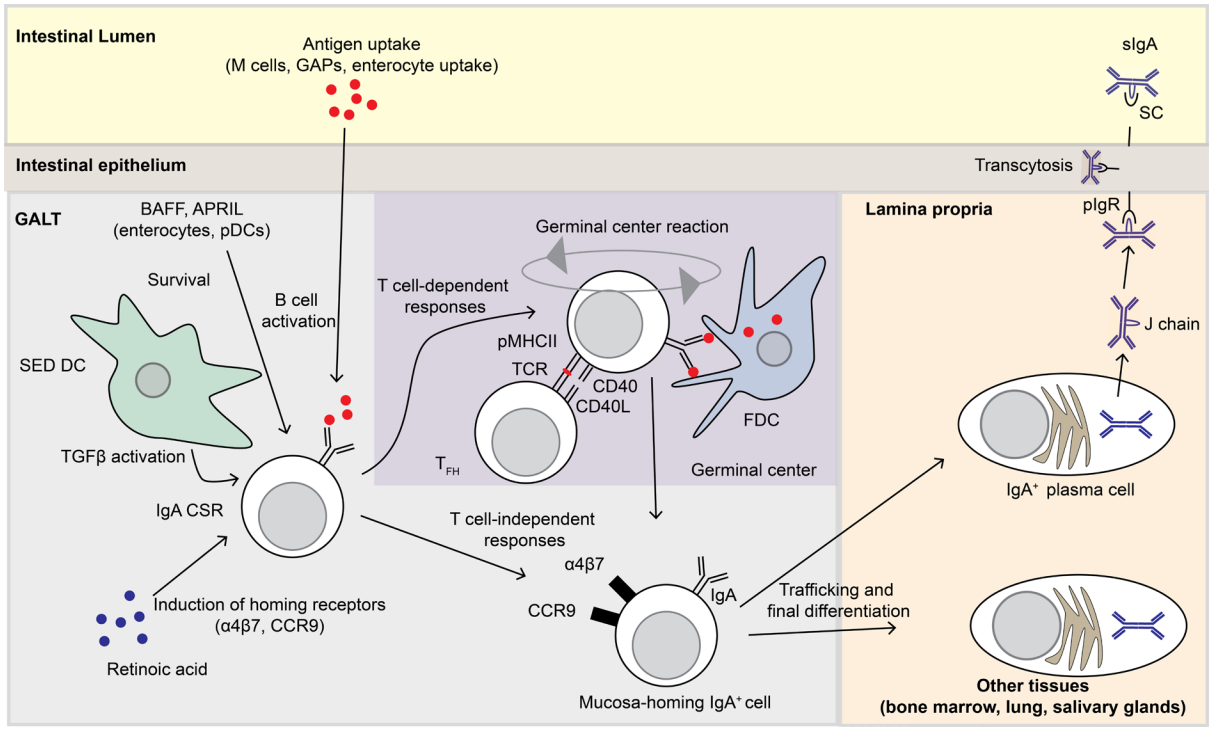

Figure 1. Classical IgA$^+$ plasma cell differentiation. Naïve B cells enter gut-associated lymphoid tissue and activate upon encounter with cognate antigen (red). Activated B cells receive local signals, such as retinoic acid, which induces expression of gut-homing receptors. Activation of latent TGFβ by subepithelial dome dendritic cells or other stromal cells, in combination with retinoic acid and interleukin signaling, initiates IgA class-switch recombination in activated B cells. Additional survival signals such as BAFF and APRIL, provided by stromal and immune cells are present. The activated B cell is induced to become an IgA$^+$ plasma cell, and either proceeds directly to the plasma cell fate or first enters a nearby germinal center to affinity mature and clonally expand. The outcome ends similarly: IgA$^+$ B cells recirculate and enter mucosal tissues, undergo final differentiation, and secrete IgA. Secreted IgA dimers bound together by the J chain are uptaken by pIgR expressed on the basolateral side of epithelial cells. IgA is transcytosed and released on the apical side of the epithelium, during which a fragment of pIgR, the secretory component, is also released and remains bound to IgA. In the lumen, the final secretory IgA complex consists of IgA dimer, J chain, and secretory component. GALT, gut-associated lymphoid tissue. GAPs, goblet cell-associated passages. SED DC, subepithelial dome dendritic cell. CSR, class-switch recombination. FDC, follicular dendritic cell. T_{FH}, follicular helper T cell. SC, secretory component.

the pIgR is cleaved off (termed secretory component (SC)) and remains bound to the J chain, possibly preventing IgA degradation in the lumen.[31] The resulting complex of dimeric IgA molecules with J chain and SC is the full secretory IgA (sIgA). Once in the lumen, at least some of the sIgA decorates the mucus.[32–34] An early connection between IgA and commensal microbiota was made when it was observed that germ-free mice have significantly reduced IgA^+ PCs and secreted IgA.[35,36] IgA has now been shown to directly bind to intestinal microbiota.[37–39] All antigens in the lumen are potential targets for IgA responses, including those of dietary origin.[40] IgA binding to microbiota was a strong indication of the broader immunologic function of mucosal antibodies. By binding bacteria, IgA has been suggested to prevent bacterial infiltration of host tissue, although contradictory results have been published.[41,42] One possible mechanism is through "enchainment" of bacterial aggregates through IgA, which ultimately are excreted from the intestine.[43] Additionally, IgA has been shown to affect the composition of the microbiota, and in some cases to facilitate enhanced colonization by certain taxa.[44,45] Further, it has been suggested that inflammatory enteric bacteria are likely to have IgA coating, perhaps limiting pathogen fitness.[37]

A more thorough understanding of the homeostatic IgA function(s) has been difficult to obtain, partly due to the vast and polyclonal nature of IgA. Genetic approaches for the removal of mucosal antibody are complicated and are prone to unintended artifacts. The least specific approach is to genetically ablate B cells either through deletion of *Ighm* or *Rag1/Rag2*, followed by B cell adoptive transfer. However, it was noted in B cell-deficient mice that Peyer's patches do not arise, meaning that any adoptively transferred cells might not follow a standard route of IgA^+ PC differentiation.[46] Due to this and other systemic defects of *Ighm*/*Rag*-deficiency, ascribing function to IgA in such models was unfeasible. A more precise attempt was made by

deleting the IgA constant region.[47] However, in this approach the researchers also deleted the switch region upstream of IgA. By doing so, B cells that would otherwise class switch to IgA after instruction by the aforementioned cytokine and growth signals, had no class to switch to, and remained as IgM-expressing cells. This is a problem on two fronts. The first is that B cells that would be secreting IgA are stuck on IgM isotype, which can also cross the mucosal epithelium through pIgR:J chain interactions as a compensatory pathway.[48] Secondly, that the specificities activated in mucosal sites remain unchanged, such that the secreted IgM still binds to the same antigenic targets that IgA would. Therefore, this is less a model of mucosal antibody deficiency and more about how IgA differs functionally from IgM in mucosal function. Some insights were made, but the results were subtle and perhaps minimized the perceived role of IgA through unnatural compensation. Another approach was made that placed a larger role on IgA but perhaps artificially so. Deletion of the *Aicda* gene, encoding AID which is expressed in pre-GC B and GC B cells, thereby preventing class switch recombination and affinity maturation, was employed to study IgA[49]. AID-deficient mice were shown to have inflammation in the gut and dysbiosis.[49] However, by removing AID, not only was class switch recombination blocked, but so was somatic hypermutation. Therefore, although IgM was secreted much like in the classic IgA knockout model, the secreted antibody was not of high affinity for antigenic targets and perhaps could not perform as it should. Compared to IgA knockout model above, these results might indicate that affinity maturation is an important part of IgA biology. However, systemic defects (no mutation for any antibody, no IgG, etc.) confound the results. A more sophisticated AID mutant line was generated, in which class-switch recombination was intact but affinity maturation ablated, and had the same result as global AID knockouts.[50] Therefore it was concluded that in order for mucosal antibodies to remain effective, somatic mutation is required.

This would point to a T-dependent, classic humoral immune response for IgA much like antibody responses of other isotypes. This may overlap with, or layer onto, the class of IgA still detectable in T cell-deficient animals.[38]

Rather than targeting B cells or IgA directly, other groups have tried to remove components of the secretory machinery to achieve functional mucosal antibody deficiencies. Even if IgA and IgM can still be produced, removal of the pIgR or J chain in theory would block epithelial transcytosis of polymeric Ig or by preventing the formation of polymeric Ig itself. In pIgR knockout mice, through unclear mechanisms, mucosal antibody is still present in the lumen of the intestine albeit at reduced levels.[51] Therefore, this model would reduce the sensitivity of subsequent assays, potentially obscuring any true functions of IgA. The J chain knockout model was flawed for other reasons. J chain is mysteriously expressed by DCs and T cells, potentially altering the cellular biology in many cell types other than mucosal plasma cells.[52] J chain knockout mice had a severe reduction in mucosal Ig, but the results, like other models, were hard to pin down to IgA function.[53] Therefore, the field of IgA research would benefit from improved models of mucosal antibody deficiency. Studying IgA function is not limited to genetic ablation; in order to properly understand IgA function, it became important to understand the antigenic targets of IgA, which would shed additional light on mucosal antibody function(s).

1.4 IgA$^+$ plasma cell ontogeny

At steady-state, a large population of IgA$^+$ PCs exists in mice, primarily in the small intestine but is also distributed across the colon, lungs, bone marrow, liver, and salivary glands. Although IgA$^+$ PCs are short lived, continual GC activity is visible in Peyer's patches, mLNs, and isolated lymphoid follicles (ILFs) which provides a source of replacement cells.[54] IgA$^+$ PCs might also arise from long-lived memory cells, maintaining a lifelong clonal presence.[55,56] The constant

induction and turnover of IgA^+ PCs suggests that specific antigens present in the mucosa might activate B cells with cognate BCRs.

While studies of polyclonal IgA indicated broad binding of intestinal bacteria, the specificities of individual IgA^+ PCs were only recently described. Employing a monoclonal antibody (mAb) generation pipeline, the Bendelac lab showed that mAbs derived from IgA^+ PCs are enriched for binding to bacteria as assessed by bacterial flow cytometry.[57] These results were confirmatory for many past studies of endogenous or polyclonal IgA binding. Yet, the broad reactivity of some monoclonal antibodies, coating upwards of 20% of the small intestinal microbiota, suggested an unusual target antigen or antibody.[57] Importantly, the enrichment of bacteria-reactive specificities among IgA^+ PCs compared with conventional B cells indicated that BCR-mediated selection into the IgA^+ PC fate might be occurring. Granted that conventional/follicular B-2 cells are the presumed precursor to IgA^+ PCs, those naïve B cells with bacteria-reactive BCRs would be selected at sites of antigen encounter and follow a standard differentiation process first through the germinal center then into the IgA^+ PC compartment. The interpretation became less clear when IgA^+ PCs from mice of different genetic backgrounds or treated under special husbandry conditions were assayed in the same way. IgA^+ PCs from T cell deficient animals had the same biased repertoire toward bacteria, suggesting that B cell selection does not require follicular T cell help.[57] The more surprising findings came from mAbs derived from IgA^+ PCs found in mouse lines kept in limited antigen environments. Mice existing in two levels of antigen limitation were tested. In the first, animals kept in germ-free isolators and fed a standard chow diet were analyzed for the presence of IgA^+ PCs. Though reduced in number, IgA^+ PCs still exist in the absence of microbiota. Moreover, when mAbs derived from germ-free IgA^+ PCs were tested for bacterial reactivity, the enrichment over B-2 cells was maintained.[57] This would

suggest that despite the absence of bacterial antigens, germ-free cells were somehow "naturally" enriched to react with foreign antigens. It was formally possible that dietary antigens, or unknown contamination of the food source with bacterial products such as LPS, were sufficient to maintain the ~10-fold-reduced IgA^+ PC population, and that this population was still being selected on the reduced foreign antigen. To address this concern, germ-free mice were weaned onto an "antigen-free" (AF) diet. The AF diet consisted of the most elementary macromolecules possible, including single amino acids, minimal saccharide moieties, and simple lipids along with essential vitamins and minerals. It was noted that AF mice still possessed IgA^+ PCs, although IgA was undetectable in a separate, recent study.[57,58] When tested, AF IgA^+ PCs also maintained an enriched repertoire for bacterial reactivity. Though the components of the AF diet were not individually tested for bacterial antigen contamination, a reasonable conclusion could be drawn that foreign antigens are not absolutely required for IgA^+ PC differentiation. Furthermore, IgA^+ PCs are being selected by specificity in the absence of all foreign antigens. These results suggested that IgA^+ PCs differentiate on self antigens. This conclusion was further supported when GF and AF IgA^+ PC mAbs were screened for polyreactivity.

Polyreactivity is an enigmatic, controversial characteristic of some mAbs. At its most base definition, polyreactivity is defined as the ability of a mAb to bind one or more model antigens in vitro. Binding is detected by enzyme-linked immunosorbent assay (ELISA) reactivity in conditions permissive to weak binding. These conditions include the use of purified water as washing buffer and protein-free blocking buffer. Additionally, the final detection step usually takes substantially more time than a typical ELISA. While no standardized practice has been reached for the *in vitro* polyreactivity assay, most research groups probe 3-7 model antigens of varied macromolecular class. Some antigens, including Keyhold Limpet Hemacyanin (KLH) are

completely novel to the animal, so resultant reactivity would indicate polyreactivity. Other antigens, such as DNA or LPS, are multivalent and are especially good at capturing low affinity antibodies. The decision to call a given antibody polyreactive has been set at reactivity to one or several antigens, depending on the total number of antigens being tested. Early hypotheses included that polyreactivity might help antibodies bind multivalent substrates, a mechanism termed "heteroligation".[59] Another is that polyreactivity might increase the innate immunity offered by serum antibodies.[60–62] The innate-like polyreactivity of "natural" IgM, for instance, was given as evidence that B-1 cells, the major provider of natural IgM, are enriched for polyreactive specificities.[63,64] The disentanglement of polyreactivity and specific reactivity to a highly conserved antigen, for example phosphatidylserine moieties, created some confusion in the field. Before the polyreactivity data of IgA^+ PCs were known, bacterial reactivity of GF and AF IgA could have been explained as cross reactivity to an ancient and conserved epitope. However, a more likely mechanism is broad, low-affinity, degenerate binding of IgA to diverse bacterial surfaces. However, polyreactivity is not necessarily a harmless property for B cells to possess. Studies in human B cells transiting through development offered some insight into the functional consequences of polyreactivity. Wardemann et al. cloned mAbs from B cells at various stages of late B cell development, including the pre-B and immature B cells stages.[65] The authors noted that as B cells proceed through development, the frequency of polyreactive was sequentially reduced.[65] A conservative conclusion from this work is that the feature of polyreactivity is associated with a BCR signaling feature, potentially polyreactivity itself, that leads to clonal deletion or altered development of the B cell possessing a polyreactive BCR (Fig.2). If indeed polyreactivity is directly responsible for clonal deletion, then it would be fair to state that

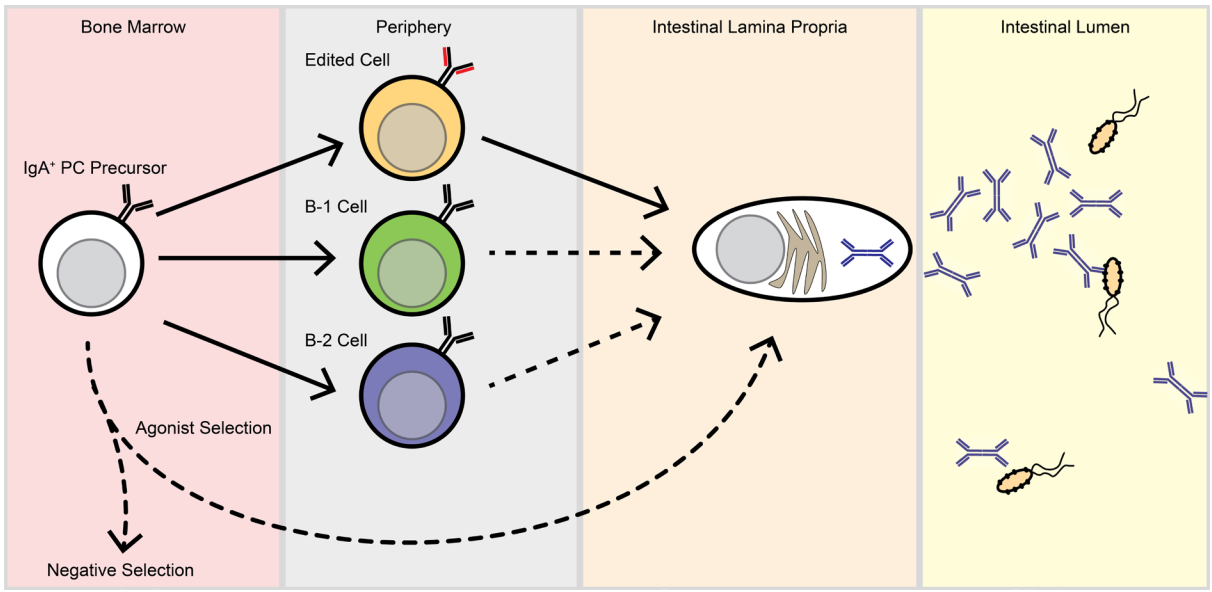

Figure 2. IgA$^+$ plasma cell ontogeny and IgA function. Recent evidence suggests that IgA$^+$ PCs potentially have unusual development and/or differentiation. A presumed IgA$^+$ PC precursor first rearranges a polyreactive, microbiota-reactive Ig pair in the bone marrow. Due to selective pressure against polyreactivity, IgA$^+$ PC precursors may exhibit clonal deletion or receptor editing. Alternatively, IgA$^+$ PC precursors might develop normally and take on a specific phenotypic fate in the periphery, such as B-1 or B-2 cells. Once differentiated, IgA$^+$ PCs secrete large amounts of IgA into the intestinal lumen, where the antibodies interact with microbial and other antigens. The function of IgA recognition of antigen in the lumen is poorly understood at present.

polyreactivity is a driving force in central tolerance, although the data are only correlative as of this writing.

Numerous reports have suggested that the IgA repertoire is polyreactive.[66–69] Most studies were limited to pooled Abs or very limited numbers of mAbs. The work done in Bunker et al. greatly increased the quality of data in the field, and largely confirmed previous findings that intestinal IgA was enriched for polyreactivity at the repertoire level.[57] Bunker et al employed a polyreactivity test against seven model antigens. They were: cardiolipin, DNA, insulin peptide, flagellin, human serum albumin, KLH, and LPS. Of these, flagellin and LPS would be present in significant quantities in the intestinal lumen. Other antigens were completely novel to the mice, or were so ubiquitous (DNA, insulin) that the antigen panel represented several self-/non-self classes in addition to structural differences. Calling polyreactivity at binding to two or more model antigens, polyreactivity was highly enriched in the intestinal IgA^+ PCs.[57] Much like the bacterial reactivity data, both GF and AF IgA^+ PCs appeared to maintain an enrichment for polyreactivity, even though these two characteristics are largely independent from each other.[57] Both lines of evidence, bacterial reactivity and polyreactivity, point toward a selection mechanism for IgA^+ PCs that is independent of foreign antigens and dependent on BCR signaling. Thus, a paradox is formed in the ontogeny of IgA^+ PCs. The feature of polyreactivity (and by extension, self-reactivity) being positively selected in IgA^+ PC differentiation, yet negatively selected during B cell lymphopoiesis, leads to the statement that cells especially likely to become IgA^+ PCs seem especially likely to be centrally tolerized. This interpretation was the driving force behind my subsequent studies on IgA^+ PC ontogeny. My work was wholly reliant on the creation of Ig knock-in lines to test monoclonal development and differentiation of IgA^+

PC-derived BCRs. In preparation for this, I also considered studying the development of B-1 lymphocytes, which have been put forward as another cellular origin of IgA^+ PCs.[70,71,71,72]

1.5 Innate-like B cell ontogeny

Several pre-immune or homeostatic subsets of B cells exist in mammals, identifiable by distinct surface marker profiles. In murine models, B cells take on at least three pre-immune phenotypes. Follicular (FO) B cells, also known as conventional B or B-2 cells (which technically includes MZ B cells but has come to refer to FO B alone), comprise the largest subset and reside primarily in secondary lymphoid tissues such as the spleen and peripheral lymph nodes. FO B cells are continuously generated throughout life and circulate the body in search of cognate antigen, carrying out classic humoral immune responses.

The remaining two subsets of B cells, classified as "innate-like" B cells, are B-1 cells and marginal zone B cells (MZ B). MZ B cells exist almost exclusively in the spleen and have primary functions other than secretion of antibody. For instance, MZ B cells have been shown to traffic antigen across splenic compartments to allow more efficient FO B cell antigen recognition and the induction of humoral immune responses.[73] In addition, MZ B cells can provide a rapidly activated pool of cells producing low-affinity antibodies.[74] The development of MZ B cells is incompletely understood, but is thought to involve signaling steps during the transitional stages of B cell development in the spleen.[75] An appreciable population of MZ B cells is not present until the organism reaches states of maturity around six weeks of age. The MZ B population is not currently thought to contribute significantly toward mucosal immune responses.

B-1 cells were first reported in 1982 as a peculiar subset of B cells predominant in the peritoneal and pleural cavities, and which express the surface antigen Ly-1 (CD5), previously thought to be

restricted to T cells.[76]. It was appreciated at the time that alongside $CD5^+$ B cells, a "sister" population of very similar B cells existed that bore resemblance to $CD5^+$ B cells but did not express CD5.[77,78] A variety of transcriptional and morphological divergences from conventional B cells has cemented the $CD5^+$ B cell lineage (and to a lesser degree, the $CD5^-$ sister population) as unique B cell subsets. These cells have come to be known as $CD5^+$ B-1a and $CD5^-$ B-1b subsets. The later designation of B-1 (and FO B/MZ B as B-2) comes from ontogenetic analysis. It was found that neonatal B cell precursors were biased toward producing B-1 cells over B-2.[79,80] The temporal dynamics of B-1a ontogeny evoked two competing but not necessarily exclusive models of B-1 cell differentiation. Succinctly, the "lineage" hypothesis predicts independent precursors for B-1 and B-2 cells, while the "induced differentiation" hypothesis predicts Ig-dependent cell fating from otherwise dually potent precursors.[81] Both hypotheses focus on the ontogeny of $CD5^+$ B-1a cells, and some evidence exists to support each individual hypothesis. In the lineage hypothesis, a temporally restricted transcriptional profile present in hematopoietic cells allows for the induction of the B-1 fate (Fig.3A). For instance, expression of the gene Lin28b has been shown to revert adult HSCs to a neonatal-like transcriptional program.[79,82] Lin28b-expressing HSCs are biased to give rise to B-1 cells.[83] Additionally, the specialized microenvironment of the neonatal hematopoietic tissue present in liver, bone marrow, or para-aortic splanchopleura might instill a B-1 fate on the earliest developing cells. At the same time, the BCR rearrangements undertaken by neonatal B cell precursors are not equivalent to those of mature B cell precursors.[84]

The induced-differentiation hypothesis puts forth that BCR signaling is the primary driver of B-1a differentiation (Fig.3A). Conclusive evidence for induced differentiation came from Ig transgenic and knock-in lines, in which quasi-monoclonal populations of B cells expressing a

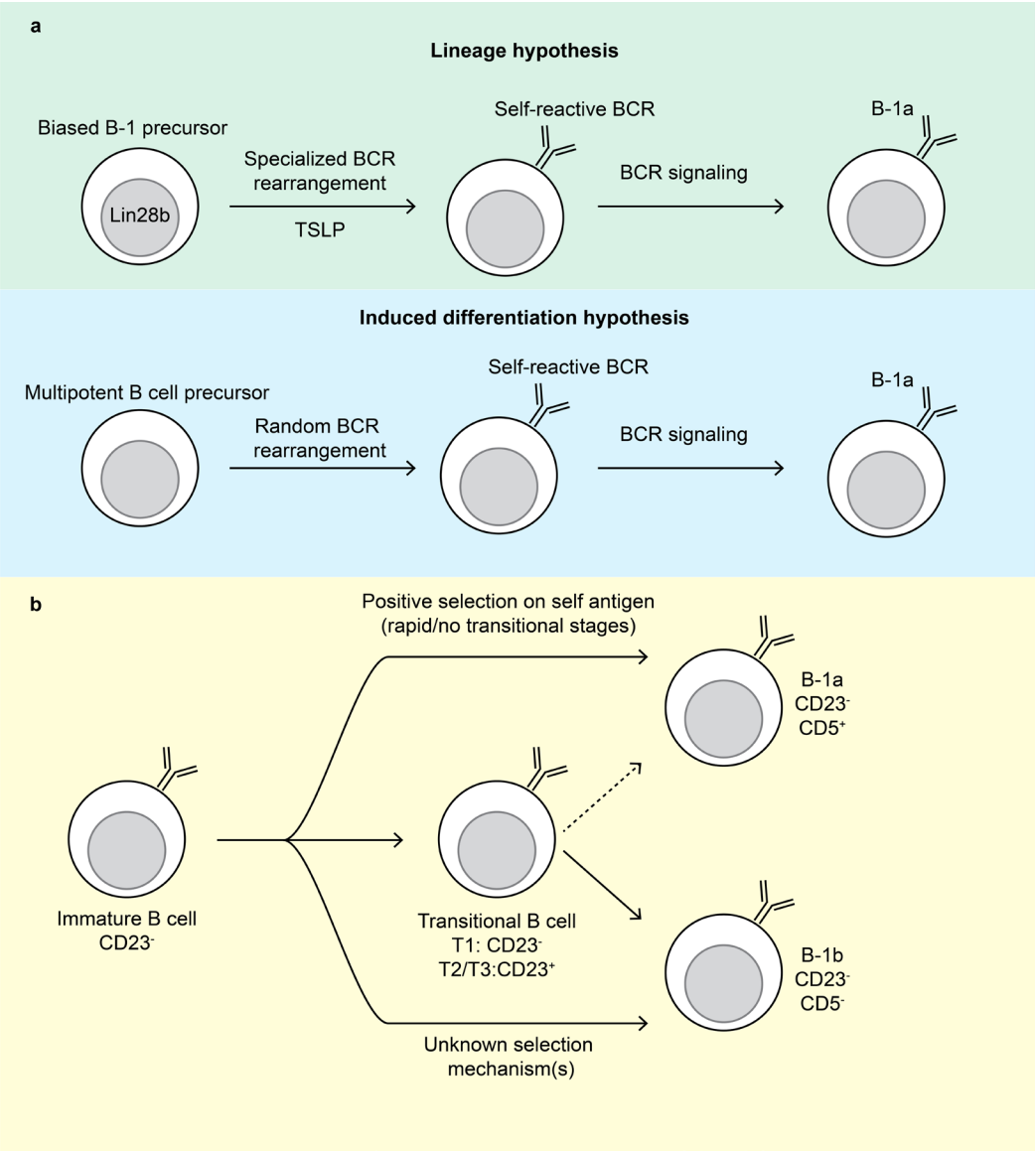

Figure 3. Known B-1 ontogeny. **A)** Models of B-1a ontogeny. The lineage hypothesis states that biased B-1 precursors, present in fetal and neonatal mice, have a specialized transcriptional profile (including the expression of Lin28b) and develop in a specialized hematopoietic niche. These factors drive the B-1a phenotype as well as non-random BCR rearrangements. The induced differentiation hypothesis holds that a single B cell precursor can give rise to B-1 and B-2 cells, with fate choice dependent on BCR signaling. Evidence for each model exists, and these hypotheses are not mutually exclusive. **B)** While fetal and neonatal lymphopoiesis are biased to produce B-1 cells, the downstream mechanisms of B-1 differentiation between early-life and adult B-1 precursors appear similar. B-1a cells are known to be positively selected on self antigens, with little evidence suggesting that any precursor stage expresses CD23. The mechanism of B-1b selection is completely unknown, but there is some evidence that a fraction of transitional B cells may give rise to B-1b cells.

canonical B-1a Ig pair using either V_H11 or V_H12 were strongly biased to the B-1a fate.[85–87] In B cells expressing B-1a BCRs diluted with B-2 BCRs, differentiation to B-1a was blocked, suggesting that some critical BCR signaling threshold must be reached to instill an innate-like phenotype in cells.[88] In a more reduced system of cells expressing BCR-signaling mimetic LMP2A, strong BCR-like signaling was sufficient to induce a B-1a fate.[89] B-1 differentiation is now known to be inducible even in mature FO B cells. Graf et al. used a genetic system in which activation of Cre recombinase swapped out an expressed B-2 BCR for a canonical B-1 BCR.[90] Mature FO B cells, now expressing a B-1a specificity, quickly differentiated to B-1a, expressing hallmark transcription factors and surface markers.[90] While BCR switching does not occur in wild type animals, this study opened the possibility that some B-1 cells might exist as FO B prior to receiving BCR signals in the periphery. A synthesis of the lineage and induced-differentiation hypotheses would best explain the ontogenetic data for B-1a cells (Fig.3B). Biased BCR rearrangements in neonatal lymphocytes give rise to high-signaling B cells, which in turn are fated to the B-1a compartment. Importantly, these models and nearly all data are confined to B-1a ontogeny, more specifically to the B-1a cells expressing canonical BCRs, such as those using V_H11 and V_H12 heavy chain variable regions. Cell-fating by non-canonical B-1a, B-1b or B-2 Ig pairs remains an understudied area of B cell biology (Fig.4)

The B-1a BCR repertoire in wild type mice does have expanded clones and biased chain usage, but it is hardly oligoclonal.[91] Many B-1a cells are rare or unique clones within the compartment, and the mechanism of differentiation for non-canonical B-1a cells may not mirror canonical pathways. Furthermore, the sizeable B-1b population has no repertoire bias.[38] By frequency, non-canonical B-1a and B-1b together may represent 50-75% of B-1 cells present in adult mice. B-1b cells are in part seeded by adult HSCs, pointing toward a different or only partially overlapping

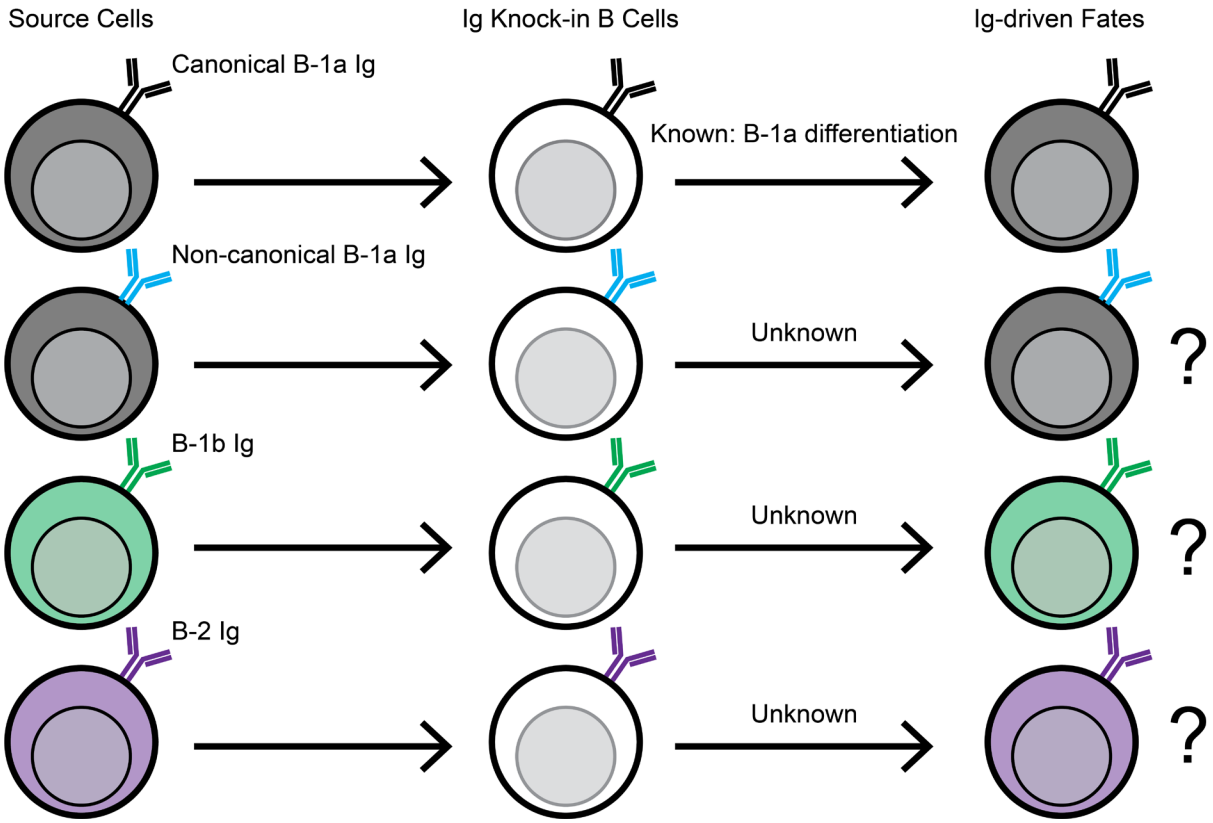

Figure 4. Ig-driven B cell ontogenies. Canonical B-1a Ig pairs including V_H11 and V_H12-using Ig drive a biased B-1a fate in expressing cells. It is unknown if Ig pairs from any other subset may drive a biased cell fate.

differentiation pathway.[92,93] Non-canonical B-1a and B-1b cell ontogeny has not been as thoroughly investigated as canonical B-1a, and for practical reasons. For instance, neither cell population has expanded clones; choosing particular Ig pairs from either group for transgenics might only reveal idiosyncratic ontogenies, not representative pathways for the greater populations. An accurate formulation of non-canonical B-1a and B-1b ontogeny may only be possible by analyzing multiple representatives from each subset (or secondary subset), so long as the representatives are phenotypically consistent. Detection of different ontogenies would call for additional representatives and would point toward additional subset heterogeneities. The sheer amount of work, and cost, of making large panels of Ig transgenic or knock-in lines has been prohibitive until now.

1.6 Approaches to study Ig-mediated B cell biology *in vivo*

The repertoire bias of B-1a cells heavily influenced the direction of B cell biological research in the 1980s and 1990s. A pressing question at the time was if B cells expressing a canonical B-1a Ig pair would be fated to the B-1 compartment. Several groups initiated genetic approaches to study monoclonal B cell behavior. By inserting a rearranged Ig pair into the genome, most B cells would express a single BCR specificity. Due to allelic exclusion and sequential Ig chain rearrangements, described above, only a relatively few endogenously rearranged BCRs progress through development. It became possible to study important questions in B cell biology, and for B-1 particularly the appropriateness of the two B-1 ontogeny models. Other applications of Ig transgenics and knock-ins have been studying B cell development, GC B dynamics, and vaccine optimization.[94–98] Ig transgenics and knock-ins represent a powerful tool in understand many aspects of B cell biology and humoral immunity.

While Ig transgenics, with randomly inserted Ig pairs, were the first to be developed and are the easiest to create, targeted integration of rearranged variable regions into the corresponding locus offered a more accurate way to study Ig-mediated B cell biology.[87,99] Ig knock-ins retain the capability to affinity mature and undergo class-switch recombination. Perhaps more importantly, knocked-in Ig genes have expression kinetics and dynamics closely approximating endogenous Ig, giving a better reflection of the developmental history and cell signaling events that the derived Ig pair might have originally undergone.[100] The only drawback of Ig knock-ins over random transgenesis is logistical. Targeted knock-in technology originated in the late 1980s.[101] Knock-in donor DNA constructs had large regions of sequence complementarity to the targeted locus flanking the cargo intended for insertion. Upon introduction to embryonic stem cells (ESCs), random DNA damage that happened in the target locus covered by construct homology arms would undergo homology-directed DNA repair. If the damaged locus used construct homology regions as a template, the cargo sequence would be added into the locus. The reliance on random double strand breaks in areas covered by homology arms necessitated large donor constructs, and even then, the chance of this event occurring in a single ESC was extremely rare. To overcome the minute frequency of the intended genetic manipulation, paired selection cassettes were often included in the knock-in cargo for positive screening of targeted hits and negative screening of cells with off-target integrations.[102] ESCs meeting these criteria were then injected into murine blastocysts. The resulting animals were therefore chimeric, with many tissues originating from blastocyst origin, and a fraction from the ESC progenitors. If the ESCs gave rise to reproductive tissues, the targeted integration may be passed on to progeny. While in theory ESC line choice is bespoke, in practice only a few lines of ESCs were used. Unless the ESC line was of the preferred background to conduct subsequent studies, most of the time ESC-

derived knock-in lines were heavily backcrossed (ten or more generations) prior to meaningful analysis. Chimerism and extensive backcrossing requirements makes traditional knock-ins time-consuming to make. Even with advances in selection, ESC lines, and donor construct designs, traditional knock-ins take the better part of a year at minimum.

Cas9-mediated gene editing using the guide RNA (gRNA) and Cas9 nuclease of the S. pyogenes CRISPR/Cas9 system) offers several advantages over traditional Ig knock-ins in theory.[103] If successful, Cas9-mediated Ig knock-ins are already on any background of choice, can be generated in around five weeks, and involve no ESC work. The primary challenge of Cas9-mediated gene editing is low efficiency of large insertions/replacements. Knocking out sections of the genome with Cas9 is trivial, with high efficiency with little dependence on distance between gRNA sites. Small edits, including point mutations, epitope tags, or loxP sites are also efficient, although at a reduced rate compared to knock outs. Once insertions/replacements begin to exceed a few hundred bp, the efficiency plummets. Because the mechanism of integration is unclear, it is currently unknown why this occurs, although I speculate on this in the discussion section given my attempts at large knock-in insertions. The first group to report larger gene edits in murine embryos with Cas9 used circular DNA donors with 2kb homology arms flanking the cargo; while reporting high efficiency, the results were hard to replicate.[103] There are valid reasons for the lack of progression regarding large knock-in insertion efficiency using Cas9.

There are no real guidelines for Cas9-mediated knock-ins to date. There is very little value in targeting the same locus with the same (or highly) similar cargo, as the resulting mouse lines would be redundant in most cases. Because of this, no group has systematically identified factors involved in integration efficiency. In fact, different targeting efficiency for similar cargo at two different loci was interpreted as a locus dependent effect.[103] While locus-dependent effects may

exist, there are likely to be several other and much more important factors. The most obvious is gRNA site selection. It is now well known that gRNA potency, as measured by the ability of the gRNA to direct Cas9 endonuclease activity, is nonuniform across sequence space.[104,105] In other words, the sequence composition of the protospacer directly affects the efficiency of Cas9 cutting, independent of the PAM. Algorithmic approaches generated from data of pooled gRNA sequences has some predictive ability in assessing gRNA on-target "quality".[106–109] The rules seem to apply to a population of gRNAs, but for any given protospacer, the actual quality may only be determined empirically.

A variety of approaches to large knock-in insertions have now been published.[106,110–112] Ig knock-ins using Cas9 have also been recently published.[113,114] Batista and colleagues used a donor DNA construct similar to those used for ESCs to install a rearranged H chain to the correct locus. However, the use of two gRNA sites led to significant rates of locus deletion, and no targeting construct for light chain insertions was published.[113] Victora and colleagues inserted both heavy and light chains into the heavy chain locus in such a way that CSR was preserved, but the expression levels and kinetics appear mismatched with endogenous B cell biology.[114] While these reports were published after I had developed a functional Ig knock-in system, I still preferred my knock-in system for reasons that will be explicated in later sections.

1.7 Summary

The function of mucosal antibodies, specifically IgA, remains poorly understood. Past genetic approaches for mucosal antibody deficiency have been imperfect. I hypothesized that if I could generate more precise genetic models, I would be able to uncover IgA functional phenotypes masked or confounded by previous approaches.

Published work, including from the Bendelac lab, suggests that IgA is enriched for polyreactive and microbiota-reactive antibodies. These traits are predicted to have direct implications for the function of IgA. However, polyreactive Ig pairs are selected against during development, creating a selection paradox. I hypothesized that if polyreactivity is instrumental in IgA^+ PC differentiation, then I would observe an associated developmental phenotype of IgA^+ PC precursors.

B-1 ontogeny has only been carefully examined for the canonical Ig pairs of the B-1a subset. No non-canonical B-1a Ig pairs, nor B-1b Ig pairs, have ever been used in the creation of an Ig knock-in line. It was therefore possible by doing so, I would uncover novel features of B-1 ontogeny. In order to address my hypotheses about B-1 cells, and about IgA^+ PC ontogeny, it was necessary to develop a highly efficient Ig knock-in system.

2. MATERIALS AND METHODS

2.1 Mice

C57BL/6J, *B6.SJL-PtprcaPepcb/BoyJ*, *CD23Cre* (B6.Cg-Tg(Fcer2a-cre)5Mbu/J)30, *hCk* (*B6;129-Igkctm1(IGKC)Mnz/J*)31, *IgHa* (*B6.Cg-Gpi1a Thy1a Igha/J*), *R26R-EYFP* (*B6.129X1-Gt(ROSA)26Sortm1(EYFP)Cos/J*)32 and *Rag1*$^{-/-}$ (*B6.129S7-Rag1tm1Mom/J*) mice were purchased from The Jackson Laboratory. *Rag2-EGFP* (*FVB-Tg(Rag2-EGFP)1Mnz/J*)33 were purchased from the Jackson Laboratory and backcrossed to C57BL/6J. Ig knock-ins, IgA^{BnS}, the *Zbtb32*^{EGFP} reporter, and the *Bhlhe41*^{Cre} lines were generated in-house. Mice deficient for the IgH J segment locus were generated in-house using Cas9 and the following protospacers: GCTACTGGTACTTCGATGTC and GCCATTCTTACCTGAGGAGA. Classic IgA^{KO} mice were generated with the following protospacers: AAGCGGCCACAACGTGGAGG and

TCAAGTGACCCAGTGATAAT. Coding sequence IgA^{KO} was generated with the following protospacers: CGGCACGATGAATGTGACCT and CCTTTAGGGGCTCAAACACT. Secretory IgA^{KO} was generated with the following protospacers: TGTCTGTGATCATGTCAGA and GGGGCCATCTCAAGAACTGC. For experiments, mice were analyzed at 3-8 weeks and compared to littermate controls. Mice were maintained in a specific pathogen-free environment at the University of Chicago. All experimental guidelines were approved by the Institutional Animal Care and Use Committee (IACUC).

2.2 Single-cell cloning of rearranged Ig genes

Single B cells were sorted as previously described[57,115,116] from the following populations using the indicated markers: IgA^+ PCs ($B220^-$ $dump^-$ (CD3e, CD4, CD8a, CD11b, CD11c, F4/80, TER119) IgA^+)Splenic B-2 ($B220^+$ $CD19^+$ $CD21^+$ $CD23^+$), peritoneal B-1a ($CD19^+$ $CD23^-$ $CD5^+$), and peritoneal B-1b ($CD19^+$ $CD23^-$ $CD5^-$). Briefly, single cells were sorted into 96-well plates (Biorad # HSP9601) containing 10µl of 1% v/v β-mercaptoethanol TCL buffer (Qiagen # 1031576) using a BD AriaII cell sorter. RNA was purified using RNAse-free SPRI beads[117,118] (GE Healthcare #65152105050250) and followed by cDNA synthesis using Superscript IV cDNA synthesis kit (Invitrogen #18091050) as described36. Rearranged Ig chains were amplified and sequenced using degenerate Ig primers.[115] In-frame variable regions were screened in IMGT39 then amplified with gene-specific overlap primers for subsequent Gibson assemblies.[119]

2.3 Guide site selection

Guide sites were identified using Integrated DNA Technologies' (IDT) selection tool (https://www.idtdna.com/site/order/designtool/index/CRISPR_CUSTOM) by inputting ~500bp

surrounding the region of interest. Individual guide sites were selected by a number of criteria, including on-target scores, off-target scores and proximity to the terminal stop codon (for non-Ig knock-ins). In general, on-target scores held primacy in selection, as off-target scores are skewed by non-PAM-led genomic hits and off-target integrations can be easily bred out unless falling near the intended target. Similar criteria were used when evaluating guide site options from CHOPCHOP (https://chopchop.cbu.uib.no/) and the Broad sgRNA designer (https://portals.broadinstitute.org/gpp/public/analysis-tools/sgrna-design).

2.4 Donor DNA construct generation

For Speed-Ig Donor DNA constructs, the pUC19 plasmid was digested with SacI and SbfI. Linearized plasmids were then assembled with overlapping homology arms encompassing both 5' and 3' arms to generate 'intermediate' targeting constructs. Promoter regions including split leader peptide sequences were amplified from genomic DNA, and full targeting constructs were obtained by assembling SalI-linearized intermediate constructs, promoter regions, and Ig variable regions. All assemblies were performed with NEB HiFi 2X Master Mix (NEB #E2621L). Assembled constructs were transformed into XL-10 Gold Ultracompetent E. coli (Agilent #200314). Colonies were miniprepped and Sanger sequenced using a set of primers to ensure proper assembly and in-frame V regions. Glycerol stocks of desired clones were midiprepped using anion-exchange columns (Invitrogen #K210015) following growth in 50ml LB + carbenicillin medium for 10-12 hours. Midiprepped DNA was then ethanol precipitated, resuspended in nuclease-free water, and passed through 0.1um filters (EMD Millipore #UFC30VV25). DNA concentration was measured by spectrophotometry on a NanoDrop; preparations falling below 1.8 A260/A280 were discarded.

2.5 Injection mix preparation

Three hours prior to microinjection, tracrRNA (IDT #1072532) and crRNA (IDT) were annealed and complexed with Cas9 protein (IDT #1081058) as described41. Briefly, 5µl of 1µg/µl cRNA was incubated with 10µl of 1µg/µl tracrRNA at 95°C for five minutes followed by cooling to 25°C with ramp speed of 5°C min-1. In a sterile nuclease-free tube (Eppendorf #022600001), 5µl of annealed crRNA:tracrRNA was then complexed with 5µl of 1µg/µl Cas9 protein at 25°C for 15 minutes in 50µl nuclease-free ultrapure water (Thermo #J71786XCR). Following gRNA:Cas9 complexing, donor DNA was added along with ultrapure water to give a final volume of 100µl and concentrations of 50ng/µl crRNA:tracrRNA (or sgRNA), 50ng/µl Cas9 protein (or 125ng/µl mRNA), and 15ng/µl targeting construct DNA. The complete injection mix was spun at 20,000 x g for ten minutes, and the top 65µl was transferred to a new sterile tube for transport to Transgenics core facilities. For injections with sgRNA and Cas9 mRNA, respective plasmids were linearized and transcribed in vitro prior to injection as described.[120]

2.6 Embryo microinjection and transgenesis

C57BL/6J female mice in diestrus between the age of 9 and 16 weeks of age were selected for superovulation. Depending on age and size of the mice, 5-7 IU of PMSG (Millipore #367222/BioVendor #RP1782721000) was injected (IP) at 2:50-3:05PM, followed by HCG 5-7 IU (Sigma CG5) 47 hours later. Mice were paired with C57BL/6J males one hour later. Females were checked the next morning for evidence of a mating plug; plugged mice were harvested for fertilized eggs. Eggs were cultured for one to three hours in KSOMaa Evolve Bicarb +BSA (Zenith Biotech #ZEKS-050). Glass needles were loaded with the described injection mix and placed on ice until used for injection. Eggs were placed on the injection slide in KSOMaa Evolve HEPES +BSA (Zenith Biotech #ZEHP-050). Fertilized eggs were injected using an Eppendorf FemtoJet apparatus. Injected eggs were returned to the incubator and cultured until embryo

transfer into 0.5d.e. pseudopregnant CD-1 females. Implanted females were observed daily and separated two days before the pups were due to deliver. Tail samples were taken between ten and 15 days for genotyping.

2.7 Ig knock-in genotyping

Tail clippings from potential founder animals were taken for genotyping. DNA was extracted in 300µl 50mM NaOH for 30 minutes at 95°C. Samples were neutralized with 25µl 1M Tris-HCl pH7.5 and used as template DNA for polymerase chain reaction (PCR) with targeting-specific primers. Reactions were carried out with OneTaq 2X master mix (NEB #M0488S) according to manufacturer instructions.

2.8 Southern blotting

DNA was extracted from spleen segments using DNeasy Blood & Tissue Kit (Qiagen #69504). 15ug of DNA were digested overnight with the indicated restriction enzymes and run on 0.8% agarose gel. Gels were denatured in 0.5M NaOH 1.5M NaCl with gentle agitation for 15 minutes twice before neutralization in 0.5M Tris-HCl pH 7.5 1.5M NaCl for 15 minutes twice. DNA was transferred from gels to positively charged nylon membranes (Invitrogen #AM10102) overnight via capillary transfer in 20X SSC (Thermo # 15557036). Prior to transfer, nylon membranes were soaked in nanopure water for five minutes followed by 20X SSC for five minutes. Following transfer, nylon membranes were soaked in 2X SSC for five minutes followed by UV cross-linking. Cross-linked membranes were blocked in pre-warmed DIG EasyHyb (Roche # 11603558001) at 43°C for four hours rolling in hybridization tubes. Custom DIG-labeled probes were generated using PCR DIG Probe Synthesis Kit (Roche #11636090910) and blots were hybridized for 16 hours at 48°C with a final concentration of 25ng/ml probe in 10ml DIG

EasyHyb buffer rolling in hybridization tubes. Following hybridization, membranes were washed twice with low stringency buffer (0.5X SSC 0.1% SDS) at 25°C for five minutes, then twice with high stringency buffer (2X SSC 0.1% SDS) at 68°C for 15 minutes. Membranes were equilibrated in wash buffer (Roche #11585762001) at 25°C for five minutes with gentle shaking, then blocked in 100ml block buffer (Roche #11585762001) at 25°C for two hours with gentle shaking. Hybridized probe was detected using AP-conjugated anti-DIG Fab fragments (Roche #11093274910) via incubation at 1:10,000 in 50ml at 25°C for 30 minutes with gentle shaking. Membranes were washed three times in wash buffer at 25°C for fifteen minutes. Membranes were equilibrated (Roche #11093274910) and CDP-Star Substrate (Invitrogen #T2145) was used to detect AP.

2.9 Lymphocyte isolation

Spleen and bone marrow were collected and passed through 70 μm cell strainers, centrifuged, and resuspended in flow cytometry buffer. For peritoneal lavage, 5ml PBS 3% FBS was injected with a 30g needle into the peritoneal cavity followed by gentle shaking. Fluid was then collected with a 25g needle, centrifuged, and resuspended in flow cytometry buffer. Small intestinal lamina propria isolation was performed as follows: tissues were excised and fat, Peyer's patches, and intestinal contents removed. Tissues were opened longitudinally, cut into ~1 cm pieces, and placed into a 50 mL tube with 10 mL RPMI 1% FCS 1 mM EDTA. Small intestines were processed as two halves in separate tubes and combined after lamina propria lymphocyte isolation as noted below. Samples were incubated at 37°C with shaking for 15 min. Pieces were collected on a 100 μm cell strainer (Fisher) and placed in fresh RPMI 1% FCS 1mM EDTA for another 15 min with shaking at 37°C. Pieces were again collected on a 100 μm cell strainer and flow-through was discarded. Intestinal pieces were then placed into 10 mL RPMI 20% FCS with

0.5 mg/mL Collagenase Type I (Gibco #17100017) and 0.1 mg/mL DNase I (Sigma #DN25) at 37°C with shaking for 30 min. Supernatant was collected by filtering through a fresh 100 μm cell strainer and intestinal pieces were placed in fresh RPMI 20% FCS with collagenase and DNase for another 30 min with shaking at 37°C. Supernatant was again collected, remaining tissues mashed, and the cell strainer was washed with 30 mL ice-cold RPMI. The two lamina propria lymphocyte fractions were combined after centrifugation and further enriched by centrifugation in 40% Percoll® (Sigma #P1644) to remove epithelial cells and debris, washed in flow cytometry buffer, and resuspended for cell staining.

2.10 Flow cytometry

Cells were incubated with anti-CD16/32 (Fc block) prior to staining with the following fluorophore or biotin conjugated monoclonal antibodies purchased from Biolegend, eBioscience, or BD unless otherwise indicated (clone in parentheses): B220 (RA3-6B2), CD4 (GK1.5), CD8α (53-6.7), CD11b, CD11b, CD19 (6D5), CD21 (7G6), CD23 (B3B4), CD43 (S7), IgD (11-26c.2a), IgM (R6-60.2), IgMa (DS-1), IgMb (AF6-78) Igκ (187.1) , F4/80 (BM8), NK1.1 (PK136), Ter119 (TER-119), goat anti-human Igκ (Southern Biotech), goat anti-mouse IgA (Southern Biotech), goat anti-mouse Igλ (Southern Biotech). Samples were run on a BD LSRII Cytometer.

2.11 Cell Sorting and adoptive transfer

Indicated populations of peritoneal B cells from multiple CD45.1-congenic wild type mice were sorted on a FACSAria II cell sorter (Becton Dickinson). After post-sort purity analysis, 1e5 cells were transferred IP into adult (8-12 week) C57BL/6J mice. Recipient mice were analyzed one week following transfer.

2.12 Non-Ig construct cloning and genotyping

Targeting constructs for knock-ins other than Speed-Ig were prepared in largely the same manner. Homology arms exactly flanking the guide site were amplified from genomic DNA of the mouse strain used as embryo donors for microinjection (typically C57BL/6J). A second cloning PCR was performed to provide Gibson overlaps to homology arms and cargo if necessary. Homology arms and cargo DNA were assembled into generic plasmids (pUC18 or pUC19) via Gibson assembly. Microinjections were carried out identically to Speed-Ig, but with crRNAs specific for the relevant guide site. Genotyping knock-in mice was performed by three separate PCRs on DNA samples from potential founder animals. First, PCRs to detect the cargo were performed to identify all mice which carried non-native DNA (e.g. EGFP). Then, cargo$^+$ animals were genotyped for targeting PCR across the 5' and 3' homology arms to detect properly targeted insertions/replacements. Amplicons arising from targeting reactions were Sanger sequenced to confirm correctly targeted alleles.

2.13 Immunohistochemistry

Intestines were dissected, flushed of contents with PBS, rolled into tissue cassettes, and incubated in formalin for 24 hours at room temperature. Cassettes were then placed into 70% EtOH and incubated for at least 12 hours. Tissues were then paraffin-embedded and sectioned for staining following standard protocols. Quantification of pSTAT3 events was performed in ImageJ using the Fiji distribution as follows: randomly selected image areas were deconvoluted for DAB signal (pSTAT3), and events were cut off at an arbitrary threshold of 180 pixel intensity to avoid background signal. Events were digitally separated by binary watershed processing, and resultant particles were counted. For duodenal images, particle counts [pSTAT3$^+$ cells] were taken for individual villi from not less than ten villi. For Peyer's patches, particle

counts were normalized to the physical area of the Peyer's patch in the image. For ileal images, villi containing any signal were counted as $pSTAT3^{+}$, and the frequency of $pSTAT3^{+}$ villi was deduced by counting a minimum of 75 individual villi per sample.

3. RESULTS

3.1 IgA Function

I sought to generate a more sophisticated model of IgA deficiency that would not have the same drawbacks as previous attempts outlined above. My objectives were to remove IgA without allowing compensatory IgM and to avoid disrupting the biology of other cell types. My efforts led to two new models of IgA deficiency. The first model, "Bait-and-Switch" (IgA^{BnS}), involved the substitution of IgA constant region with a constant region from IgG1 or IgG2a (Fig.5A). The concept of IgA^{BnS} was straightforward: cells that have been instructed to class-switch to the IgA isotype were still capable of using the IgA switch region, thereby permanently switching away from IgM expression. However, the isotype present after the IgA switch region was IgG, which cannot cross intact epithelial layers as would be needed for luminal deposition. I used Cas9 to cut immediately upstream of the IgA constant region coding region, leaving the switch region intact, replacing only the structural domains of IgA with that of IgG1. The replacement of IgA coding regions with that of IgG1[a] was confirmed by genotyping PCR of founder animals across the homology arms (Fig.5A). I left intact the transmembrane region of IgA at the 3' end of the locus and made our knocked-in IgG1 splice-competent with this transmembrane region (Fig.5A). This was a difficult replacement of approximately 1.7kb of the

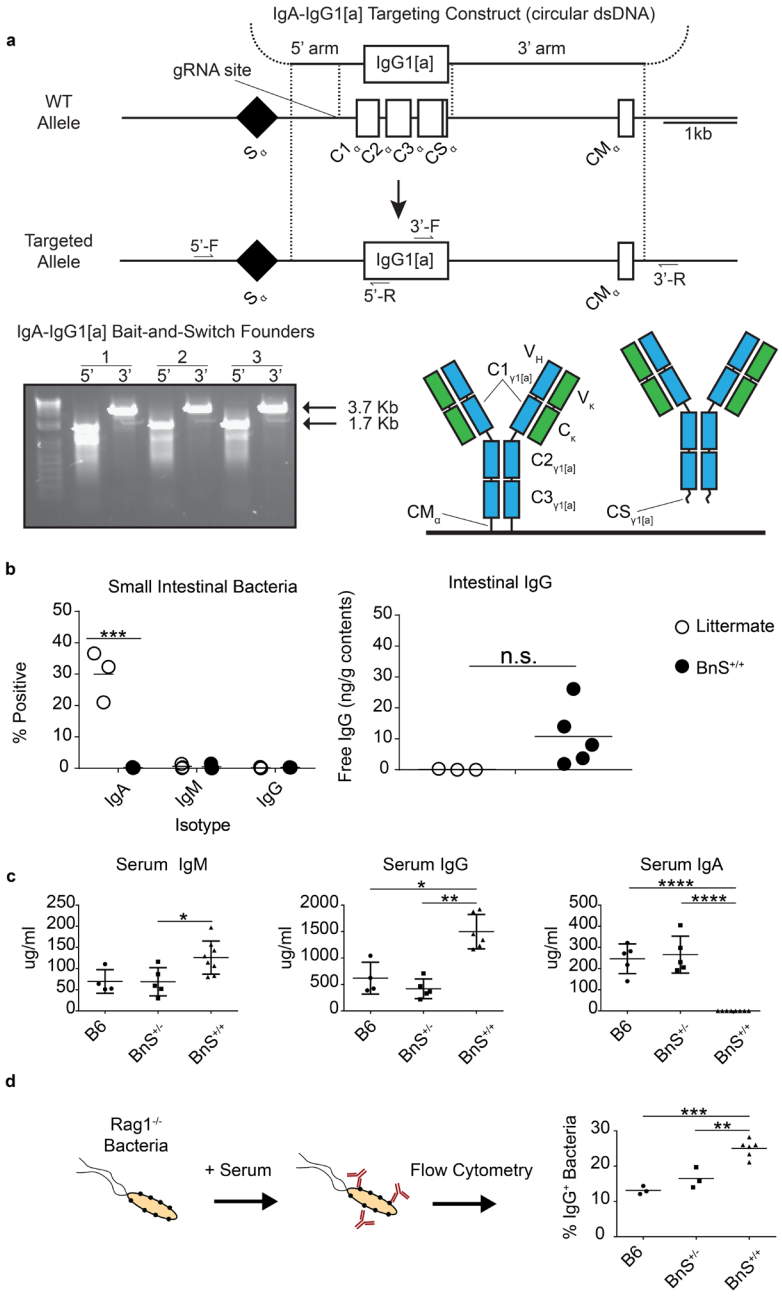

Figure 5. The IgA^{BnS} Model. A) [Top] Knock-in scheme to replace IgA coding sequence with IgG1. [Bottom] Genotyping of IgA^{BnS} founders and cartoon depiction of IgA^{BnS} antibodies. **B)** Bacterial flow cytometry of small intestinal bacteria, and free intestinal IgG in IgA^{BnS} homozygous animals. Significance determined by Student's T Test. **C)** Serum IgM, IgG, and IgA in IgA^{BnS} heterozygous and homozygous animals. Significance determined by one-way ANOVA with post-hoc Tukey test. **D)** Coating of Rag1$^{-/-}$ small intestinal bacteria by IgA^{BnS} serum with detection by flow cytometry. Significance determined by one-way ANOVA with post-hoc Tukey test. n.s., not significant.

IgA locus with 1.2kb of IgG1 and an upstream splice region. I installed a allotype IgG1 cDNA such that I could distinguish serum IgG1[a] derived from IgA^{BnS} cells apart from unaltered IgG1[b] secreted by normal $IgG1^{+}$ plasma cells found in all B6 mice. My construct successfully targeted and disrupted the normal IgA locus, and I was able to detect the full replacement of IgA as intended.

I took several steps to validate the IgA^{BnS} model. IgA^{BnS} were deficient in mucosal antibody coating of intestinal bacteria, a critical improvement over most other IgA deficiency models (Fig.5B). I detected some shifts in serum concentrations of IgG and IgM, and no IgA in homozygous IgA^{BnS} mice (Fig.5C). I performed a complementary experiment by taking serum IgG from IgABnS mice, and used these sera to stain intestinal bacteria from a $Rag1^{-/-}$ animal. IgA^{BnS} was better able to bind to bacteria than serum IgG taken from wild type mice, demonstrating that IgA^{BnS} antibodies are successfully rerouted to the serum (Fig.5D).

Having validated the IgA^{BnS} model, I performed a number of preliminary experiments to explore possible functions of mucosal antibody deficiency. I was interested in observing whether IgA^{BnS} mice had an altered microbiota composition, as had been observed in other IgA deficiency models. Using 16s rRNA analysis, I observed no consistent shift in the fecal microbiota of IgA^{BnS} animals compared to cage-mate, littermate controls (Fig.6A). It was likely that co-housing animals equilibrated the cage-wide microbiota composition, so any effects of mucosal antibody deficiency might be masked by such experimental setups. I was also interested to know the broader reactivity profile of IgA^{BnS} mice. Since IgA^{+} PCs are polyreactive— and from our previous work, thought to be self-reactive— I screened IgA^{BnS} serum against a protein microarray containing mostly self-antigens. This array was carried out under more stringent conditions than polyreactivity ELISAs, so low-affinity interactions are more easily washed away.

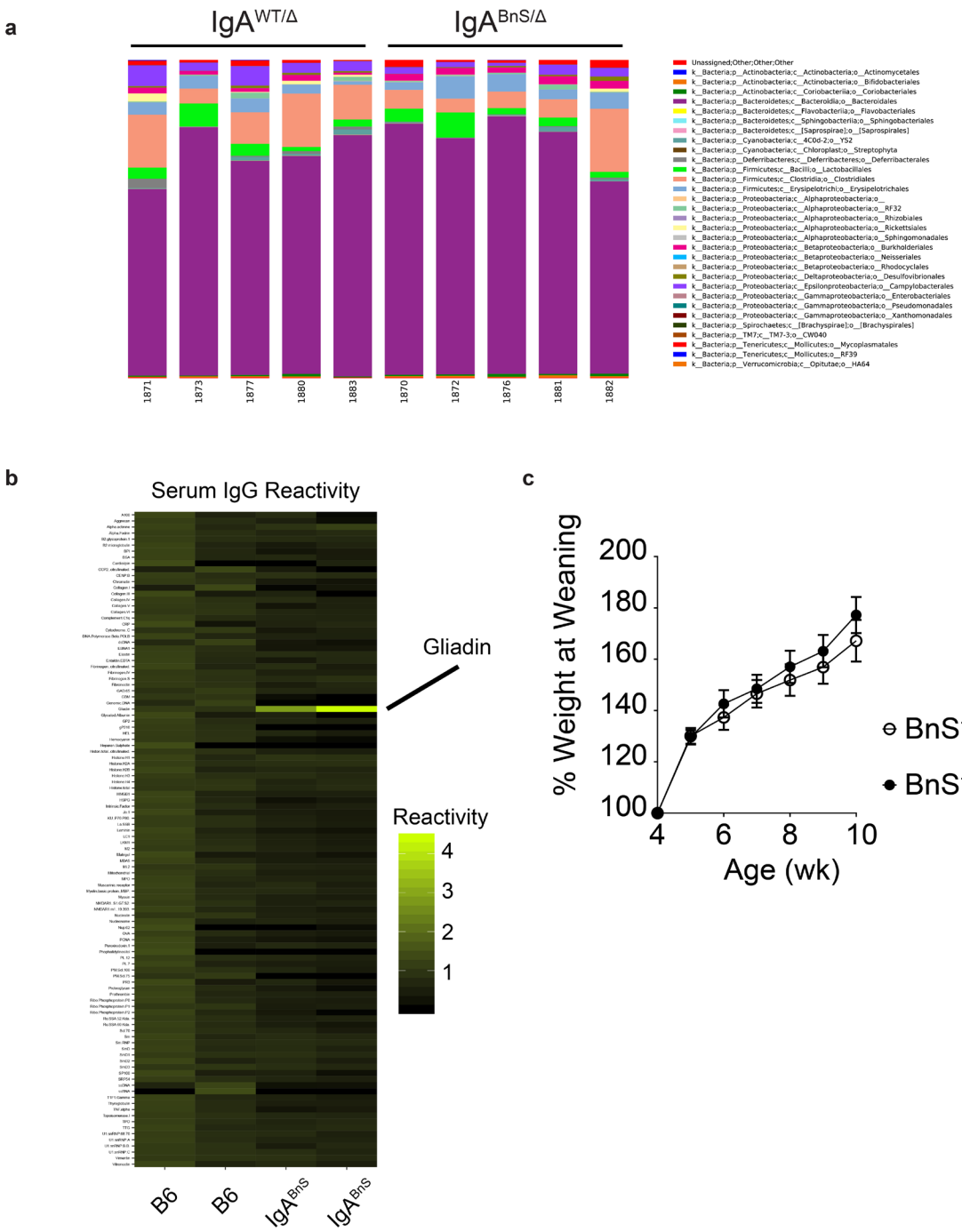

Figure 6. Effects of mucosal antibody deficiency in IgA^{BnS} mice. A) Order-level 16s rDNA compositional analysis of fecal bacteria from IgA$^{BnS/\Delta}$ and littermate/cagemate mice. B) autoantigen protein microarray reactivity of serum IgG from B6 and IgA^{BnS} homozygous mice. Reactivity values were normalized to B6 average and square-root transformed to adjust display scale. C) Weight gain of IgA^{BnS} heterozygous and homozygous mice through 6 weeks after weaning.

Notably, IgA^{BnS} serum was not enriched for self-reactivity compared to wild type mice (Fig.6B). IgA^{BnS} serum did strongly react with deamidated gliadin, one of the control proteins on the microarray (Fig.6B) Gliadin is a dietary protein, and the strong reactivity would suggest that some IgA is directed against dietary antigens. IgA is known to bind food antigens, so my findings are consistent with that literature.[40,121] This also served as some evidence that IgA^+ PCs were not being selected on specific self-antigens, although the microarray was not exhaustive. Still, it was possible that IgA^{BnS} antibodies, with low affinity for many self-antigens, might cause general morbidity. I tracked the weight gain of cohorts of heterozygous and homozygous IgA^{BnS} littermates. All animals gained weight at the same rate, suggesting no fulminant autoimmunity was progressing due to IgA^{BnS} antibodies (Fig.6C).

I then looked at the histology of the small intestine in IgA^{BnS} mice. The intestine was morphologically unperturbed, however with immunohistochemistry I observed an increased frequency of $pSTAT3^+$ cells throughout the intestines of IgA^{BnS} mice (Fig.7). In the duodenum, I saw that $pSTAT3^+$ cells were mostly localized to the lamina propria, with little epithelial STAT3 signaling (Fig.7). The Peyer's patches had distributed $pSTAT3^+$ cells, with no clear microanatomical enrichment (Fig.7). In the ileum, both the epithelial cells and lamina propria cells were positive for pSTAT3 (Fig.7). The pSTAT3 staining pattern suggests that loss of IgA differentially affects homeostatic signaling pathways in different intestinal locations. This result was of great interest and may hint at a multiple homeostatic functions of IgA.

My second model of IgA deficiency was less acrobatic and was based off an approach used by Neuberger and colleagues for the removal of secretory IgM[63,122]. When IgA^+ GC B cells transit through the GC, they use transmembrane IgA for signaling purposes and only when committing to the plasma cell fate are genes upregulated that force transcript termination ahead of this

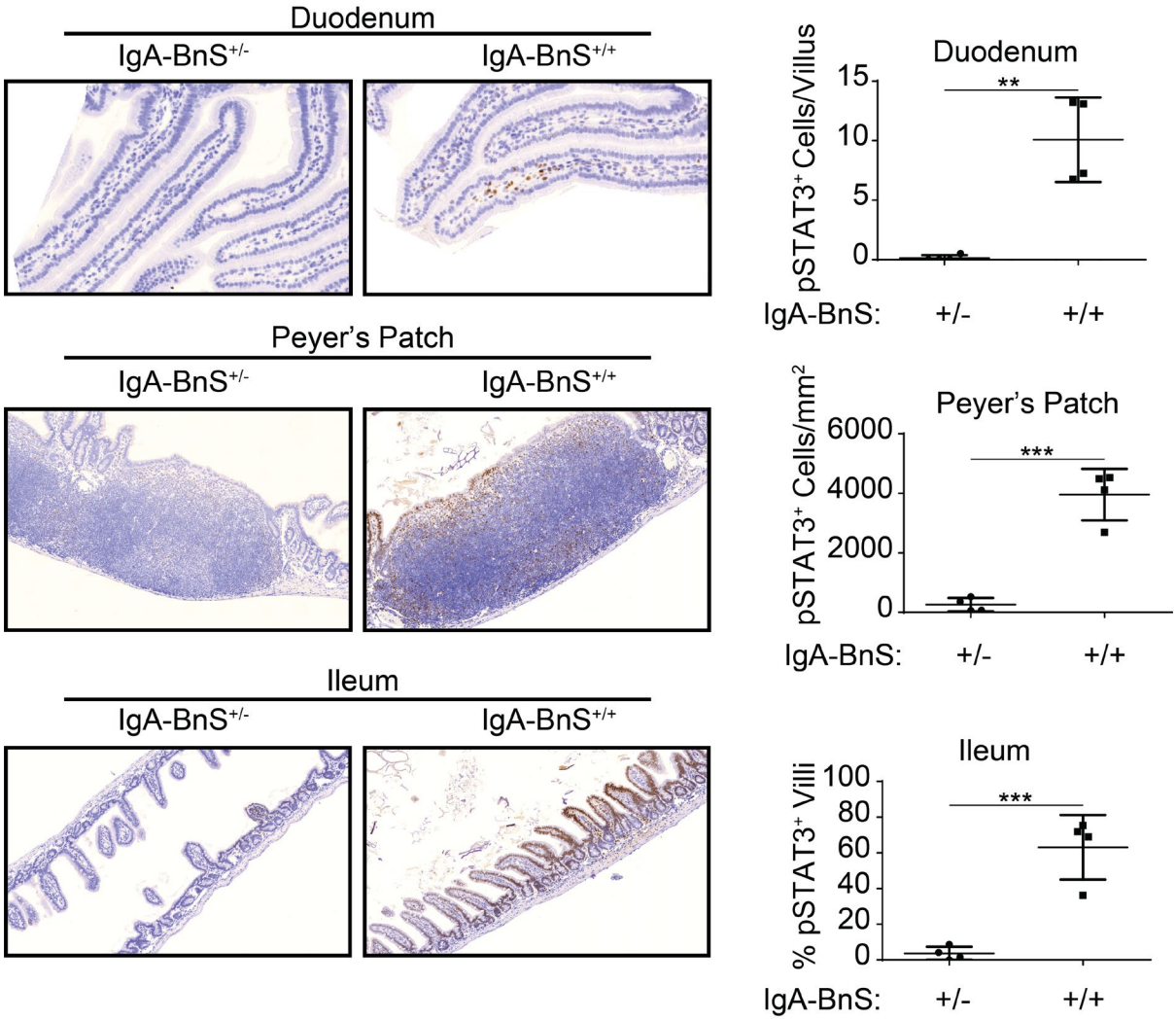

Figure 7. Elevated intestinal STAT3 signaling in IgA^{BnS} mice. Sections of the intestine from littermate heterozygous and homozygous IgA^{BnS} mice were stained for pSTAT3 and counterstained with hematoxylin. Representative images of duodenal villi, Peyer's patches, and ileal villi which showed increased pSTAT3 in homozygous IgA^{BnS} mice. In the duodenum, pSTAT3^{+} cells were mostly localized to the lamina propria, while the ileum had pSTAT3^{+} epithelial and lamina propria cells. Peyer's patches displayed distributed pSTAT3^{+} cells. Significance determined by Student's T-test.

domain.[123] By virtue of "premature" splicing, IgA molecules are forced to encode a small secretory tailpiece prior to a stop codon terminating the coding region.[124] In this way, secretory IgA is formed, and the secretory tailpiece is involved in bonding to the J chain and formation of dimers or polymers. I identified gRNA sites that would remove the secretory tailpiece and secretory isoform polyadenylation signal while leaving the remaining IgA exons splice-competent to the transmembrane region (Fig.8A). One gRNA site targeted within the tailpiece sequence, after the donor splice site of the final Ig fold coding region. The other targeted slightly upstream of the transmembrane coding region, after the stop following the tailpiece. Proper resection of this region would lead to the inability of IgA to be secreted with no other defects. I was successful in generating the intended deletion (Fig.8B). I was also successful in generating a replication of the original IgA knockout line, removing the switch sequence and a portion of the first coding region (Fig.8A-B). As an alternative, I also generated an IgA knockout allele with switch region intact but missing the major coding elements of IgA (Fig.8A-B). While I did not assess the original knockout replica, nor the coding sequence mutant, these lines may prove to be useful controls for future experiments done in the Jabri lab. I was able to do preliminary validations of the IgA^{SecKO} line. I saw that no bacteria were coated with IgA, similar to IgA^{BnS} mice (Fig.8C), I also observed that no bacteria had IgM coatings, which suggest the IgA^{SecKO} model is a good model for mucosal antibody deficiency.

3.2 Ig knock-ins using a Cas9-mediated approach

Both the IgA^{+} PC ontogeny project and the innate-like B cell ontogeny project required Ig knock-in lines. In order to make solid conclusions about the nature of each population, it was important to have multiple representatives, thus avoiding biases from potential outlier Ig pairs. Each full Ig knock-in line required the separate installation of a heavy and light chain, and each

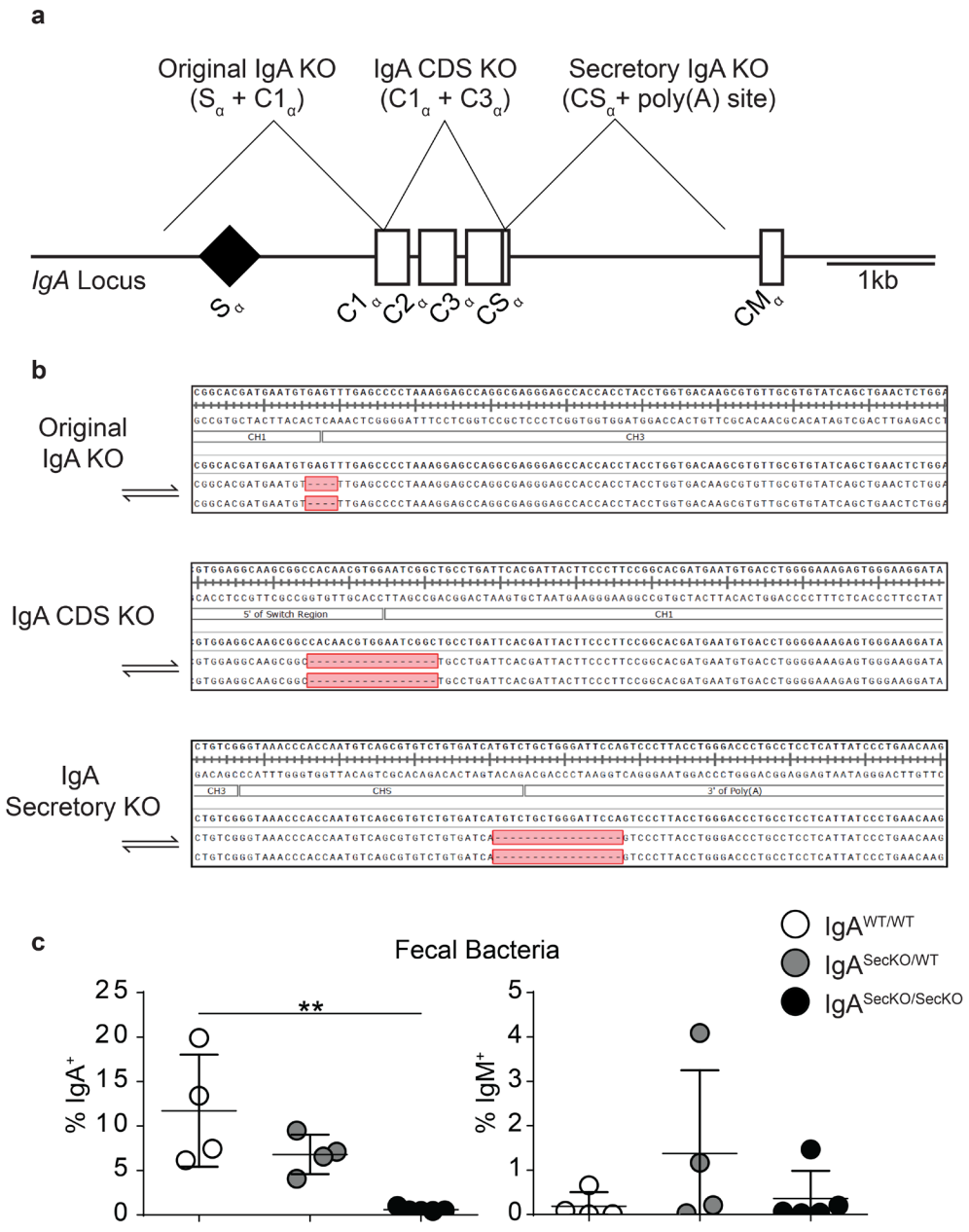

Figure 8. Additional genetic models of IgA deficiency. A) Depiction of the IgA constant region locus with Cas9-mediated deletions indicated. **B)** Sanger sequencing of founder animals carrying deletions of the indicated type. Potential founders were genotyped by PCR across the prospective deletions and amplicons of the expected size were sequenced from both directions. Sequences were aligned to mock-ups of the indicated deletion. Red dashes indicate absent nucleotides in the founder sequence. **C)** Early validation of the IgA^{SecKO} model. Homozygous IgASecKO animals had no IgA^{+} bacteria in the feces. Significance determined by one-way ANOVA with post-hoc Tukey test.

project required at least six different Ig knock-in lines. To produce 24 knock-in lines, I needed to carefully consider the methodological approach in order to accomplish this task. Random transgenesis of Ig pairs was a possibility and has been used in the past to understand the developmental biology of B cells.[125–128] However, random transgenics are not typically competent to switch isotypes to IgA, precluding analysis of terminal differentiation. Moreover, random transgenic insertions have non-uniform expression patterns, and as proper Ig expression is critically important to B cell development, this option was not ideal. I tried, and failed, to make Ig retrogenics, which has proven fruitless in the past.[129] Therefore the only reasonable option at the time, although it had never been accomplished, was to use Cas9-mediated knock-in technology to create my genetic lines. While Cas9-mediated gene edits such as deletions and small epitope-tag knock-ins have become trivial, large insertions or replacements are difficult and no existing guidelines were available for implementation. I initiated a series of attempts to create Ig knock-in lines using Cas9 in order to proceed with my research. To maximize the biological relevance and utility of my Ig knock-in approach, I had the following objectives: (1) to remove the endogenous J segment loci, thereby preventing secondary Ig rearrangements after successful integrations; (2) to use fixed promoter regions which would allow for phenotypic comparisons across mouse lines in a truly Ig-dependent manner; and (3) to minimize targeting construct size and synthesis time such that panels of Ig knock-in mice could be generated quickly and efficiently.

To insert rearranged Ig genes into their corresponding loci, I first selected one guide RNA (gRNA) site each for J_H1 and $J_\kappa1$, directly upstream of the gene segment coding regions. This was already a break from similar replacement approaches, in which two gRNA sites are used to remove the endogenous sequence prior to installation of intended cargo. I settled on a directional

approach with one gRNA, with the expectation that synthesis-dependent strand annealing would be the mechanism of action.[130] I then generated targeting constructs with short (~800bp) "proximal" and long (~2.2kb) "distal" homology arms bookending all endogenous J segments (Figs.9-10A). Using a single Cas9 guide site, only the proximal homology arm directly abutted the double-strand break and served as an anchor for the intended synthesis-dependent strand annealing. The intervening genomic DNA between the guide RNA site and the beginning of the distal homology arm had no complementarity present in the donor DNA and was excised upon construct integration (Fig.10A). Therefore, upon successful integration of the targeting construct, the entire J segment clusters were deleted, preventing secondary Ig rearrangements on the targeted allele. The distal homology arms were selectively increased in length as longer distal, but not proximal, homology arms were demonstrated to increase efficiency of large gene replacements in vitro.[131] Promoter regions 800-1200 base pairs in size including split leader peptide sequences were cloned from the V_H1 family for heavy chain constructs and the $V_\kappa10$ family for kappa constructs based on usage patterns in wild type B cell repertoires.[57] Rearranged Ig chains amplified from cDNA of single sorted B cells were assembled seamlessly with promoters into respective targeting constructs using Gibson assembly (Fig.9).[119] This modular construct assembly allowed for rapid and scalable Ig cloning combined with flexibility in promoter choice. Fertilized murine oocytes were microinjected at the one-cell stage with targeting constructs and either single-guide RNA (sgRNA) with Cas9 mRNA or pre-complexed gRNA:Cas9 ribonucleoproteins (RNPs) (Fig.7B). Potential Ig knock-in founders were screened for intact Ig insertions via "targeting" PCR which was accommodated by homology arms much shorter than those used in traditional knock-in transgenesis (Fig.10C). Ig inserts were further verified by southern blotting (Fig.10D). Rarely, some founder animals possessed off-target

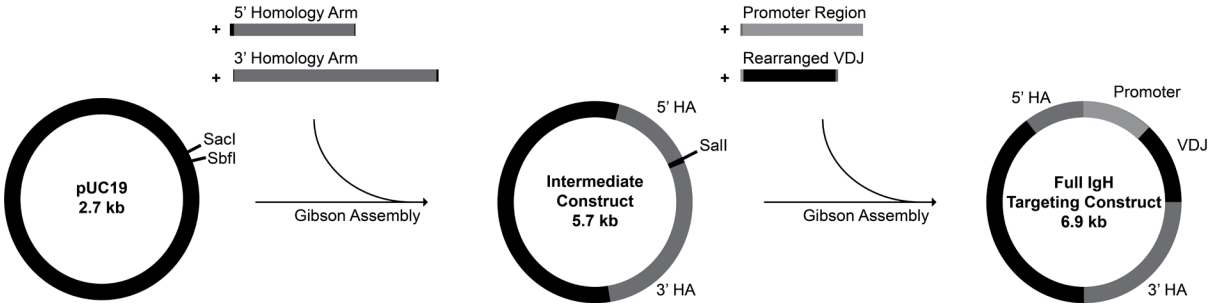

Figure 9. Rapid *IgH* targeting construct generation. A generic plasmid backbone was digested with SacI and SbfI, allowing assembly of homology arms into an intermediate targeting construct. Intermediate constructs were digested with SalI, followed by final assembly with an Ig-specific promoter region and Ig variable regions of interest. Regions of assembly overlaps at the ends of inserts are color-matched to construct sequence. A similar assembly pipeline was done for *Igκ* targeting constructs. Not depicted to scale.

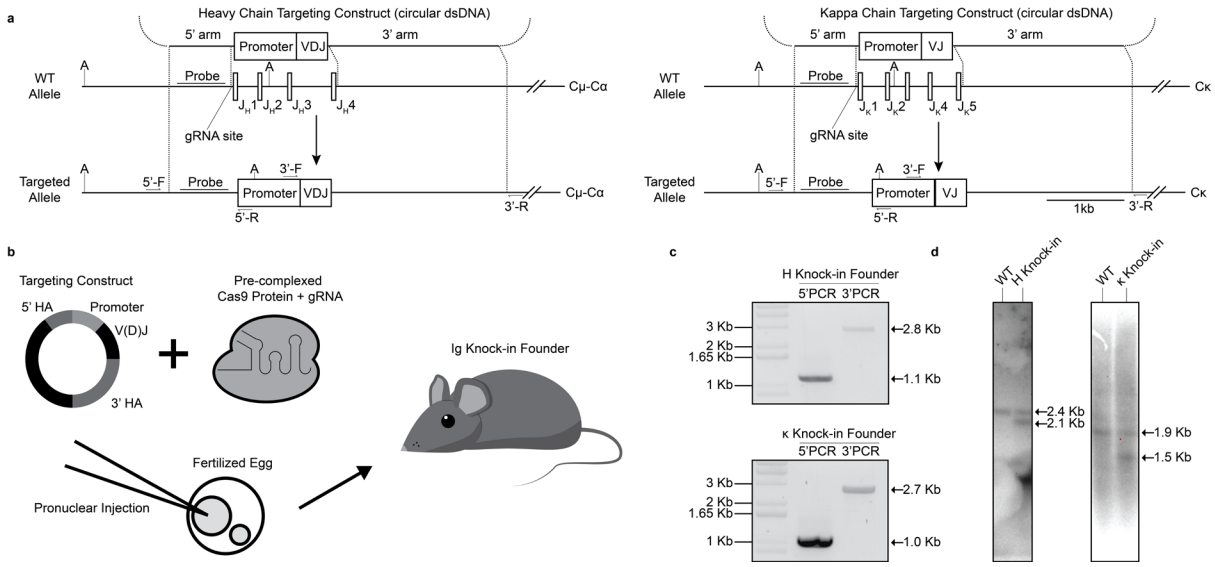

Figure 10. Targeted integration of rearranged V regions at the JH/Jκ loci. A) Targeting approach to replace endogenous J segments with rearranged VDJH/VJκ. Dashed lines indicate areas of complementarity for homology arms. **B)** Schematic diagram of pronuclear injection **C)** Genotyping of H and κ knock-in founders using paired targeting PCRs. Corresponding primers are depicted in panel A. **D)** Southern blotting of H and κ knock-in mice. Genomic DNA was digested with ApoI (for H) or AccI (for κ) and probed within the 5' homology arm. A: ApoI/AccI sites.

integrations (Fig.11). After several rounds of optimization, successful Ig integrations/J cluster deletions ultimately reached 20.7% of live-born mice for heavy chains and 23.3% for kappa chains (Table 1). Successful knock-ins were only recovered from the injection of targeting constructs with longer 3' homology arms (Table 1). Notably, the use of gRNA:Cas9 RNPs was superior to sgRNA/Cas9 mRNA, similar to recent reports.[106,110]

I performed a series of experiments to evaluate the utility of Speed-Ig mice in studying B cell biology, a hallmark of prior Ig knock-in approaches. Heavy chain and light chain expression were measured independently by flow cytometry. Progeny from H knock-in mice (on the IgH^b C57BL/6J background) bred to IgH^a allotype mice demonstrated knock-in chain expression at the protein level (Fig.12A, left panels). As expected, the knocked-in chain, due to its rearranged state and ensuant expression kinetics, prevented endogenous rearrangements and therefore excluded IgH^a allele expression.[132] On an IgH^{Δ} background, knocked-in heavy chains were capable of driving normal B cell development (Fig.13A). Furthermore, the surface expression of IgM and IgD were comparable between wild type B cells and B cells from $IgH^{KI/\Delta}$ mice (Fig.13A). The IgH^{Δ} background also provided an opportunity to assess class-switch recombination in Speed Ig mice. As expected, B cells forced to use knocked-in H chains were able to switch to the IgA isotype in mucosal tissue, a firm indication that our Speed-Ig lines retain this important capability (Fig.13B). These data confirm the functionality of the targeting approach, promoter regions, and Ig integrations for H knock-ins. Similar experiments were performed using κ knock-in mice. κ knock-ins were bred to mice possessing the human kappa constant region to allow for allele-specific flow cytometry staining.[133] κ knock-in mice with Vκ10-96 promoters had normal mIgκ surface expression and outcompeted the human kappa

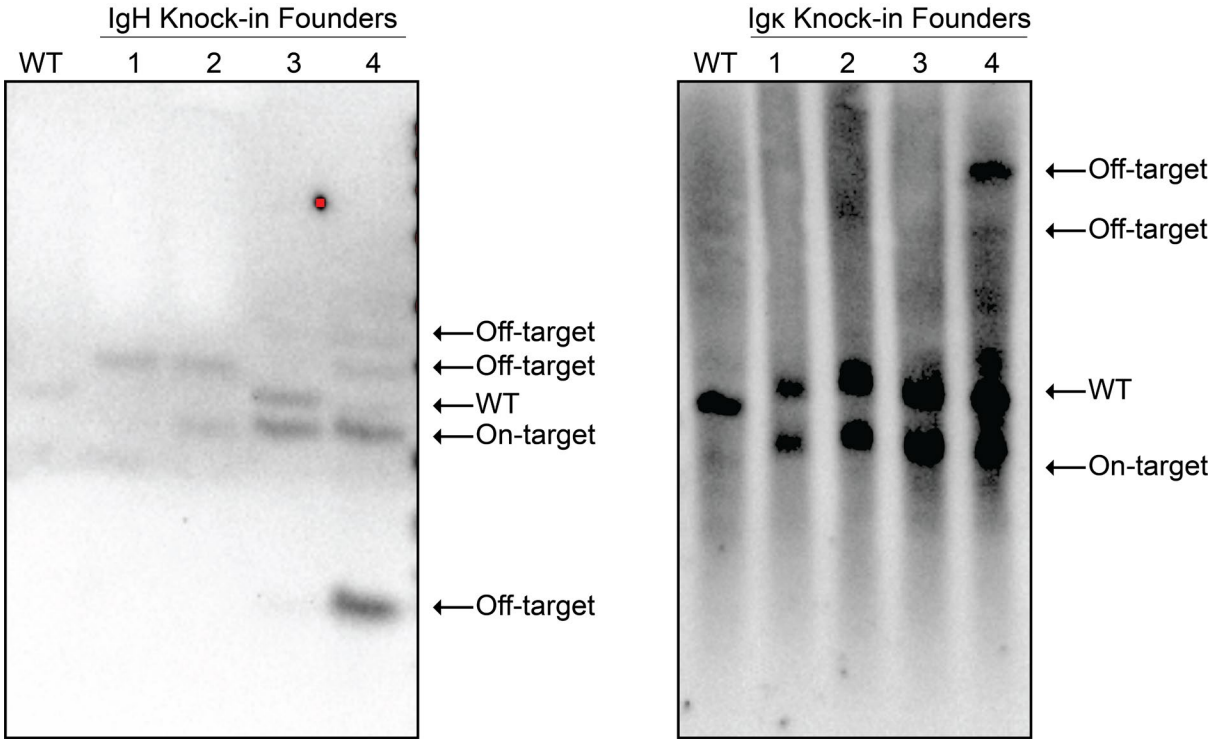

Figure 11. Off-target analysis of H and κ knock-in founder animals. Genomic DNA was digested with ApoI (for H) or AccI (for κ) and probed within the 5' homology arm. Wild type, on-target, and off-target bands are indicated by arrows. Panels include representatives from four different knock-in lines.

Heavy Chain

Version	Protospacer	gRNA/Cas9 Modality	Homology Arms (5':3')[bp]	Promoter family/size [bp]	Total Pups	Positive	%
1	A	R	800:800	IgHV1-18, 874	33	0	0.00
2	A	R	800:2200	IgHV1-18, 874	222	6	2.70
3	A	P	800:2200	IgHV1-18, 874	161	10	6.21
4	B	P	800:2200	IgHV1-18, 874	163	9	5.52
5	C	P	800:2200	IgHV1-18, 874	198	41	20.71

Kappa Chain

Version	Protospacer	gRNA/Cas9 Modality	Homology Arms (5':3')[bp]	Promoter family/size [bp]	Total Pups	Positive	%
1	D	R	800:800	IgKV4-53, 729	15	0	0.00
2	D	R	800:2200	IgKV4-53, 729	214	9	4.21
3	D	P	800:2200	IgKV4-53, 729	129	30	23.26
4	D	P	800:2200	IgKV10-96, 1179	479	70	14.61

Table 1. Speed-Ig knock-in efficiencies. Several iterations of Ig knock-in approaches differing in protospacers, Cas9 form, homology arm lengths and promoter sizes had different targeting efficiencies. A-C, different protospacers used to target the heavy chain locus. D, a single protospacer was used to target the kappa chain locus. R, Cas9 mRNA and in vitro transcribed sgRNA. P, protein Cas9 and bipartite crRNA:tracrRNA.

allele (Fig.12A, right panels). This contrasted with κ knock-in mice generated with Vκ4-53 promoter regions, which had poor kappa expression (Fig.14). Although the Vκ4-53 promoter region was selected based on published work, I did not observe adequate Igκ expression in our lines, prompting my use of a larger promoter region from a different Igκ family.[134] I then examined full (H + κ) Ig knock-in mice (henceforth with V_{κ}10-96 promoters) for B cell developmental progression. It has been previously noted that, in Ig knock-in mice, developing B cells transit the pre-B stage faster than wild type cells due to pre-rearranged Ig expression.[89,100,128,135] My knock-in lines demonstrated a reduction in pre-B frequency, consistent with prior knock-in approaches and further validation of knocked-in Ig expression (Fig.12B). Taken together, these results suggested that Speed-Ig mice display physiologic Ig chain expression levels and that knocked-in Igs predominate over endogenous chains. In summary, my results demonstrated that the Speed-Ig system is a robust tool for *in vivo* studies of monoclonal B cell biology.

The difficulty in utilizing CRISPR/Cas9 for larger (>1kb) genome insertions/replacements has stood at odds with the highly efficient knockout and small knock-in data in the field. My iterative testing of the H and κ loci provided empirical evidence into the effects of homology arm length and Cas9 modalities in a locus-controlled manner *in vivo*. The methodological modifications leading to elevated targeting efficiency were additive and consistent across both loci. Accordingly, I reasoned that such modifications would be broadly applicable toward knock-in insertions and replacements elsewhere in the genome. To this end, Shan Kasal and I generated targeting constructs to place IRES-led reporter genes or similarly sized modifications into the 3'

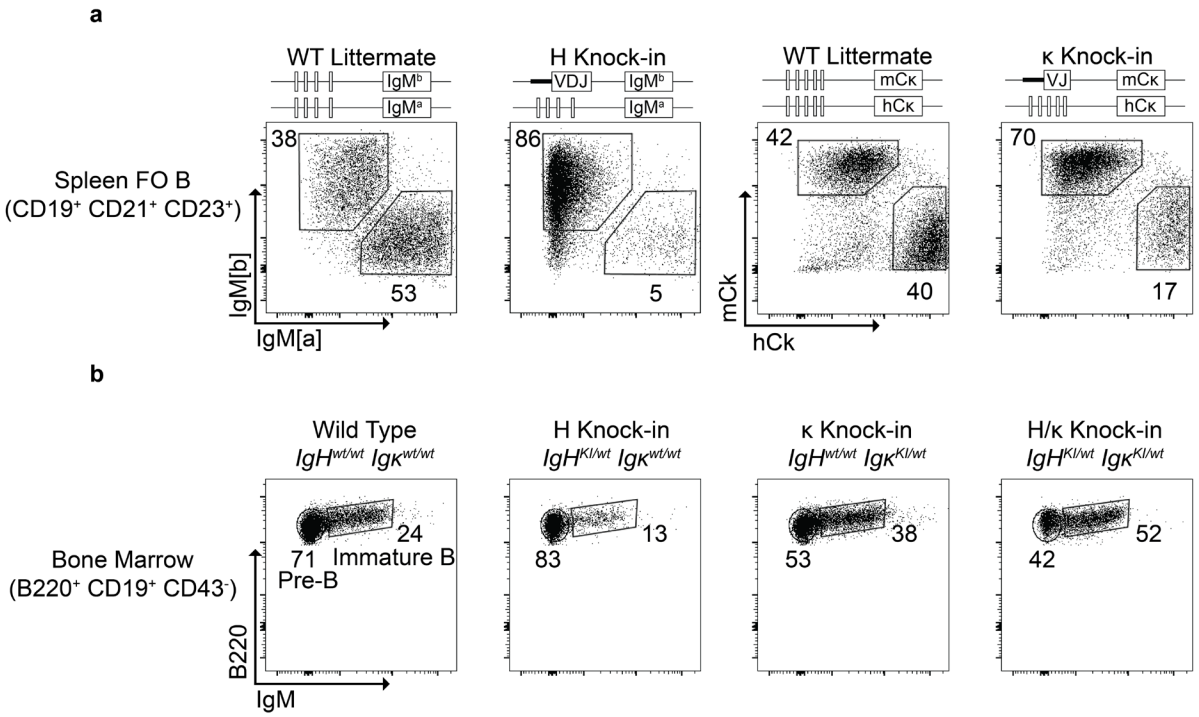

Figure 12. Speed-Ig gene expression and B cell development. A) Knocked-in H and κ chains dominate over endogenous alleles. [Left panels] Flow cytometry of splenic follicular B cells (CD19$^+$ CD21$^+$ CD23$^+$) from *IgH*$^{b/a}$ and *IgH*$^{KI/a}$ littermates stained with allotype-specific anti-IgM antibodies. *IgH* locus genotype indicated above plots. [Right panels] Flow cytometry of splenic follicular B cells from *Igκ*$^{m/h}$ and *Igκ*$^{KI/h}$ littermates stained with human and mouse-specific anti-IgK antibodies. *Igκ* locus genotype indicated above plots. **B)** Bone marrow development of Speed-Ig B cells expressing H, k, or both Ig knock-in chains. All panels are representative of n ≥ 3 mice.

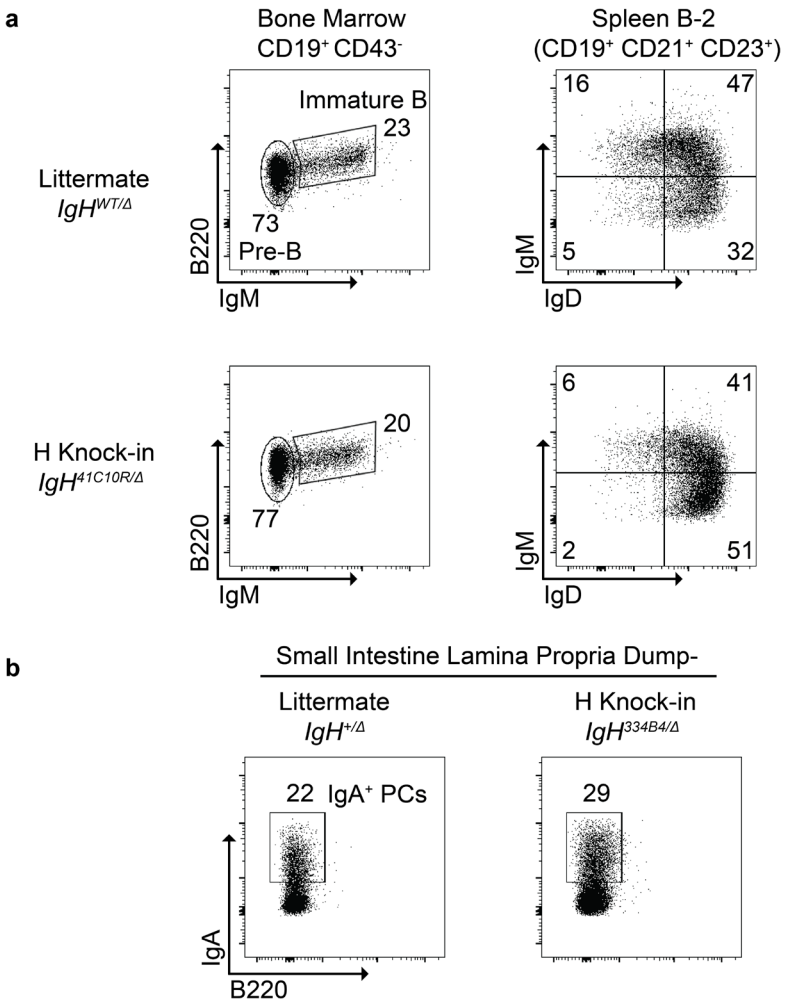

Figure 13. H knock-ins are sufficient in the absence of endogenous alleles and can class switch. **A)** [Left panels] Flow cytometry of developing B cells in the bone marrow and [right panels] mature B cells in the spleen of an H knock-in mouse on an IgH-deficient background. **B)** Class switching to IgA in the gut lamina propria of an $IgH^{KI/\Delta}$ mouse All panels are representative of n ≥ 3 mice.

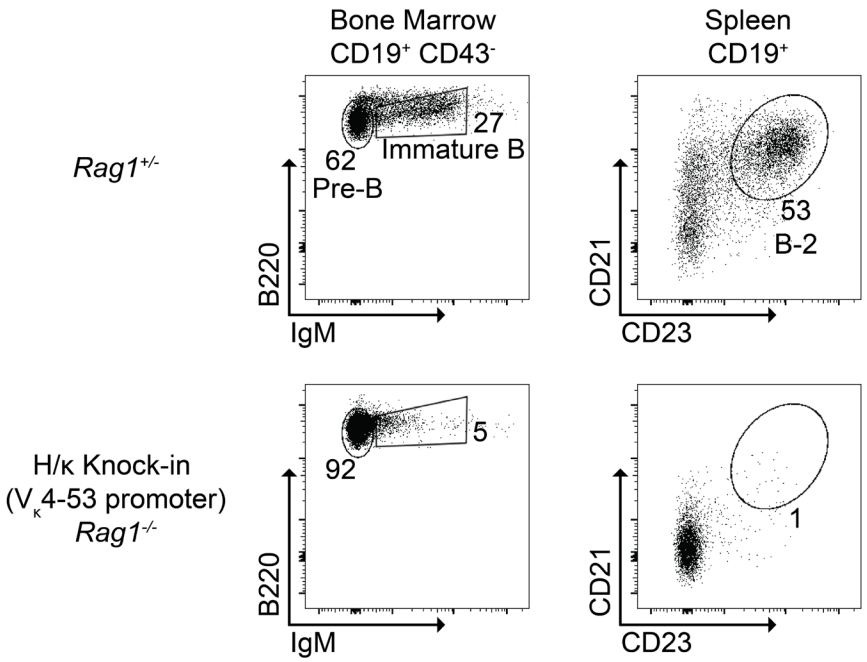

Figure 14. A V_κ4-53 promoter fragment is insufficient to drive Igκ knock-in expression. [Left panels] B cell development in the bone marrow gated on $CD19^+$ cells past the Pro-B ($CD43^+$) stage. [Right Panels] surface expression of CD21 and CD23 on splenic $CD19^+$ B cells. All panels are representative of n≥ 3 mice from 5 separate lines using the V_κ4-53 promoter

untranslated regions of several previously untested target loci. Inserted cargo ranged from approximately 1.4kb to 2.0kb (Table 3). Guide sites were chosen by high on-target scores as assigned by Integrated DNA Technologies' (IDT) selection tool (Table 3). For knock-in insertions without deletion of genomic DNA, both homology arms in effect abut the Cas9 cut site, and no determination can be made regarding the directionality of knock-in integration via synthesis dependent strand annealing. Therefore, the orientation of short and long homology arms was arbitrary relative to the inserted cargo. However, I speculated that having only one long homology arm would be sufficient to increase targeting efficiency to levels seen in Speed-Ig. Strikingly, using asymmetric homology arms and pre-complexed Cas9/gRNA RNPs yielded correctly targeted mice at a rate of 18.4% across eight loci (Table 3). Therefore, my insights from the Speed-Ig approach elevated integration efficiencies across many loci, allowing me to generalize Cas-mediated gene editing principles in the mouse. With the Ig knock-in tool in hand, I was able to pursue the questions I had about IgA^+ PC ontogeny and innate-like B cell ontogeny.

3.3 IgA^+ plasma cell ontogeny

One angle to approach the question of IgA function has been understanding the binding specificities of the cells selected into the IgA^+ PC repertoire. This angle was undertaken following the prior work in the lab, which suggested that IgA^+ PCs are polyreactive and/or self-reactivity.[57] I first selected representative Ig pairs from B-2 cells and IgA^+ PC cells (Table 3). Ig pairs were selected for their potential to give me the most dramatic phenotype, if any, as possible. This meant that selecting B-2 cells with the lowest polyreactivity and microbiota reactive, and conversely selecting some of the most polyreactive IgA^+ PCs. Ig pairs were diverse in V, D, and J gene segment usage, and in cases where mutations were present in the recovered Ig, reverted to a predicted germ-line configuration to best model the development prior to

Gene	Protospacer	On-Target Score [a]	Insertion	Insertion size (bp)	Homology Arms [5':3'](kb)	Pups	Knock-ins	%
Bhlhe41	CTTTAGAGGACGTTTGAACT	71	IRES-Cre	1638	1.0:3.0	22	5	22.73
Gata3	AAAACGCAAGTAGAAGGGGT	57	IRES-mCitrine	1330	3.0:1.0	15	3	20.00
Igha	TGGAGCGCTAGACTGCTCAG	37	IgG1 [b]	1211	0.8:2.7	53 [c]	9	16.98
Rorc	GTCCTACAAGGCAAGCCTAG	69	IRES-Thy1.1	1157	1.0:3.0	59 [c]	13	22.03
Tbx21	ACTAACTTAGAAAACAGACG	53	IRES-mCerulean3	1330	1.0:3.0	10	2	20.00
Tcf7	CGACCTGAGAATGTTGGTGC	49	IRES-mCherry	1387	1.0:3.0	24	2	8.33
Zbtb16	CGAGCTAGAACCAGACAAAG	60	IRES-hCD4	1950	1.0:3.0	29	4	13.79
Zbtb32	ACAGGAGCTACGAACCCTTC	68	IRES-Cre	1593	0.8:2.6	22	5	22.73

Table 2. Generic improvements of Cas9-mediated large insertions and replacements. Donor DNA constructs with indicated cargo were targeted to different loci. a, protospacer on-target scored ascribed by IDT. b, replacement of endogenous sequence of similar size. c, combined counts from multiple injection days.

Follicular B Cell Ig Knock-in Lines	
Ig Name	Average Polyreactivity (Bunker et al 2017)
292D8	0.075
305E7	0.170
334B4	0.049
335A3	0.087

IgA+ Plasma Cell Ig Knock-in Lines	
Ig Name	Average Polyreactivity (Bunker et al 2017)
377A2R	1.269
41C10R	0.824
41D3	1.015
43G10R	1.080

Table 3. Ig knock-in lines used to study IgA$^+$ Plasma Cell Ontogeny. Average polyreactivity values of each chain against seven model antigens used in *Bunker et al 2017.*

somatic hypermutation. All Ig pairs were taken from B cells/PCs found in wild type and otherwise unmanipulated C57BL/6J mice.[57] I chose to make four lines for each subset. Using my validated knock-in approach, I sought to compare the ontogeny of IgA^+ PCs with control follicular B cells. The earliest stages of B cell development take place in the bone marrow, involving the rearrangement of Ig gene segments and eventual production of an intact Ig pair. Owing to the pre-rearranged status of our knocked-in Igs, I focused on the critical transition at which nascent B cells begin expressing surface IgM. All knock-in lines analyzed had an elevated frequency of IgM^+ immature B cells over non-transgenic animals (Fig.15A). Otherwise, there appeared to be no block in bone marrow development of control B-2 or polyreactive IgA^+ PC knock-in lines, suggesting that IgA^+ PC precursors are not subjected to clonal deletion at a group-level (Fig.15A). In line with proper B cell development, all Ig knock-in lines had similar numbers of FO B cells and MZ B cells in the spleen (Fig.15B). An alternative outcome to clonal deletion is receptor editing in which self-reactive immature B cells, upon suprathreshold BCR signaling, undergo further rearrangements of κ and λ light chain genes. In some cases, this can reduce self-reactivity to a tolerable level, allowing the previously self-reactive clone to proceed towards further maturation. I did not observe a significant increase in Ig lambda usage in any line, providing evidence that IgA^+ PC precursors do not exhibit high enough self reactivity to induce receptor editing (Fig.15C). Taken together, these data demonstrate that polyreactive IgA^+ PC precursors develop similarly to normal B cells.

Two observations were made that, at the time, I considered to be some evidence of unusual IgA^+ PC ontogeny. The first came with analysis of a polyreactive IgA mouse line, 377A2R. When stained for lambda chain, 377A2R Ig knock-in cells were largely positive, while at the same time

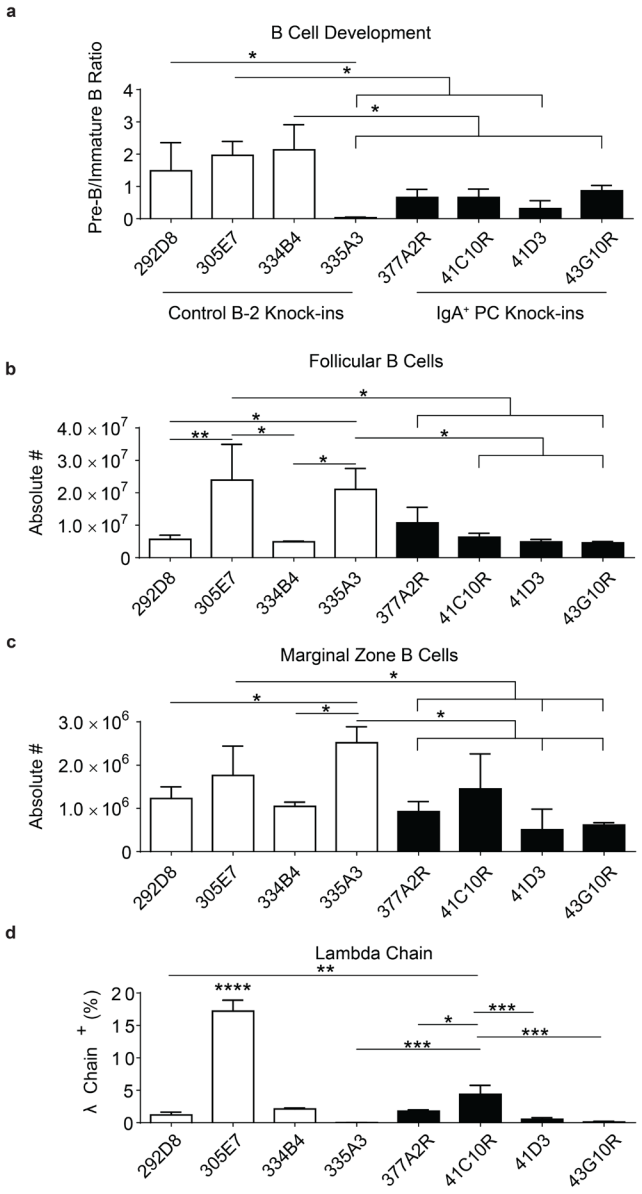

Figure 15. IgA$^+$ PC Ontogeny. B cells from control B-2 and polyreactive IgA+ PC Ig knock-in lines were analyzed for developmental and maturation phenotypes. A) Potential developmental blockade assessed by taking the ratio of Pre-B to immature B cells in the bone marrow. B) Follicular B-2 cell counts in Ig knock-in lines. C) Marginal Zone B cell counts in Ig knock-in lines. D) Receptor editing in Ig knock-in lines as measured by percent of splenic B-2 cells using a lambda light chain. Significant differences determined by one-way ANOVA with post-hoc Tukey test. n≥3 for each line analyzed.

having near-normal levels of surface kappa expression (Fig.16A). As no other line displayed this behavior, I further pursued the finding. 377A2R cells became “lambda positive” at the expected immature B cell stage in the bone marrow. Only cells bearing the full Ig pair drove the phenotype, as H or κ knock-ins in isolation did not produce the result. However, the cells were also staining for kappa expression, indicating that the original BCR was still expressed to some extent on the cell surface. The conclusive evidence of a staining artifact came from 377A2R Ig knock-in mice backcrossed to the *Rag1*-deficient background. On the *Rag1*-deficienct background, 377A2R cells still stained positive for lambda expression (Fig.16A). No lambda rearrangement can occur in these settings, so I concluded that the paratope of 377A2R was capable of binding to goat polyclonal antibodies, which was my reagent for staining the lambda chain.

A second Ig knock-in line bore a similar, yet distinct result worth mentioning. The mouse line 41C10R, harboring a highly polyreactive, highly bacteria-reactive Ig pair, displayed unusual staining patterns (Fig.16B). 41C10R seems to specifically bind to PE-Cy7. This was demonstrated by staining 41C10R cells with a variety of monoclonal antibodies conjugated to different fluorophores (Fig.16B). To my confusion, a variant line of 41C10R, 41C10RY37A-R112A, which has two alanine substitutions in the heavy chain CDRs meant to ablate polyreactivity, was unable to bind to PE-Cy7 (Fig.16B). While at first I associated the staining patterns with the presence or absence of polyreactivity, it became clear that the Ig pair was capable of binding to flow cytometry reagents. This is unlikely to be due to polyreactivity, as the binding occurred in the presence of blocking serum and with low reagent concentrations.

The line 377A2R was the first IgA^+ PC Ig knock-in line I had available for analysis, and the line I focused on for detecting terminal differentiation of precursor cells to the PC fate. Both *Rag1*-

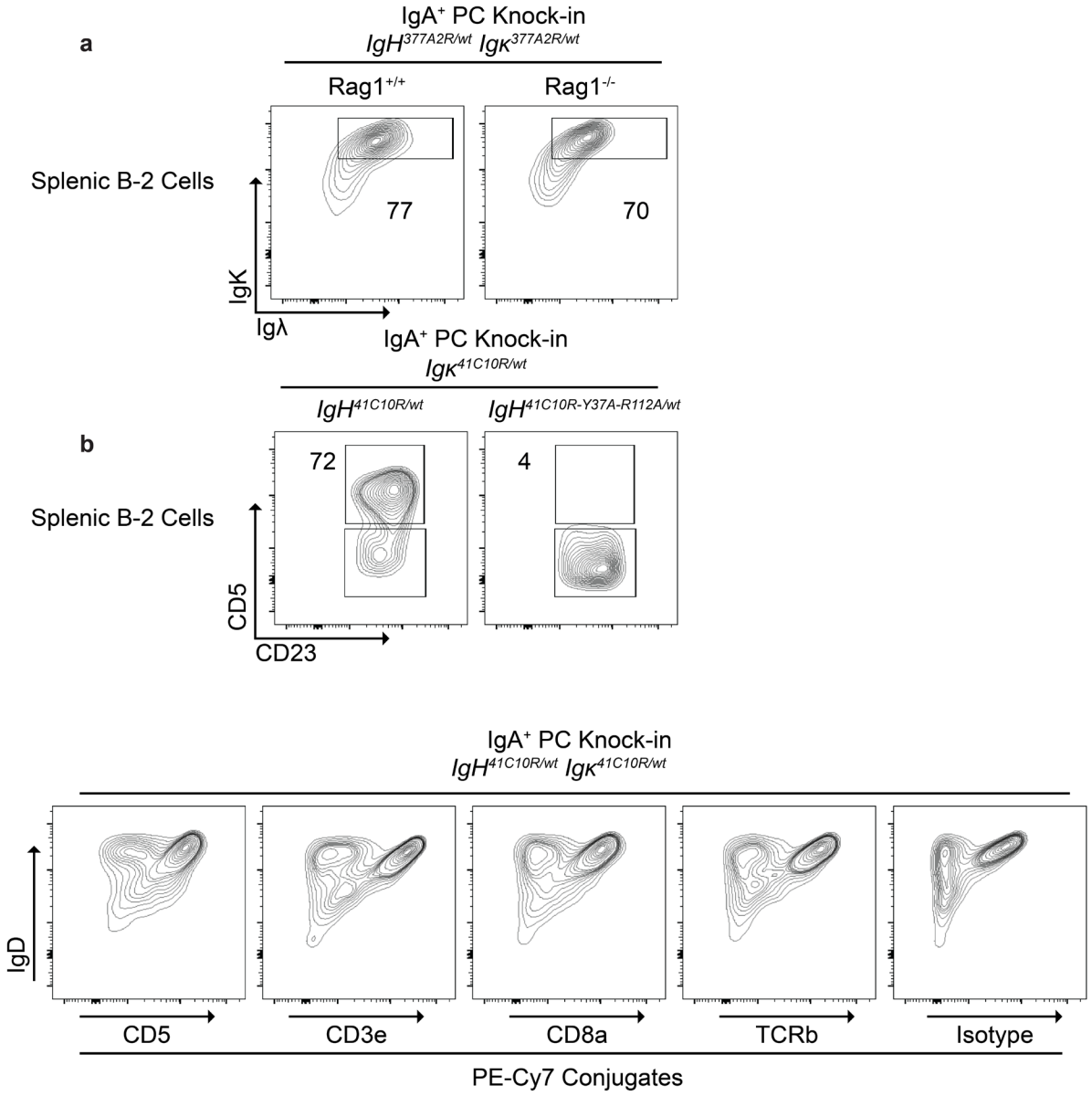

Figure 16. Ig knock-in reactivities to flow cytometry reagents. A) Splenic B-2 cells from the Ig knock-in line 377A2R on *Rag1* sufficient and deficient backgrounds. Ig knock-in B cell still stain positive for lambda chain expression in the absence of Rag1. B) [Top] Apparent CD5 positivity among splenic B-2 cells from the Ig knock-in line 41C10R. [Bottom] staining of splenic B-2 cells from 41C10R with a variety of PE-Cy7 conjugates. 41C10R cells stain positively with any PE-Cy7 conjugate.

sufficient and -deficient 377A2R mice had appreciable B cells in the periphery, albeit at reduced levels compared to nontransgenic animals (Fig.17A). Even with reduced peripheral B cell levels, I detected normal frequencies of SILP IgA$^+$ PCs 377A2R on a *Rag1*-sufficient background (Fig.17B). However, when I analyzed *Rag1*-deficient 377A2R knock-in mice, SILP IgA$^+$ PCs were largely absent (Fig.17B). This surprising outcome could be due to artifacts of the Ig knock-in approach, the complex phenotype of the *Rag1*-deficient background, or other more biologically meaningful reasons.

3.4 B-1 cell lineage relationships in the peritoneal cavity

B-1 ontogeny was the second major application I intended for my Ig knock-in system. I sought to understand the ontogeny of the less well-studied innate-like B cell populations: non-canonical B-1a and B-1b cells. To do so, I created mouse lines with Ig pairs from randomly selected B-1b clones or non-expanded B-1a clones (Table 4)[57]. Additionally, I created a canonical B-1a V_H11-$V_\kappa9$ Ig line "321C6" to serve as a control for BCR-driven cell fating[128,136]. Both canonical and non-canonical B-1a Ig knock-in mice harbored populations of B cells strongly biased towards the B-1a fate (Fig.18A-B). B-1b Ig knock-in mice, on the other hand, gave rise to both B-1 and B-2 cell subsets in the peritoneal cavity, albeit with a reduction in B-1a (Fig.18A-B). The same result was observed in B-2 Ig knock-in lines, such that B-1b and B-2 Ig knock-in lines were phenotypically indistinguishable. Given the possibility that some endogenous early-life B-1a precursors escaped allelic exclusion, I bred one B-1a line, "416C1, and B-1b line, "301G2", to *Rag1*-deficient backgrounds. In this setting, virtually all peritoneal B cells in 416C1/*Rag1*$^{-/-}$ mice were of the B-1a phenotype as expected (Fig.18C). Conversely, 301G2/*Rag1*$^{-/-}$ mice had minimal B-1a cells, confirming that the knocked-in Ig pair was incapable of giving rise to the B-1a subset (Fig.18C). However, there was no loss of peritoneal cavity B-2 cells, suggesting that some Ig pairs

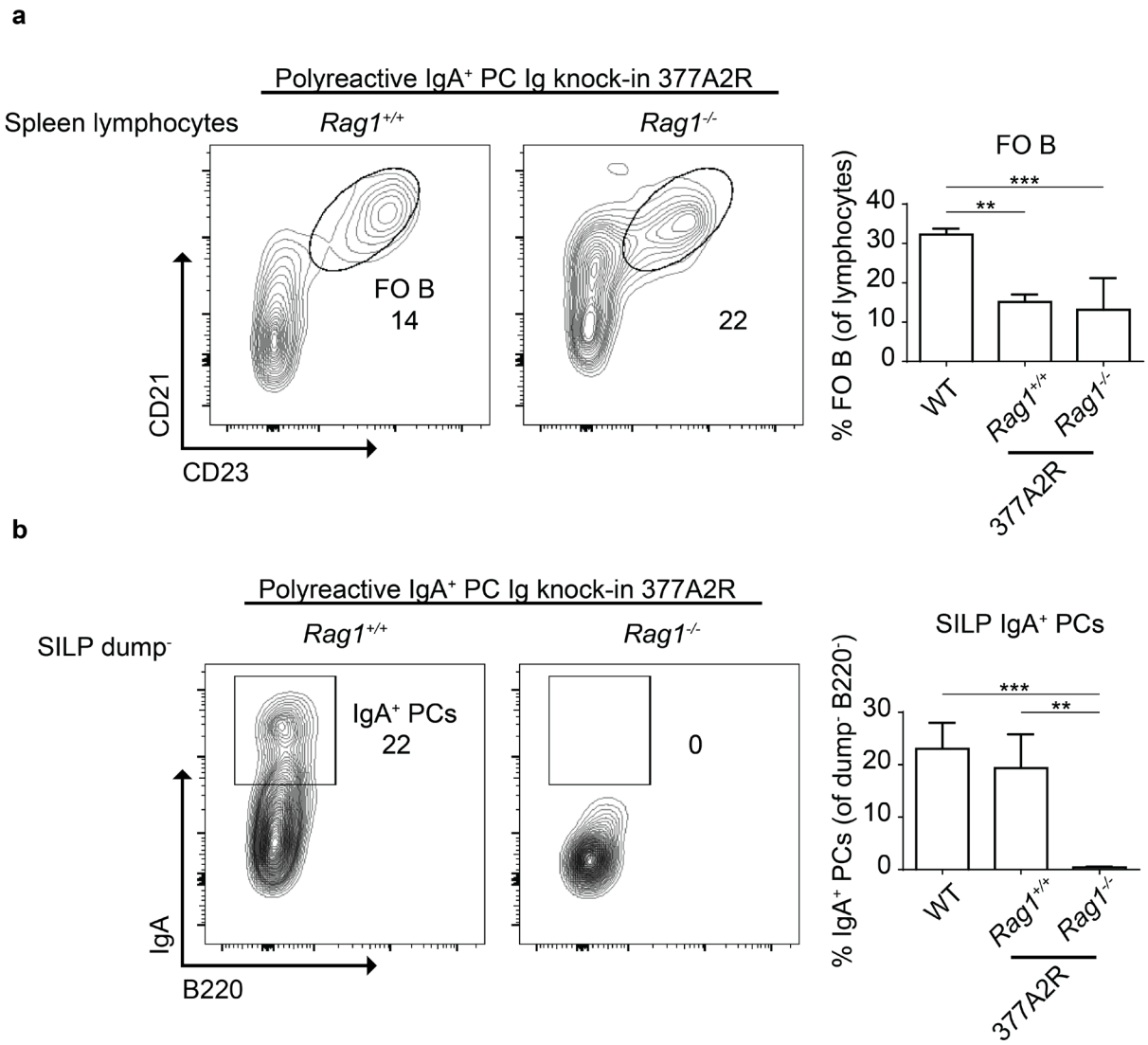

Figure 17. IgA$^+$ plasma cells in the Ig knock-in line 377A2R. A) Splenic FO B cells in 377A2R on *Rag1*-sufficient and -deficient backgrounds. [Left] Representative flow cytometry plots of splenic lymphocytes. [Right] Quantification. **B)** 377A2R *Rag1*$^{-/-}$ mice do not have IgA$^+$ plasma cells. [Left] Representative flow cytometry plots of small intestinal lamina propria cells in *Rag1*-sufficient or -deficient 377A2R knock-in mice. [Right] Quantification of the frequency of IgA$^+$ plasma cells in wild type, *Rag1*-sufficient, and *Rag1*-deficient 377A2R mouse lines. Significance determined by one-way ANOVA with post-hoc Tukey test. n≥3 mice per genotype.

B-1 Ig Knock-in Lines	
Ig Name	Subset Source
321C6	B-1a (canonical)
320F7	B-1a (non-canonical)
416C1	B-1a (non-canonical)
301G2	B-1b
319F1	B-1b

Table 4. Ig knock-in lines used to study B-1 ontogeny. Ig pair name and subset source. each chain against seven model antigens used in *Bunker et al 2017.*

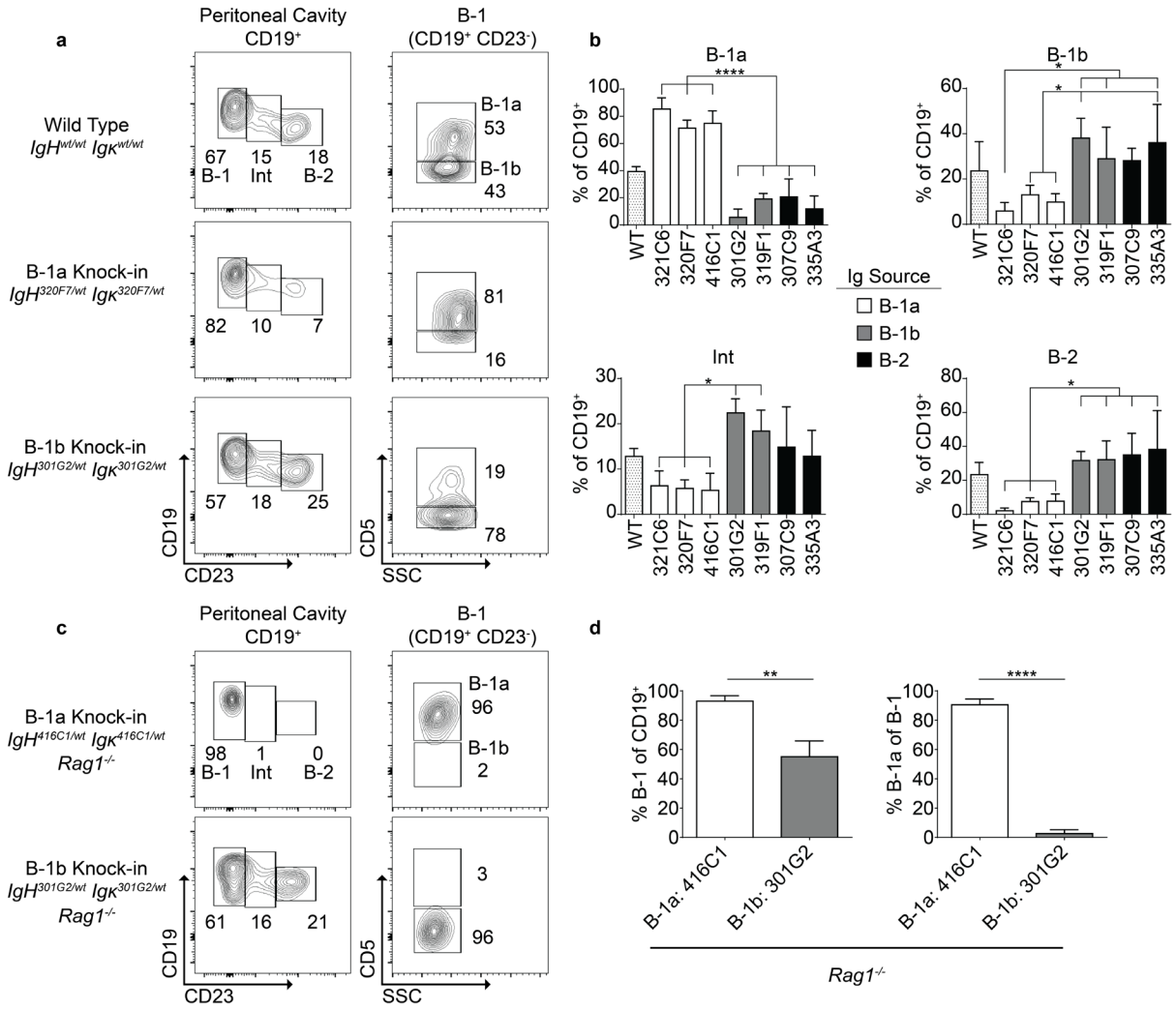

Figure 18. B-1b and B-2 Ig knock-ins display unpredicted phenotypic flexibility. A) [Left] Representative plots of peritoneal B cells in wild type, non-canonical B-1a, and B-1b Ig knock-in mice. [Right] Frequencies of B-1 cells of all peritoneal B cells in Ig knock-in lines. Significance determined by one-way ANOVA with post-hoc Tukey test. **B)** [Left] Breakdown of B-1a and B-1b cells present in the B-1 gate of representative Ig knock-in lines as in A. [Right] Frequencies of B-1a and B-1b cells in all Ig knock-in lines. Significance determined by one-way ANOVA with post-hoc Tukey test. **C)** Comparison of a non-canonical B-1a line and a B-1b line on Rag1-defecient backgrounds. **D)** frequency of B-1 among all B cells and B-1a among B-1 cells in Rag1-deficient Ig knock-in lines. Significance determined by Student's T-test. n≥ 3 biological replicates for all panels.

can seed both B-1b and B-2 subsets. Interestingly, ~15% of the B cells present in B-1b and B-2 Ig knock-in lines did not fully conform to either the B-1 or B-2 lineages, appearing as CD23 "intermediate" (Int or B^{int}) cells. As B^{int} cells persisted in the *Rag1*-deficient 301G2 line, I hypothesized that shared origins between the B-1b and B-2 subsets might exist in wild type animals. However, due to the lack of markers used to identify B-1b cells, it was possible that immature or transitional B cells were present in my samples. To rule out the presence of young $CD23^{variable}$ B cells which might appear in the B^{int} gate, I used the *Rag2-EGFP* reporter line. In these animals, ~80% of splenic transitional stage 1 (T1) and stage 2 (T2) cells still had residual EGFP signal, indicative of recent development (Fig.19A). Splenic FO B cells and MZ B cells were largely $EGFP^-$, in concordance with their temporal separation from lymphopoiesis (Fig.19A). Virtually all cells in the peritoneal cavity were $EGFP^-$, suggesting that the large fraction of poorly defined B^{int} B cells present are not recent bone marrow emigrants (Fig.15A). As another determination of lineage relationships, I pursued a fate-mapping experiment by crossing *CD23-Cre* with *R26R-EYFP* mice. CD23 expression initiates at the T2 stage of development and is ubiquitously expressed by B-2 cells. In the peritoneal cavity, approximately 98% of B-2 phenotype cells were fate-mapped, demonstrating efficient and robust Cre activity driven by the CD23 promoter (Fig.19B). Nearly 90% of B^{int} cells were also $EYFP^+$, in line with the variable but apparent surface CD23 expression. Notably, ~70% of B-1b cells were also fate-mapped, suggesting prominent seeding of the B-1b compartment by cells that had expressed CD23 during a precursor stage (Fig.19B). B-1a cells displayed the lowest fate-mapping by CD23, with approximately 30% $EYFP^+$ (Fig.19B). Taken together, these data suggest that some fraction of each B-1 lineage has origins in mature, $CD23^+$ precursors. Furthermore, the ability of a single Ig

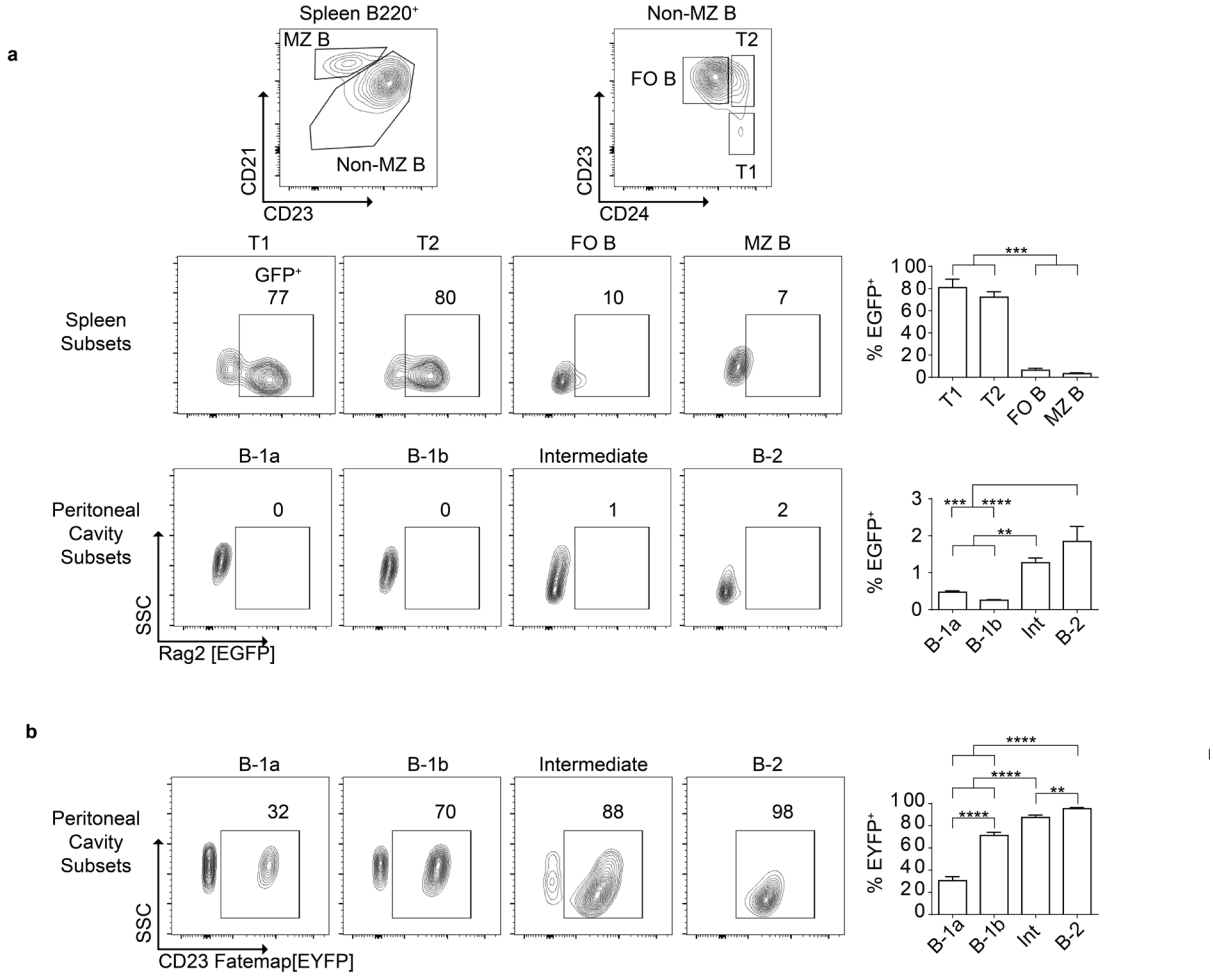

Figure 19. CD23$^+$ precursors contribute to B-1 subsets with minimal contribution from recent bone marrow emigrants. A) [Top panels] gating strategy for splenic T1, T2, FO B and MZ B subsets in *Rag2-EGFP* mice. [Bottom panels] frequency of GFP$^+$ (recent bone marrow emigrants) in splenic and peritoneal B cell subsets. Significance determined by one-way ANOVA with post-hoc Tukey test. **B)** Peritoneal B cells from *CD23-Cre* x *R26R-EYFP* mice. Significance determined by one-way ANOVA with post-hoc Tukey test. n≥ 3 biological replicates for all panels.

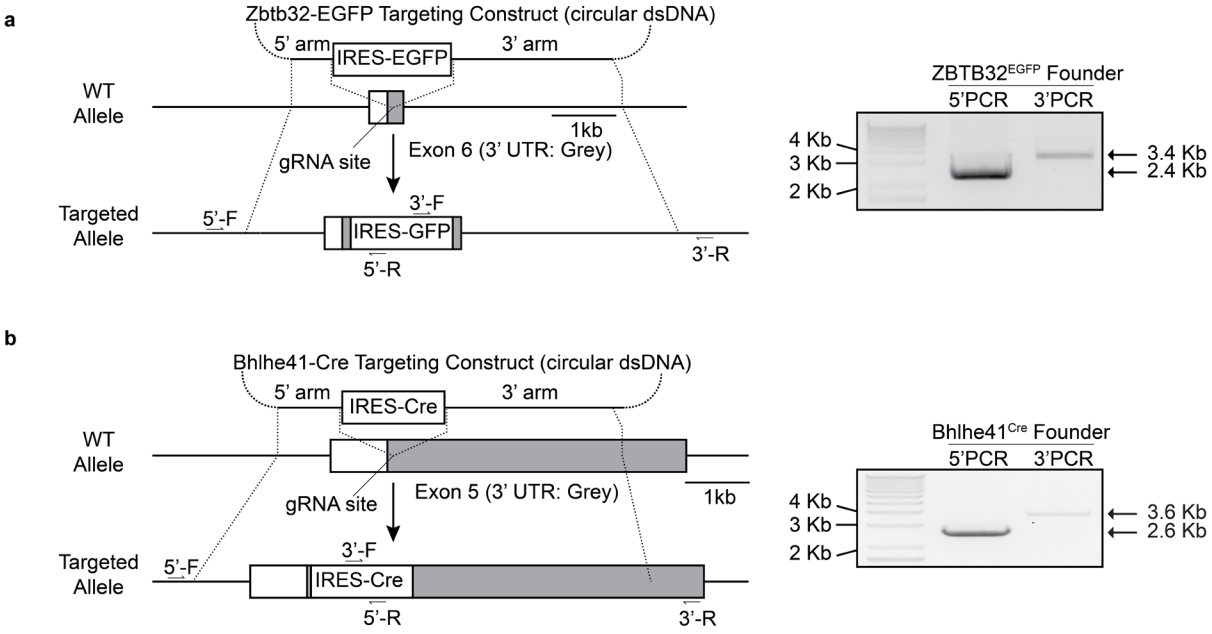

Figure 20. Generation of *Zbtb32*^{EGFP} and *Bhlhe41*^{Cre} lines. A) [Left]Targeting strategy for Cas9-mediated insertion of IRES-led EGFP into the 3' UTR of the *Zbtb32* locus. [Right] Genotyping PCR bands of a founder animal. **B)** [Left] Targeting strategy for Cas9-mediated insertion of IRES-led Cre into the 3' UTR of the *Bhlhe41* locus. [Right] Genotyping PCR amplicons of a founder animal.

pair to drive B-1b, B-2, and intermediate cell phenotypes establishes the possibility of shared B cell lineages in the peritoneal cavity.

To further analyze the ontogeny of B-1 cells, I created a *Zbtb32* transcription factor reporter line (Fig.20A). Zbtb32 is highly upregulated in B-1 cells, but has minimal expression in follicular B cells[90,137]. As expected, virtually all peritoneal B-1 cells were $EGFP^+$ (Fig.21A-B). Interestingly, B^{int} cells were largely positive for EGFP expression and a small fraction of B-2 also had expression (Fig.21A-B). The mean fluorescence intensity of EGFP across the three populations suggests a gradual phenotypic transition from B-2 to B-1 (Fig.21B**,** right panel). I then compared B-2 cells grouped by the presence or absence of EGFP expression. Across a variety of markers and cell size and granularity, $EGFP^+$ B-2 cells were skewed toward a B-1 phenotype compared to $EGFP^-$ B-2 cells (Fig.21C). Zbtb32 expression therefore directly correlates with B-1 phenotype polarization, and putative B-1 precursors present within the B-2 subset can be identified by Zbtb32 expression. I further probed peritoneal B cell lineage relationships by generating a *Bhlhe41*^{Cre} line (Fig.20B). *Bhlhe41* is a master factor in B-1 differentiation and like *Zbtb32* is highly expressed in B-1 cells with negligible expression in other B cell subsets[90,137,138]. Like *CD23*^{Cre}, I crossed the *Bhlhe41*^{Cre} line to *R26R-EYFP* mice to delineate the ontogeny of B-1 and B^{int} cells. I observed that all B-1 cells were fate-mapped by *Bhlhe41*^{Cre}, as were ~90% of B^{int} cells (Fig.21D-E) Consistent with the Zbtb32 reporter data, a fraction of peritoneal B-2 cells were fate-mapped by Bhlhe41Cre, providing a second line of evidence for transcriptional heterogeneity of the peritoneal B-2 compartment (Fig.21D-E). Gating fate-mapped peritoneal B-2 cells from $EYFP^-$ B-2 cells confirmed that fate-mapped B-2 appear more B-1-like across a variety of markers in addition to cell size and granularity (Fig.21F). These data were consistent with observations in the *Zbtb32*

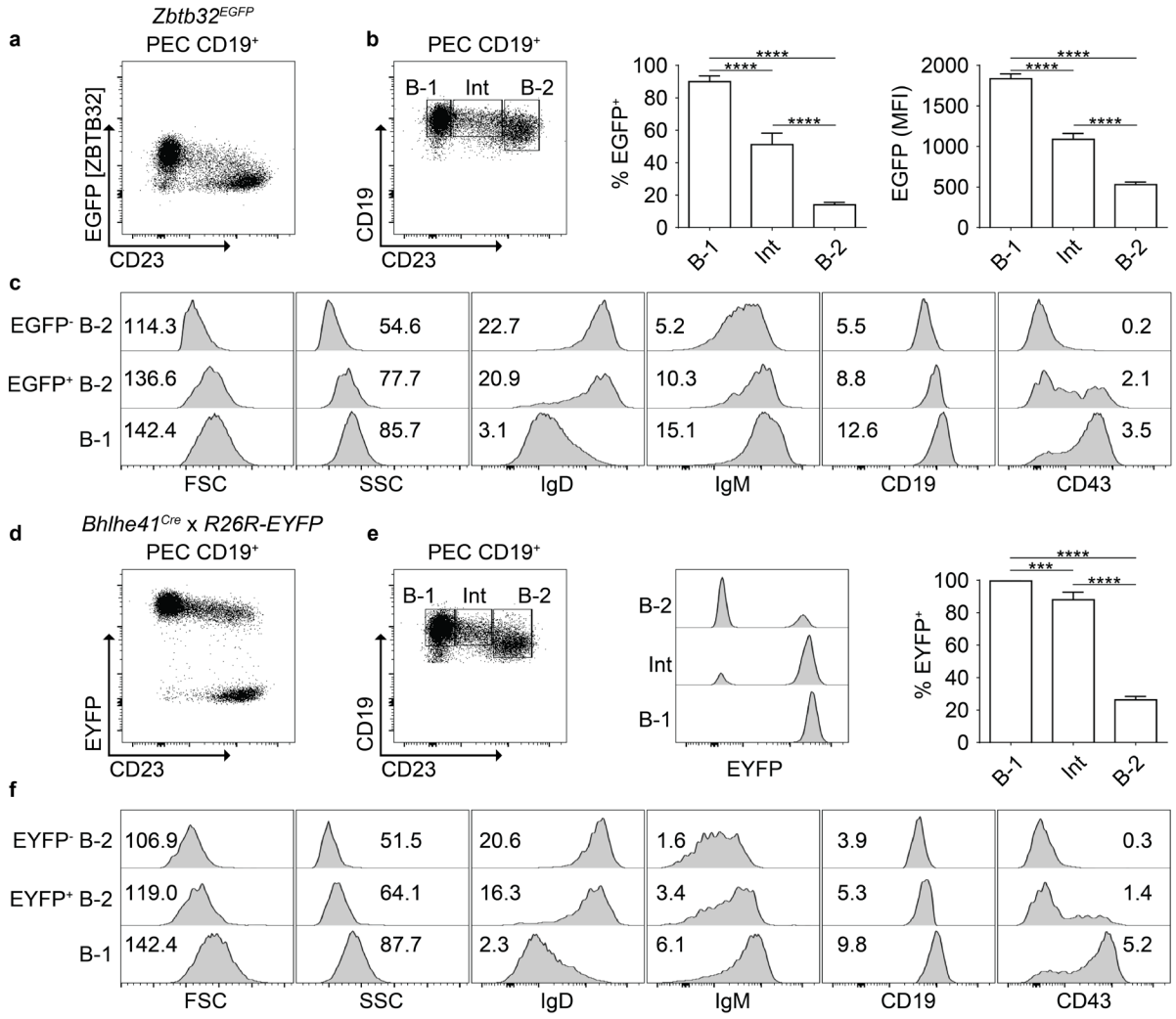

Figure 21. A *Zbtb32* reporter and *Bhlhe41* Cre-driver reveal B-1-like phenotypic changes in peritoneal B cells. A) Zbtb32 expression reported by EGFP in peritoneal B cells. **B)** EGFP$^+$ frequency and mean fluorescence intensity in peritoneal B cell subsets. Significance determined by one-way ANOVA with post-hoc Tukey test. **C)** Histograms of scatter values and fluorescence intensities for indicated cell subsets. Mean fluorescence intensities given as 1x10^3. **D)** Fate-mapping of peritoneal B cells in *Bhlhe41^{Cre}* x *R26R-EYFP* mice. **E)** EYFP$^+$ frequency in peritoneal B cell subsets. Significance determined by one-way ANOVA with post-hoc Tukey test. **F)** Histograms of scatter values and fluorescence intensities for indicated cell subsets. Mean fluorescence intensities given as 1x10^3. n≥ 4 biological replicates for all panels

reporter line. Taken together with results from Speed-Ig lines, I hypothesized that some peritoneal B-2 cells were triggered to differentiate to a B-1 phenotype, and that B^{int} cells represent ex-B-2 cells en route to the B-1 cell fate.

To test the ability of peritoneal B-2 and B^{int} cells to seed the B-1 compartment, I performed an adoptive transfer experiment using congenically marked but otherwise wild type B cells (Fig.22A). Cells were FACS-purified and assessed for purity prior to intraperitoneal injection into C57BL/6J hosts (Fig.22A-B). After one week, I collected cells from recipient animals by peritoneal lavage and stained for B cell makers. Both B-1a and B-1b subsets largely retained their original phenotypes following transfer, consistent with a previous report[139] (Fig.22B-C).Transferred B^{int} cells closely resembled the phenotype of transferred B-1 cells, with most cells now falling into a $CD23^{lo/-}$ gate (Fig.22B-C). A large fraction of transferred B-2 cells also fell into the B-1 gate at a frequency in line with the *Zbtb32*^{EGFP} and *Bhlhe41*^{Cre} results (Fig.22B-C). The presence of host B cells allowed me to directly compare the marker profiles of host and donor cells. Not only had donor B^{int} and B-2 cells now appearing in the B-1 gate lost surface expression of CD23, they had gained a marker profile consistent with the B-1 phenotype (Fig.22D). Regardless of original cell phenotype, the donor cells falling into a B-1 gate were indistinguishable from bona fide host B-1 cells, allowing me to conclude that some B-2 and most B^{int} cells can differentiate to the B-1 fate.

I performed a preliminary experiment to analyze the signal(s) that might be inducing B-2 cells to activate and differentiate to B-1. To do so, I analyzed peritoneal B cells in Ig-stimulated and -unstimulated conditions using antibodies against the phosphorylated forms of several signal transducers (Fig.23). I observed that at baseline, B-1a and B-1b cells had elevated pPLCy2, pErk, and pSTAT3 compared to B-2 cells. B^{int} cells also had elevated pSTAT3 compared to B-2, and a

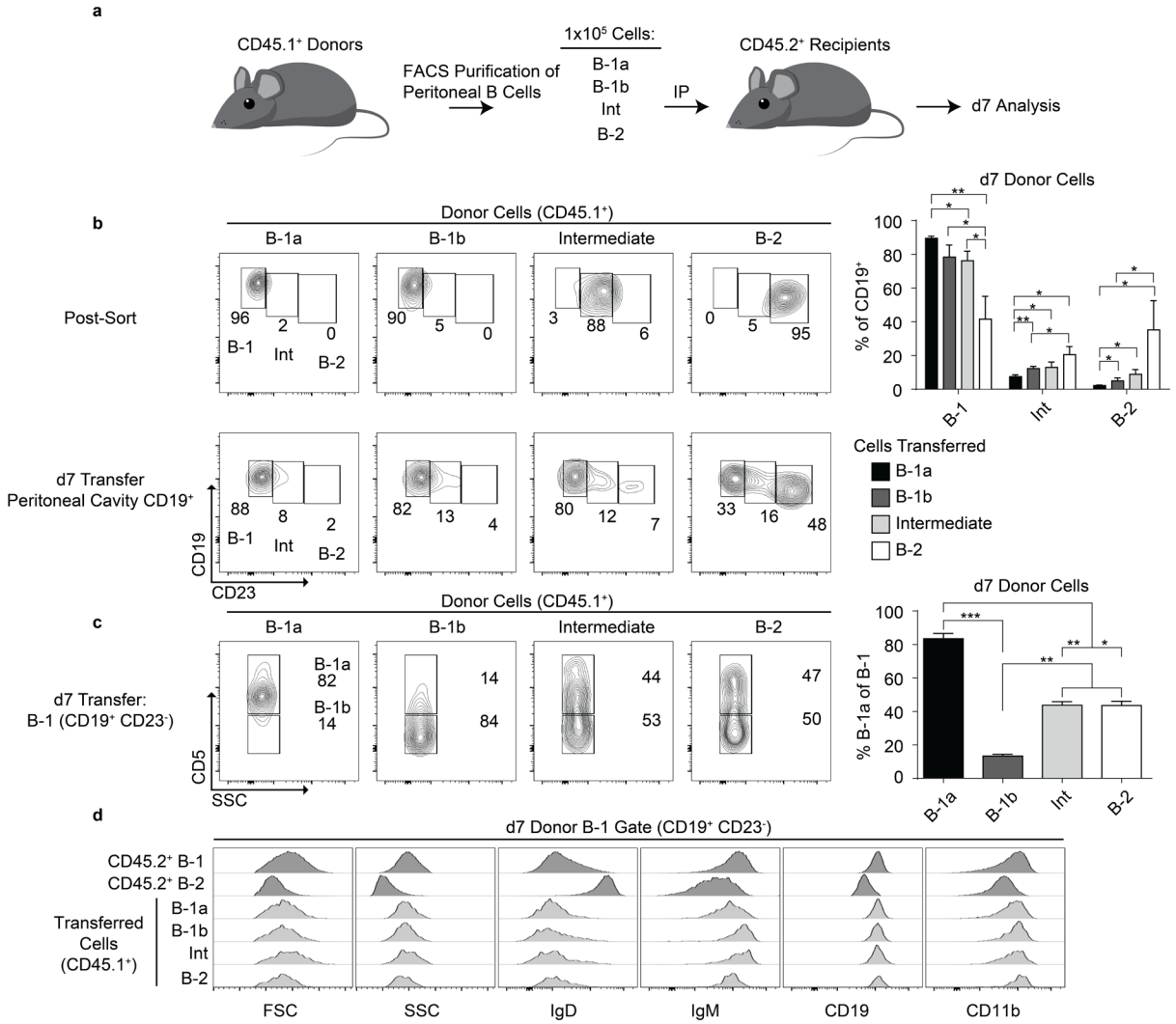

Figure 22. Adoptively transferred peritoneal B-2 and Intermediate cells give rise to B-1 cells. A) adoptive transfer scheme. **B)** Post-sort and d7 analysis of donor cells. Significance determined by Student's T-test. **C)** Breakdown of B-1a and B-1b subsets within the B-1 gate of donor cells. Significance determined by one-way ANOVA with post-hoc Tukey test. **D)** Histograms of scatter and mean fluorescence intensities for donor cells present in the B-1 gate compared to host B-1 and B-2 cells. n≥ 3 biological replicates for all panels.

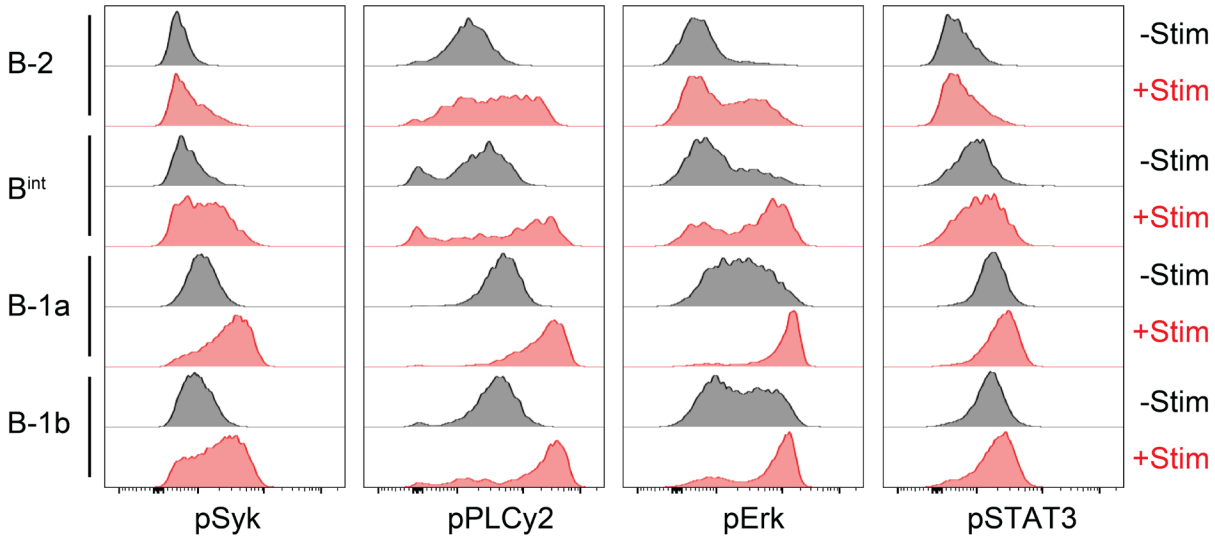

Figure 23. Phosphorylation of signal transducers in peritoneal B cells. B cells from the peritoneal cavity were extracted and stained for surface markers. Cells were then incubated in PBS or PBS + 10ug/ml anti-IgM for five minutes at 37°C. Cells were fixed in 1.6% paraformaldehyde for ten minutes at room temperature before permeabilization in ice-cold methanol. Cells were then stained for the indicated phosphorylated signal transducers. n=1

fraction of B^{int} cells appeared to have elevated pErk. Following stimulation, a fraction of cells in each subset had increased phosphorylation of Syk, PLCy2, and Erk while pSTAT3 levels remained relatively stable.

In summary, the Speed-Ig knock-in lines, transcription factor genetic approaches, and adoptive transfers all suggest an unappreciated B-1 precursor exists within the conventional B-2 population, which may give rise to the majority of B-1b cells and a minority of B-1a cells. Thus, I proposed a model of additional complexity for B-1 ontogeny (Fig.24). Some B-1a cells either arrive in the peritoneal cavity already fully of the B-1a phenotype or as B-2 phenotype cells which rapidly transit the B^{int} stage to a final B-1 phenotype. B cells destined for the B-1b subset enter the peritoneal cavity as B-2 phenotype cells, upregulate B-1 transcription factors, and gradually shed the B-2 phenotype for that of B-1b (Fig.24).

4. DISCUSSION

4.1 IgA Function

Genetic models of IgA deficiency were imprecise prior to this work. I generated two new models of IgA deficiency that have some overlapping and some non-overlapping applications.

The IgA^{BnS} model is a significant improvement over previous genetic approaches to IgA deficiency. My objectives were to remove IgA, avoid compensatory IgM, and have minimal impact on other cell types if possible. As seen from the various readouts, I accomplished these objectives with the IgA^{BnS} line. IgA^{BnS} mice have virtually no intestinal luminal antibodies of any isotype. Bacteria in IgA^{BnS} mice are devoid of antibody coating, as all microbiota-reactive antibody in IgA^{BnS} mice is trapped in the serum. To formally demonstrate this, I used the serum from IgA^{BnS} to stain bacteria and saw that IgA^{BnS} serum was enriched for microbial-reactive

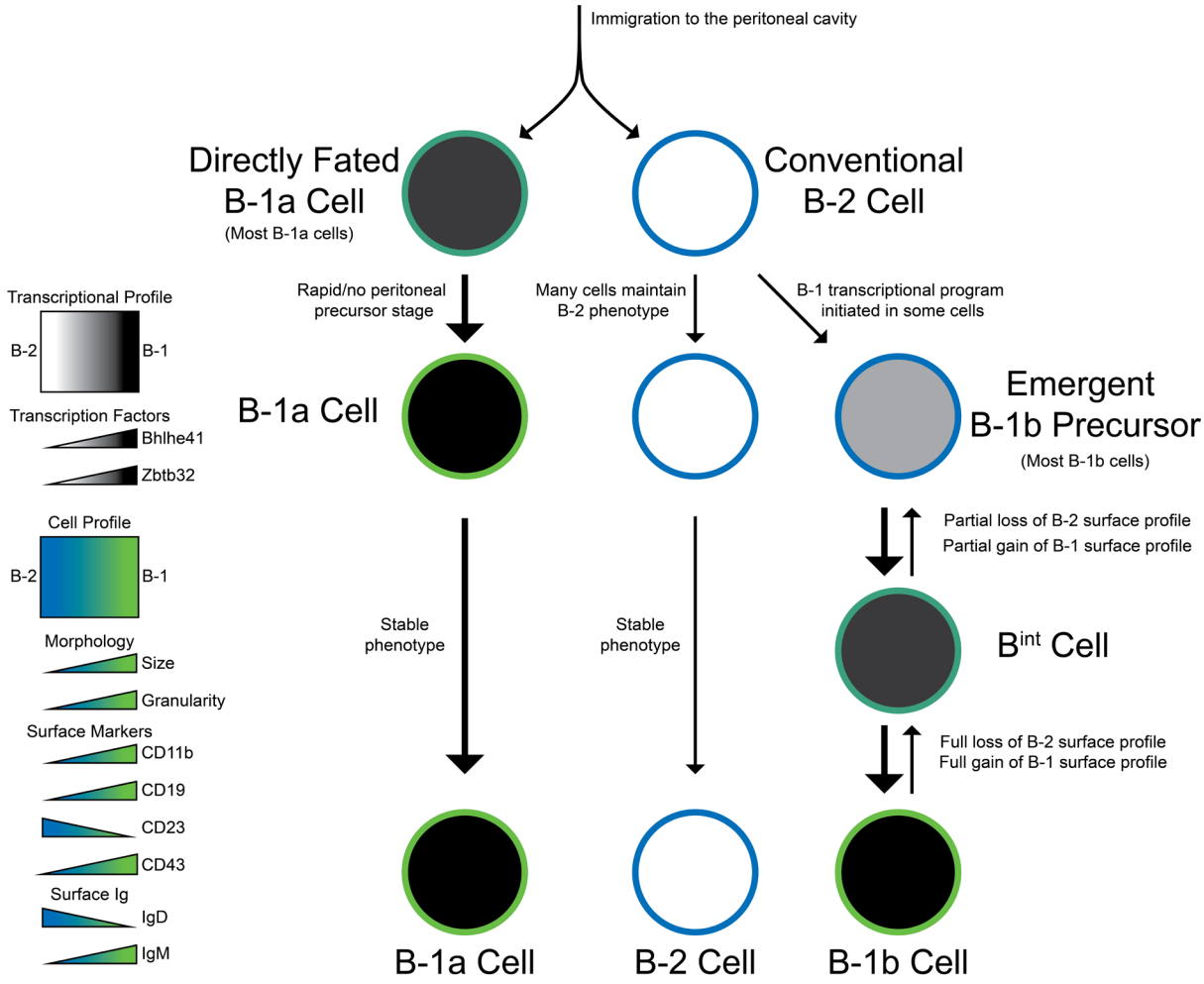

Figure 24. A novel B-1b precursor stage. Peritoneal B cells at steady state display a continuum of surface phenotypes between classically gated B-1 and B-2 cells. B-1b precursor cells initially upregulate B-1 transcription factors. B-1 precursors gradually replace B-2 characteristics with B-1 characteristics. At the B^{int} stage, cells are committed to the B-1 phenotype but still have residual B-2 characteristics. Cells then completely shed B-2 characteristics and display a classic B-1 cellular profile. The majority of B-1a cells arise through differentiative pathways with transient or negligible CD23 expression.

antibody compared to wild type mice. Therefore, antibody specificities destined to become IgA were successfully trapped on the IgG1 isotype, which cannot be deposited in the intestinal lumen. The functional phenotype of mucosal antibody deficiency using the IgA^{BnS} model was minor. No major shifts in the composition of the microbiota were observed between co-housed IgA^{BnS} and littermate animals. It is likely that co-housing mice of different genotypes caused an equilibration of intestinal bacteria between all cage-mates, thereby limiting my detection of a major shift. Future experiments involving isolated mice might clarify compositional phenotypes of the IgA^{BnS} line. The elevated STAT3 signaling seen in IgA^{BnS} mice was a more dramatic phenotype. IgA^{BnS} mice had more $pSTAT3^{+}$ cells than littermate/cage-mate animals, most prominently in the duodenum, Peyer's patches, and ileum. In the ileum, $pSTAT3^{+}$ cells were detected in the epithelial lining of villi and extended into cells residing in the lamina propria. This result was not unlike that of Germain and colleagues, who observed elevated STAT3 signaling in the intestine under a variety of conditions.[140] It is worth noting that group focused on the ileum and might have missed B cell phenotypes in the upper small intestine, where I saw unusual pSTAT3 levels. The cause of STAT3 signaling in IgA^{BnS} is unknown but is limited to a short list of known cytokines. For instance, IL-6, IL-10, and IL-22 are all known to be produced in gut tissue, and all are capable of downstream phosphorylation of STAT3.

One application unique to the IgA^{BnS} model is in studying the true targets of IgA. Because specificities which would normally switch to IgA are stuck on a serum-bound isotype, the serum contains large amounts of these specificities. Because the IgA^{BnS} isotype of IgG1[a] is allotypic to the genetic background the line was created on (IgG1[b]), IgA^{BnS} antibodies can be purified away from host antibodies. A purified pool of IgA^{BnS} antibodies may offer insights into the reactivities of IgA as a whole. For instance, as shown above, IgA^{BnS} antibodies are enhanced for

bacterial binding. Additionally, IgA^{BnS} antibodies reacted with a known dietary antigen. This tool could shed light on the antigenic universe of the intestinal tract through the perspective of the immune system.

Using purified IgA^{BnS} antibodies over purification of endogenous IgA is superior for two reasons. Endogenous IgA must be purified from within the intestinal lumen, so endogenous IgA has likely already encountered (and may still be bound to) target antigens. Furthermore, several important targets may bind to IgA in a non-specific manner. While still important for the overall biological functions of IgA, non-specific IgA binding (e.g. bacterial recognition of the J chain or SC) might confound analysis of Fab-dependent interactions between mucosal antibodies and antigens. For these reasons, the IgA^{BnS} model affords cleaner antibodies on an isotype unlikely to obscure the data.

IgA^{secKO} is likely the best model for in vivo studies of IgA function. I had the same objectives with this line as I did for IgA^{BnS}. I successfully depleted both IgA and IgM antibodies from the intestinal lumen. The nature of the genetic deletion should have no intrinsic effect on other cell types, as no cells other than IgA^{+} PCs (and IgA^{+} memory cells) express IgA. Even in these cell types, the surface-bound IgA BCR is intact, which allows for important survival signaling. The IgA^{secKO} model is superior to IgA^{BnS} for studying in vivo IgA function because IgA^{secKO} mice do not have a surplus of gut antigen-reactive IgG in their sera, which might mask inflammatory or bacterial dissemination phenotypes.

4.2 Cas9-mediated Ig knock-ins

I developed an efficient and robust Cas9-mediated method to generate Ig knock-in mice. My method retains all the biologically useful features of targeted Ig mouse lines while increasing

throughput and reducing generation time. Knocked-in Igs expressed at levels similar to wild-type mice, strongly excluded endogenous rearrangements, and recapitulated physiologically relevant BCR signaling. Using identical promoter regions across Speed-Ig lines provides several advantages over using V region-specific promoters. The promoters themselves are now well validated to provide robust expression. Phenotypic comparisons between Speed-Ig lines can be directly attributed to different V regions, as only these will differ among lines.

My approach complements the elegant method recently reported by Victora and colleagues[114]. Their strategy effectively halves the number of mouse lines required to study any given Ig pair by virtue of integrating both Ig chains into the heavy chain locus. Such mouse lines are a valuable tool to study mature B cell responses to cognate antigens. My method, while still requiring separate integration events at the *IgH* and *Igκ* loci, represents a closer approximation of endogenous Ig expression kinetics and amplitude. Depending on the biological question, each strategy has clear advantages and disadvantages. My heavy chain knock-in approach is similar to that of Batista and colleagues; Lin et al. demonstrated impressive integration efficiencies at the *IgH* locus[113]. The main difference between our approaches is the length of targeting construct homology arms. Increasing the homology arms to lengths commonly used for embryonic stem cell constructs might afford the greatest efficiency. My chief comparative advantage is the ability to genotype via targeting PCR across both homology arms to ensure correct integrations, in addition to my description of *Igκ* knock-ins. Nevertheless, there is clearly a relationship between cargo size and homology arm lengths that affects integration efficiency. The Speed-Ig strategy stands to be improved by further studies into optimal homology arm length, especially for the longer distal arm. Guide site selection was originally conducted by analyzing loci with CHOPCHOP and the Broad Institute's sgRNA Designer[104,105,107]. These algorithms are based off screening results of sgRNA

libraries in cell lines. Later guide site selection was through the IDT design tool for crRNA:tracrRNA bipartite gRNA which may behave differently from sgRNA *in vivo*[110]. While all targeted integrations were achieved regardless of predicted score, my highest efficiencies came from guides with on-target scores above 60 per IDT. However, guide site quality is only one factor in determining knock-in rates, as the length of inserted cargo can also have an effect[141]. My results are informative on the insertion of cargo up to at least two kilobases. This range includes most if not all reporter genes and a variety of genetic tools, including Cre recombinase and luciferases. In conclusion, my method may serve as a platform for universally successful gene editing in the mouse.

4.3 IgA$^+$ plasma cell ontogeny

The original goal of the IgA ontogeny aim was to understand the early development of IgA$^+$ PC precursors. The background data for this project suggested that IgA$^+$ PC precursors would be subjected to negative selective pressure.

I observed that the development of IgA$^+$ PC precursors was similar to control B-2 Ig pairs. There was some variability between lines, but these variabilities were larger within groups than across groups. All lines gave rise to B cells that proceeded through development until reaching a follicular B-2 stage. There was no enrichment of lambda chain usage in IgA+ PC precursors, which suggests limited to no receptor editing. In limited studies, there was no evidence of a large increase or decrease of IgA PCs in these lines. Two exceptional cases of Ig knock-ins binding to flow cytometry staining reagents delayed my overall interpretation of the results. I originally misinterpreted the findings to think that receptor editing was occurring in one line, and a novel B cell phenotype occurring in the other. However, with further experimentation I was able to conclude that these phenotypes were artifacts induced by Ig-binding to flow cytometry reagents.

Having appropriately ruled out these artifacts, the evidence was overwhelming in favor of IgA^+ PC precursors having no observable pre-PC phenotype. Analyzing SILP IgA^+ PCs, I saw that while the IgA^+ PC Ig knock-in line 377A2R had normal frequencies of plasma cells compared to non-transgenic animals, on a $Rag1^{-/-}$ background, 377A2R mice had very few or no plasma cells. This result was difficult to fit with our expectations and with published data regarding IgA^+ PC differentiation in T cell-deficient animals. 377A2R is a polyreactive, microbiota reactive Ig pair, and represents a prototypical IgA^+ PC specificity. The predicted selection mechanism for such specificities was not expected to be dependent on T cells, yet I saw no IgA^+ PC differentiation in $Rag1^{-/-}$ Ig knock-in animals. These data suggest that either the Ig knock-in system is not conducive to normal IgA^+ PC differentiation, or that T cells do have a larger role in IgA^+ PC differentiation than previously expected. My Ig knock-ins are splice-competent with isotypes beyond IgM and IgD, but I cannot definitively state that CSR is unaffected by knock-in transgenesis. The $Rag1^{-/-}$ background is not identical to a pure T cell-deficient background, and other factors may have contributed to my observations. For instance, the absence of polyclonal B cell populations may limit the generation of IgA^+ PC differentiation. The reduction of peripheral B cell populations of Ig knock-in lines may also contribute to the absence of IgA^+ PCs in $Rag1^{-/-}$ 377A2R mice. While a ~two-fold reduction of conventional B cells alone cannot explain my data, as every B cell present in 377A2R $Rag1^{-/-}$ mice is an ideal candidate for IgA^+ PC differentiation, it is possible that altered cell trafficking, follicle localization, or other unknown artifacts contributed to the absence of IgA^+ PCs.

4.4 B-1 cell ontogeny

My novel insights into B-1 ontogeny, specifically the identification of a novel B-1b precursor stage, principally arose from observations in Speed-Ig mice. The ability of a single Ig pair to drive

cells into the B-2 and B-1b subsets, and for conversion of B-2 cells to B-1b, has not been previously reported. Recent evidence for B-1 lineage plasticity *in vivo* using an inducible Ig expression system demonstrated the ability of B-2 cells to acquire a B-1 phenotype[90]. While elegant, this approach was still limited to the biology of canonical B-1a signaling and differentiation. In a related study, BCR signaling blockade prevented B-1a Ig transgenic cells from assuming a full B-1a phenotype[85]. The apparent heterogeneity of peritoneal B cell subsets limits extrapolation of these findings. I expanded on existing data by showing that a monoclonal knocked-in Ig pair can give rise to diverse B cell subsets, and that a phenotypic spectrum is apparent in wild type mice. The polarity of cells toward the B-1 phenotype was directly correlated with the expression of hallmark B-1 transcription factors, regardless of CD23 surface expression. Furthermore, I observed rapid differentiation of peritoneal B-2 and B^{int} cells into B-1 cells following adoptive transfer. Similar results were observed in an adoptive transfer experiment using peritoneal B-2 cells, but not splenic B-2 cells[142]. These data suggest that BCR-independent signaling events occurring in the peritoneum might drive acquisition of the B-1 phenotype in a broad range of B cells. This argument is supported by the fact that peritoneal B-2 cells have no repertoire bias[91]. The continual presence of B^{int} cells in wild type mice opens the possibility that at steady-state, there is perpetual seeding of the B-1 compartment by non-B-1 precursors. Moreover, in combination with data from B-1b and B-2 Ig knock-in mice, there appears to be some factor(s) limiting the size of the B-1 niche. Both BCR-dependent and -independent mechanisms are possible, and further studies are needed to identify the rules governing innate-like B cell fating.

While my work revealed a novel ontogenetic pathway for B-1b cells (and some B-1a), it opened up many questions about how cells are instructed to switch phenotypes *in situ*. While B-1a differentiation is absolutely dependent on BCR signaling, little evidence exists to suggest a similar

dependence for B-1b cells. I observed that both B-1b and B-2 Ig knock-in mouse lines possessed B-1b cells. This can be taken to mean that all non-B-1a BCRs are permissive to B-1b differentiation. If BCR signals are still important for the differentiation of B-1b, then either heightened tonic signaling or a limited antigen pool, present in the peritoneal cavity, would explain the distribution of cells in my Ig knock-in mice.[143,144] The repertoire diversity of B-1b, and the precursor B-2 populations, cast doubt on the possibility of a specialized antigenic trigger in the peritoneal cavity. Analysis of Ig knock-in lines of known specificity (e.g. anti-Ovalbumin Ig knockins), in which the Ig pair is specifically reactive to a foreign antigen, might clarify the nature of B-1b induction. However, it will be difficult to rule out the presence of an alternative antigen in all cases, and foreign antigen-reactive B cells are not guaranteed to possess zero reactivity to other antigens. The finding that peritoneal B-2 cells, but not splenic B-2 cells, could give rise to B-1-like cells following adoptive transfer suggests that local environmental cues are important in the differentiation process.[142] Residing in the peritoneal cavity for any length of time might predispose B-2 cells toward B-1b differentiation, accomplished by alterations in BCR signaling sensitivity, perception of localized cytokine signals, or other mechanisms. To formally test this, an experiment can be envisioned in which splenic B-2 cells are parked in host mice for different lengths of time, such that adequate conditioning in the peritoneal cavity is allowed. If splenic B-2 cells still prove incapable of differentiating to B-1b cells, it would suggest the normal peritoneal cavity B-2 population is already enriched for B-1b precursors. Another approach would be to use the reporter and Cre recombinase lines I generated to transfer specific populations of B-2 cells, in order to observe if different fractions of B-2 cells have nonuniform differentiative capabilities.

At least one BCR-independent signaling mechanism is known to be present in peritoneal B-1 cells. All B-1 cells have constitutive STAT3 phosphorylation, which would suggest ongoing cytokine

signaling.[145] B-1 cells are known to express the majority of B cell-derived IL-10, one of many cytokines that acts through the STAT3 signal transduction pathway.[146] Investigations of the cytokine(s) responsible for B-1 STAT3 phosphorylation, particular in precursor stages such as B^{int} or peritoneal B-2, might reveal triggering events important for lineage conversion. My preliminary experiment did not decisively rule out any signaling pathways, and BCR-dependent and -independent signals may alone or in combination induce B-1 differentiation.

The observation of sizable B-1 precursor cell populations in wild type mice opens another set of questions about B cell population dynamics in the peritoneal cavity. All wild type mice examined had B^{int} cells, and *Bhlhe41*^{Cre} fate-mapping experiments suggested that up to a third of peritoneal B-2 cells had expressed that B-1 master transcription factor. These data suggest that at steady-state, there is continual influx of cells to the B-1 compartment. However, the B-1 compartment is relatively stable in number, and some B-1 constituents are able to undergo homeostatic proliferation.[147] Therefore, two possibilities exist to explain these otherwise opposing observations. It is possible that significant efflux from the B-1 compartment occurs during homeostasis, with cells either losing the B-1 phenotype locally or emigrating to other tissues. B-1 cells are known to emigrate through thoracic duct lymph nodes.[148] Perhaps, if B-1 cells leave and take up residence in new tissue sites, the B-1 phenotype can be shed, leading to negative identification. Using the Bhlhe41Cre, or another B-1-specific Cre, B cells residing in other tissues may be fate-mapped back to the B-1 subset. B-1 cells are already known to give rise to IgA^{+} PCs, but the relative contribution of B-1 versus B-2 is unknown.[72,72,149] It is also possible that the B^{int} cells I detected are not rapidly differentiating to B-1. Given the stable B-1 cell numbers, B^{int} cells might be arrested at the intermediate phenotype, and only upon openings in the B-1 niche would B^{int} cells proceed to terminal differentiation. An inducible fate-mapping

experiment could likely address this possibility. For example, by pulsing *CD23*$^{Cre\text{-}ER}$ fate-mapper mice with tamoxifen, waves of developing and undifferentiated B cells might be separable from pre-existing cells. The rate at which pulse-labeled B cells differentiate from B-2 to B-1 in the peritoneal cavity might then be determined.

I did not address a considerable portion of B-1 ontogeny in my studies, which is the difference between neonatal and adult lymphopoiesis and cell fating. I had no knowledge of when B cells bearing the Ig pairs I used for my knock-in studies had first developed in the original animal. This would most affect my conclusions about B-1a Ig pairs, coming from a source population known to derive primarily from neonatal HSCs. It is possible that my observations of B-1a ontogeny. Most of the cells I observed in these mice could have been generated during early life, after all B^{int} or B-2 phenotype cells had fully differentiated. Future experiments should include analysis of B-1a Ig pairs at different developmental timepoints to determine if this variable affects my observations. I have reason to conclude that my observation of a B-1b precursor, and more specifically the B^{int} population in wild type mice, suggests I uncovered a real biological phenomenon. However, I did not carefully analyze the B^{int} population in very young or very old mice. Under the right conditions, the very first wave of B^{int} cells might be observed. Independent of that, B^{int} cells may deplete as the mouse ages, which would have important implications for B-1 function over time. This is an interesting set of experiments that will better define the nature of B^{int} cells and B-1 cell ontogeny.

5. REFERENCES

1. Sarma, J. V. & Ward, P. A. The complement system. *Cell Tissue Res.* **343**, 227–235 (2011).

2. Holmskov, U., Thiel, S. & Jensenius, J. C. Collectins and Ficolins: Humoral Lectins of the Innate Immune Defense. *Annu. Rev. Immunol.* **21**, 547–578 (2003).

3. Bottazzi, B., Doni, A., Garlanda, C. & Mantovani, A. An Integrated View of Humoral Innate Immunity: Pentraxins as a Paradigm. *Annu. Rev. Immunol.* **28**, 157–183 (2010).

4. Tonegawa, S. Somatic generation of antibody diversity. *Nature* **302**, 575–581 (1983).

5. Hozumi, N. & Tonegawa, S. Evidence for somatic rearrangement of immunoglobulin genes coding for variable and constant regions. *Proc. Natl. Acad. Sci. U. S. A.* **73**, 3628–3632 (1976).

6. van Bebring, E. The mechanism of immunity in animals to diphtheria and tetanus. 3.

7. Avery, O. T. THE DISTRIBUTION OF THE IMMUNE BODIES OCCURRING IN ANTIPNEUMOCOCCUS SERUM. *J. Exp. Med.* **21**, 133–145 (1915).

8. Tiselius, A. Electrophoresis of serum globulin. *Biochem. J.* **31**, 1464–1477 (1937).

9. Tiselius, A. & Kabat, E. A. AN ELECTROPHORETIC STUDY OF IMMUNE SERA AND PURIFIED ANTIBODY PREPARATIONS. *J. Exp. Med.* **69**, 119–131 (1939).

10. Mackay, F., Schneider, P., Rennert, P. & Browning, J. BAFF and APRIL: A Tutorial on B Cell Survival. *Annu. Rev. Immunol.* **21**, 231–264 (2003).

11. Merrell, K. T. *et al.* Identification of Anergic B Cells within a Wild-Type Repertoire. *Immunity* **25**, 953–962 (2006).

12. Oliver, P. M., Vass, T., Kappler, J. & Marrack, P. Loss of the proapoptotic protein, Bim, breaks B cell anergy. *J. Exp. Med.* **203**, 731–741 (2006).

13. Yarkoni, Y., Getahun, A. & Cambier, J. C. Molecular underpinning of B-cell anergy: BCR signaling in anergic B cells. *Immunol. Rev.* **237**, 249–263 (2010).

14. Cambier, J. C., Gauld, S. B., Merrell, K. T. & Vilen, B. J. B-cell anergy: from transgenic models to naturally occurring anergic B cells? *Nat. Rev. Immunol.* **7**, 633–643 (2007).

15. Victora, G. D. & Nussenzweig, M. C. Germinal Centers. *Annu. Rev. Immunol.* **30**, 429–457 (2012).

16. Victora, G. D. *et al.* Germinal Center Dynamics Revealed by Multiphoton Microscopy with a Photoactivatable Fluorescent Reporter. *Cell* **143**, 592–605 (2010).

17. Gitlin, A. D. *et al.* Independent Roles of Switching and Hypermutation in the Development and Persistence of B Lymphocyte Memory. *Immunity* **44**, 769–781 (2016).

18. Stavnezer, J., Guikema, J. E. J. & Schrader, C. E. Mechanism and Regulation of Class Switch Recombination. *Annu. Rev. Immunol.* **26**, 261–292 (2008).

19. Honjo, T., Kinoshita, K. & Muramatsu, M. Molecular mechanism of class switch recombination: linkage with somatic hypermutation. *Annu. Rev. Immunol.* **20**, 165–196 (2002).

20. Roco, J. A. *et al.* Class-Switch Recombination Occurs Infrequently in Germinal Centers. *Immunity* **51**, 337-350.e7 (2019).

21. Kunkel, E. J. & Butcher, E. C. Plasma-cell homing. *Nat. Rev. Immunol.* **3**, 822–829 (2003).

22. Craig, S. W. & Cebra, J. J. Peyer's patches: an enriched source of precursors for IgA-producing immunocytes in the rabbit. *J. Exp. Med.* **134**, 188–200 (1971).

23. Chodirker, W. B. & Tomasi, T. B. Gamma-Globulins: Quantitative Relationships in Human Serum and Nonvascular Fluids. *Science* **142**, 1080–1081 (1963).

24. Tomasi, T. B., Tan, E. M., Solomon, A. & Prendergast, R. A. CHARACTERISTICS OF AN IMMUNE SYSTEM COMMON TO CERTAIN EXTERNAL SECRETIONS. *J. Exp. Med.* **121**, 101–124 (1965).

25. Zhang, Y.-A. *et al.* IgT, a primitive immunoglobulin class specialized in mucosal immunity. *Nat. Immunol.* **11**, 827–835 (2010).

26. Mashoof, S. *et al.* Ancient T-independence of mucosal IgX/A: gut microbiota unaffected by larval thymectomy in Xenopus laevis. *Mucosal Immunol.* **6**, 358–368 (2013).

27. Halpern, M. S. & Koshland, M. E. Novel Subunit in Secretory lgA. 3 (1970).

28. Mestecky, J., Zikan, J. & Butler, W. T. Immunoglobulin M and Secretory Immunoglobulin A: Presence of a Common Polypeptide Chain Different from Light Chains. *Science* **171**, 1163–1165 (1971).

29. Brandtzaeg, P. & Prydz, H. Direct evidence for an integrated function of J chain and secretory component in epithelial transport of immunoglobulins. *Nature* **311**, 71–73 (1984).

30. Mostov, K., Su, T. & ter Beest, M. Polarized epithelial membrane traffic: conservation and plasticity. *Nat. Cell Biol.* **5**, 287–293 (2003).

31. Lindh, E. Increased Resistance of Immunoglobulin a Dimers to Proteolytic Degradation after Binding of Secretory Component. *J. Immunol.* **114**, 284–286 (1975).

32. Clamp, J. R. The Relationship Between Secretory Immunoglobulin A and Mucus. *Biochem. Soc. Trans.* **5**, 1579–1581 (1977).

33. Crottet, P. & Corthésy, B. Secretory Component Delays the Conversion of Secretory IgA into Antigen-Binding Competent F(ab′)2: A Possible Implication for Mucosal Defense. *J. Immunol.* **161**, 5445–5453 (1998).

34. Phalipon, A. & Corthésy, B. Novel functions of the polymeric Ig receptor: well beyond transport of immunoglobulins. *Trends Immunol.* **24**, 55–58 (2003).

35. Benveniste, J., Lespinats, G. & Salomon, J.-C. Serum and Secretory IgA in Axenic and Holoxenic Mice. *J. Immunol.* **107**, 1656–1662 (1971).

36. Moreau, M. C., Ducluzeau, R., Guy-Grand, D. & Muller, M. C. Increase in the Population of Duodenal Immunoglobulin A Plasmocytes in Axenic Mice Associated with Different Living or Dead Bacterial Strains of Intestinal Origin. *Infect. Immun.* **21**, 532–539 (1978).

37. Palm, N. W. *et al.* Immunoglobulin A Coating Identifies Colitogenic Bacteria in Inflammatory Bowel Disease. *Cell* **158**, 1000–1010 (2014).

38. Bunker, J. J. *et al.* Innate and Adaptive Humoral Responses Coat Distinct Commensal Bacteria with Immunoglobulin A. *Immunity* **43**, 541–553 (2015).

39. Kau, A. L. *et al.* Functional characterization of IgA-targeted bacterial taxa from undernourished Malawian children that produce diet-dependent enteropathy. *Sci. Transl. Med.* **7**, 276ra24–276ra24 (2015).

40. Coppo, R. *et al.* IgA Antibodies to Dietary Antigens and Lectin-Binding IgA in Sera From Italian, Australian, and Japanese IgA Nephropathy Patients. *Am. J. Kidney Dis.* **17**, 480–487 (1991).

41. Fransen, F. *et al.* BALB/c and C57BL/6 Mice Differ in Polyreactive IgA Abundance, which Impacts the Generation of Antigen-Specific IgA and Microbiota Diversity. *Immunity* **43**, 527–540 (2015).

42. Harris, N. L. *et al.* Mechanisms of Neonatal Mucosal Antibody Protection. *J. Immunol.* **177**, 6256–6262 (2006).

43. Moor, K. *et al.* High-avidity IgA protects the intestine by enchaining growing bacteria. *Nature* **544**, 498–502 (2017).

44. Donaldson, G. P. *et al.* Gut microbiota utilize immunoglobulin A for mucosal colonization. *Science* **360**, 795–800 (2018).

45. Bollinger, R. R. *et al.* Secretory IgA and mucin-mediated biofilm formation by environmental strains of Escherichia coli: role of type 1 pili. *Mol. Immunol.* **43**, 378–387 (2006).

46. Golovkina, T. V. Organogenic Role of B Lymphocytes in Mucosal Immunity. *Science* **286**, 1965–1968 (1999).

47. Harriman, G. R. *et al.* Targeted Deletion of the IgA Constant Region in Mice Leads to IgA Deficiency with Alterations in Expression of Other Ig Isotypes. *J. Immunol.* **162**, 2521–2529 (1999).

48. Mueller, C. & Macpherson, A. J. Layers of mutualism with commensal bacteria protect us from intestinal inflammation. *Gut* **55**, 276–284 (2006).

49. Fagarasan, S. Critical Roles of Activation-Induced Cytidine Deaminase in the Homeostasis of Gut Flora. *Science* **298**, 1424–1427 (2002).

50. Wei, M. *et al.* Mice carrying a knock-in mutation of Aicda resulting in a defect in somatic hypermutation have impaired gut homeostasis and compromised mucosal defense. *Nat. Immunol.* **12**, 264–270 (2011).

51. Johansen, F.-E. *et al.* Absence of Epithelial Immunoglobulin a Transport, with Increased Mucosal Leakiness, in Polymeric Immunoglobulin Receptor/Secretory Component–Deficient Mice. *J. Exp. Med.* **190**, 915–922 (1999).

52. Castro, C. D. & Flajnik, M. F. Putting J Chain Back on the Map: How Might Its Expression Define Plasma Cell Development? *J. Immunol.* **193**, 3248–3255 (2014).

53. Erlandsson, L., Andersson, K., Sigvardsson, M., Lycke, N. & Leanderson, T. Mice with an inactivated joining chain locus have perturbed IgM secretion. *Eur. J. Immunol.* **28**, 2355–2365 (1998).

54. Mattioli, C. A. & Tomasi, T. B. THE LIFE SPAN OF IgA PLASMA CELLS FROM THE MOUSE INTESTINE. *J. Exp. Med.* **138**, 452–460 (1973).

55. Lindner, C. *et al.* Age, microbiota, and T cells shape diverse individual IgA repertoires in the intestine. *J. Exp. Med.* **209**, 365–377 (2012).

56. Lindner, C. *et al.* Diversification of memory B cells drives the continuous adaptation of secretory antibodies to gut microbiota. *Nat. Immunol.* **16**, 880–888 (2015).

57. Bunker, J. J. *et al.* Natural polyreactive IgA antibodies coat the intestinal microbiota. *Science* **358**, eaan6619 (2017).

58. Kim, K. S. *et al.* Dietary antigens limit mucosal immunity by inducing regulatory T cells in the small intestine. *Science* **351**, 858–863 (2016).

59. Mouquet, H. *et al.* Polyreactivity increases the apparent affinity of anti-HIV antibodies by heteroligation. *Nature* **467**, 591–595 (2010).

60. Chen, Z. J. *et al.* Polyreactive antigen-binding B cells are the predominant cell type in the newborn B cell repertoire. *Eur. J. Immunol.* **28**, 989–994 (1998).

61. Gunti, S. & Notkins, A. L. Polyreactive Antibodies: Function and Quantification. *J. Infect. Dis.* **212**, S42–S46 (2015).

62. Zhou, Z.-H. *et al.* The Broad Antibacterial Activity of the Natural Antibody Repertoire Is Due to Polyreactive Antibodies. *Cell Host Microbe* **1**, 51–61 (2007).

63. Baker, N. & Ehrenstein, M. R. Cutting Edge: Selection of B Lymphocyte Subsets Is Regulated by Natural IgM. *J. Immunol.* **169**, 6686–6690 (2002).

64. Ehrenstein, M. R. & Notley, C. A. The importance of natural IgM: scavenger, protector and regulator. *Nat. Rev. Immunol.* **10**, 778–786 (2010).

65. Wardemann, H. *et al.* Predominant Autoantibody Production by Early Human B Cell Precursors. *Science* **301**, 1374–1377 (2003).

66. Vassilev, T. L. & Veleva, K. V. Natural Polyreactive IgA and IgM Autoantibodies in Human Colostrum. *Scand. J. Immunol.* **44**, 535–539 (1996).

67. Mestecky, J. & Russell, M. W. Specific antibody activity, glycan heterogeneity and polyreactivity contribute to the protective activity of S-IgA at mucosal surfaces. *Immunol. Lett.* **124**, 57–62 (2009).

68. Quan, C. P., Berneman, A., Pires, R., Avrameas, S. & Bouvet, J. P. Natural polyreactive secretory immunoglobulin A autoantibodies as a possible barrier to infection in humans. *Infect. Immun.* **65**, 3997–4004 (1997).

69. SHIMODA, M., INOUE, Y., AZUMA, N. & KANNO, C. Natural polyreactive immunoglobulin A antibodies produced in mouse Peyer's patches. *Immunology* **97**, 9–17 (1999).

70. Grootjans, J. *et al.* Epithelial endoplasmic reticulum stress orchestrates a protective IgA response. *Science* **363**, 993–998 (2019).

71. Kroese, F. G. *et al.* Many of the IgA producing plasma cells in murine gut are derived from self-replenishing precursors in the peritoneal cavity. *Int. Immunol.* **1**, 75–84 (1989).

72. Suzuki, K., Maruya, M., Kawamoto, S. & Fagarasan, S. Roles of B-1 and B-2 cells in innate and acquired IgA-mediated immunity. *Immunol. Rev.* **237**, 180–190 (2010).

73. Cinamon, G., Zachariah, M. A., Lam, O. M., Foss, F. W. & Cyster, J. G. Follicular shuttling of marginal zone B cells facilitates antigen transport. *Nat. Immunol.* **9**, 54–62 (2008).

74. Martin, F., Oliver, A. M. & Kearney, J. F. Marginal Zone and B1 B Cells Unite in the Early Response against T-Independent Blood-Borne Particulate Antigens. *Immunity* **14**, 617–629 (2001).

75. Hammad, H. *et al.* Transitional B cells commit to marginal zone B cell fate by Taok3-mediated surface expression of ADAM10. *Nat. Immunol.* **18**, 313–320 (2017).

76. Hardy, R. R., Hayakawa, K., Haaijman, J. & Herzenberg, L. A. B-cell subpopulations identifiable by two-color fluorescence analysis using a dual-laser FACS. *Ann. N. Y. Acad. Sci.* **399**, 112–121 (1982).

77. Lalor, P. A., Stall, A. M., Adams, S. & Herzenberg, L. A. Permanent alteration of the murine Ly-1 B repertoire due to selective depletion of Ly-1 B cells in neonatal animals. *Eur. J. Immunol.* **19**, 501–506 (1989).

78. Lalor, P. A., Herzenberg, L. A., Adams, S. & Stall, A. M. Feedback regulation of murine Ly-1 B cell development. *Eur. J. Immunol.* **19**, 507–513 (1989).

79. Montecino-Rodriguez, E. & Dorshkind, K. B-1 B Cell Development in the Fetus and Adult. *Immunity* **36**, 13–21 (2012).

80. Montecino-Rodriguez, E. & Dorshkind, K. Formation of B-1 B Cells from Neonatal B-1 Transitional Cells Exhibits NF-κB Redundancy. *J. Immunol.* **187**, 5712–5719 (2011).

81. Baumgarth, N. The double life of a B-1 cell: self-reactivity selects for protective effector functions. *Nat. Rev. Immunol.* **11**, 34–46 (2010).

82. Dorshkind, K. & Montecino-Rodriguez, E. Fetal B-cell lymphopoiesis and the emergence of B-1-cell potential. *Nat. Rev. Immunol.* **7**, 213–219 (2007).

83. Zhou, Y. *et al.* Lin28b promotes fetal B lymphopoiesis through the transcription factor Arid3a. *J. Exp. Med.* **212**, 569–580 (2015).

84. Hardy, R. R. B-1 B Cell Development. *J. Immunol.* **177**, 2749–2754 (2006).

85. Arnold, L. W., McCray, S. K., Tatu, C. & Clarke, S. H. Identification of a Precursor to Phosphatidyl Choline-Specific B-1 Cells Suggesting That B-1 Cells Differentiate from Splenic Conventional B Cells In Vivo: Cyclosporin A Blocks Differentiation to B-1. *J. Immunol.* **164**, 2924–2930 (2000).

86. Hardy, R. R. Positive selection of natural autoreactive B cells. *Science* **285**, (1999).

87. Taki, S., Meiering, M. & Rajewsky, K. Targeted insertion of a variable region gene into the immunoglobulin heavy chain locus. *Science* **262**, 1268–1271 (1993).

88. Lam, K.-P. & Rajewsky, K. B cell antigen receptor specificity and surface density together determine B-1 versus B-2 cell development. *J. Exp. Med.* **190**, 471–478 (1999).

89. Casola, S. *et al.* B cell receptor signal strength determines B cell fate. *Nat. Immunol.* **5**, 317–327 (2004).

90. Graf, R. *et al.* BCR-dependent lineage plasticity in mature B cells. *Science* **363**, 748–753 (2019).

91. Yang, Y. *et al.* Distinct mechanisms define murine B cell lineage immunoglobulin heavy chain (IgH) repertoires. *eLife* **4**, (2015).

92. Kantor, A. B., Stall, A. M., Adams, S., Herzenberg, L. A. & Herzenberg, L. A. Differential development of progenitor activity for three B-cell lineages. *Proc. Natl. Acad. Sci.* **89**, 3320–3324 (1992).

93. Li, Y.-S. *et al.* A developmental switch between fetal and adult B lymphopoiesis. *Ann. N. Y. Acad. Sci.* **1362**, 8–15 (2015).

94. Goodnow, C. C. *et al.* Altered immunoglobulin expression and functional silencing of self-reactive B lymphocytes in transgenic mice. *Nature* **334**, 676–682 (1988).

95. Burnett, D. L. *et al.* Germinal center antibody mutation trajectories are determined by rapid self/foreign discrimination. *Science* **360**, 223–226 (2018).

96. Abbott, R. K. *et al.* Precursor Frequency and Affinity Determine B Cell Competitive Fitness in Germinal Centers, Tested with Germline-Targeting HIV Vaccine Immunogens. *Immunity* **48**, 133-146.e6 (2018).

97. Dosenovic, P. *et al.* Anti-HIV-1 B cell responses are dependent on B cell precursor frequency and antigen binding affinity. (2018) doi:10.1101/275438.

98. Verkoczy, L. *et al.* Autoreactivity in an HIV-1 broadly reactive neutralizing antibody variable region heavy chain induces immunologic tolerance. *Proc. Natl. Acad. Sci.* **107**, 181–186 (2010).

99. Zou, Y.-R., Takeda, S. & Rajewsky, K. Gene targeting in the lgx locus: efficient generation of X chain-expressing B cells, independent of gene rearrangements in lgx. 10.

100. Pelanda, R., Schaal, S., Torres, R. M. & Rajewsky, K. A Prematurely Expressed Ig□ Transgene, but Not a V□J□ Gene Segment Targeted into the Ig□ Locus, Can Rescue B Cell Development in □5-Deficient Mice. 11.

101. Thomas, K. R. & Capecchi, M. R. Site-directed mutagenesis by gene targeting in mouse embryo-derived stem cells. *Cell* **51**, 503–512 (1987).

102. Wu, S., Ying, G., Wu, Q. & Capecchi, M. R. A protocol for constructing gene targeting vectors: generating knockout mice for the cadherin family and beyond. *Nat. Protoc.* **3**, 1056–1076 (2008).

103. Yang, H. *et al.* One-Step Generation of Mice Carrying Reporter and Conditional Alleles by CRISPR/Cas-Mediated Genome Engineering. *Cell* **154**, 1370–1379 (2013).

104. Montague, T. G., Cruz, J. M., Gagnon, J. A., Church, G. M. & Valen, E. CHOPCHOP: a CRISPR/Cas9 and TALEN web tool for genome editing. *Nucleic Acids Res.* **42**, W401–W407 (2014).

105. Labun, K., Montague, T. G., Gagnon, J. A., Thyme, S. B. & Valen, E. CHOPCHOP v2: a web tool for the next generation of CRISPR genome engineering. *Nucleic Acids Res.* **44**, W272–W276 (2016).

106. Quadros, R. M. *et al.* Easi-CRISPR: a robust method for one-step generation of mice carrying conditional and insertion alleles using long ssDNA donors and CRISPR ribonucleoproteins. *Genome Biol.* **18**, (2017).

107. Doench, J. G. *et al.* Optimized sgRNA design to maximize activity and minimize off-target effects of CRISPR-Cas9. *Nat. Biotechnol.* **34**, 184–191 (2016).

108. Sanson, K. R. *et al.* Optimized libraries for CRISPR-Cas9 genetic screens with multiple modalities. *Nat. Commun.* **9**, 1–15 (2018).

109. Kim, H. K. *et al.* Deep learning improves prediction of CRISPR–Cpf1 guide RNA activity. *Nat. Biotechnol.* **36**, 239–241 (2018).

110. Aida, T. *et al.* Cloning-free CRISPR/Cas system facilitates functional cassette knock-in in mice. *Genome Biol.* **16**, (2015).

111. Chu, V. T. *et al.* Increasing the efficiency of homology-directed repair for CRISPR-Cas9-induced precise gene editing in mammalian cells. *Nat. Biotechnol.* **33**, 543–548 (2015).

112. Ran, F. A. *et al.* Genome engineering using the CRISPR-Cas9 system. *Nat. Protoc.* **8**, 2281–2308 (2013).

113. Lin, Y. *et al.* One-step CRISPR/Cas9 method for the rapid generation of human antibody heavy chain knock-in mice. *EMBO J.* **37**, e99243 (2018).

114. Jacobsen, J. T. *et al.* One-step generation of monoclonal B cell receptor mice capable of isotype switching and somatic hypermutation. *J. Exp. Med.* **215**, 2686–2695 (2018).

115. Tiller, T., Busse, C. E. & Wardemann, H. Cloning and expression of murine Ig genes from single B cells. *J. Immunol. Methods* **350**, 183–193 (2009).

116. Ho, I. Y. *et al.* Refined protocol for generating monoclonal antibodies from single human and murine B cells. *J. Immunol. Methods* **438**, 67–70 (2016).

117. Rohland, N. & Reich, D. Cost-effective, high-throughput DNA sequencing libraries for multiplexed target capture. *Genome Res.* **22**, 939–946 (2012).

118. DeAngelis, M. M., Wang, D. G. & Hawkins, T. L. Solid-phase reversible immobilization for the isolation of PCR products. *Nucleic Acids Res.* **23**, 4742–4743 (1995).

119. Gibson, D. G. *et al.* Enzymatic assembly of DNA molecules up to several hundred kilobases. *Nat. Methods* **6**, 343–345 (2009).

120. Mao, A.-P., Ishizuka, I. E., Kasal, D. N., Mandal, M. & Bendelac, A. A shared Runx1-bound Zbtb16 enhancer directs innate and innate-like lymphoid lineage development. *Nat. Commun.* **8**, (2017).

121. Hara, S. *et al.* Dietary Antigens Induce Germinal Center Responses in Peyer's Patches and Antigen-Specific IgA Production. *Front. Immunol.* **10**, 2432 (2019).

122. Ehrenstein, M. R., O'Keefe, T. L., Davies, S. L. & Neuberger, M. S. Targeted gene disruption reveals a role for natural secretory IgM in the maturation of the primary immune response. *Proc. Natl. Acad. Sci.* **95**, 10089–10093 (1998).

123. Bruce, S. R., Dingle, R. W. C. & Peterson, M. L. B-cell and plasma-cell splicing differences: A potential role in regulated immunoglobulin RNA processing. *RNA* **9**, 1264–1273 (2003).

124. Seipelt, R. L. & Peterson, M. L. Alternative processing of IgA pre-mRNA responds like IgM to alterations in the efficiency of the competing splice and cleavage-polyadenylation reactions. *Mol. Immunol.* **32**, 277–285 (1995).

125. Pelanda, R. *et al.* Receptor Editing in a Transgenic Mouse Model: Site, Efficiency, and Role in B Cell Tolerance and Antibody Diversification. *Immunity* **7**, 765–775 (1997).

126. Tiegs, S. L., Russell, D. M. & Nemazee, D. Receptor editing in self-reactive bone marrow B cells. *J. Exp. Med.* **177**, 1009–1020 (1993).

127. Chumley, M. J. *et al.* A VH11V 9 B Cell Antigen Receptor Drives Generation of CD5+ B Cells Both In Vivo and In Vitro. *J. Immunol.* **164**, 4586–4593 (2000).

128. Arnold, L. W., Pennell, C. A., McCray, S. K. & Clarke, S. H. Development of B-1 cells: segregation of phosphatidyl choline-specific B cells to the B-1 population occurs after immunoglobulin gene expression. *J. Exp. Med.* **179**, 1585–1595 (1994).

129. Freitag, J. *et al.* Towards the generation of B-cell receptor retrogenic mice. *PloS One* **9**, e109199 (2014).

130. Haber, J. E. Partners and pathways: repairing a double-strand break. *Trends Genet.* **16**, 259–264 (2000).

131. Byrne, S. M., Ortiz, L., Mali, P., Aach, J. & Church, G. M. Multi-kilobase homozygous targeted gene replacement in human induced pluripotent stem cells. *Nucleic Acids Res.* **43**, e21–e21 (2015).

132. Vettermann, C. & Schlissel, M. S. Allelic exclusion of immunoglobulin genes: models and mechanisms. *Immunol. Rev.* **237**, 22–42 (2010).

133. Casellas, R. *et al.* Contribution of receptor editing to the antibody repertoire. *science* **291**, 1541–1544 (2001).

134. Ota, T. *et al.* B Cells from Knock-in Mice Expressing Broadly Neutralizing HIV Antibody b12 Carry an Innocuous B Cell Receptor Responsive to HIV Vaccine Candidates. *J. Immunol.* **191**, 3179–3185 (2013).

135. Rickert, R. C. & Rajewsky, K. Impairment of T-cell-dependent B-cell responses and B-1 cell development in CD19-deficient mice. 4.

136. Kurosaki, T., Shinohara, H. & Baba, Y. B Cell Signaling and Fate Decision. *Annu. Rev. Immunol.* **28**, 21–55 (2010).

137. Mabbott, N. A. & Gray, D. Identification of co-expressed gene signatures in mouse B1, marginal zone and B2 B-cell populations. *Immunology* **141**, 79–95 (2014).

138. Kreslavsky, T. *et al.* Essential role for the transcription factor Bhlhe41 in regulating the development, self-renewal and BCR repertoire of B-1a cells. *Nat. Immunol.* **18**, 442–455 (2017).

139. Haas, K. M., Poe, J. C., Steeber, D. A. & Tedder, T. F. B-1a and B-1b Cells Exhibit Distinct Developmental Requirements and Have Unique Functional Roles in Innate and Adaptive Immunity to S. pneumoniae. *Immunity* **23**, 7–18 (2005).

140. Mao, K. *et al.* Innate and adaptive lymphocytes sequentially shape the gut microbiota and lipid metabolism. *Nature* **554**, 255–259 (2018).

141. Moehle, E. A. *et al.* Targeted gene addition into a specified location in the human genome using designed zinc finger nucleases. *Proc. Natl. Acad. Sci.* **104**, 3055–3060 (2007).

142. Hastings, W. D., Tumang, J. R., Behrens, T. W. & Rothstein, T. L. Peritoneal B-2 cells comprise a distinct B-2 cell population with B-1b-like characteristics. *Eur. J. Immunol.* **36**, 1114–1123 (2006).

143. Monroe, J. G. Ligand-independent tonic signaling in B-cell receptor function. *Curr. Opin. Immunol.* **16**, 288–295 (2004).

144. Stadanlick, J. E. *et al.* Tonic B cell antigen receptor signals supply an NF-κB substrate for prosurvival BLyS signaling. *Nat. Immunol.* **9**, 1379–1387 (2008).

145. Karras, J. G. *et al.* Signal Transducer and Activator of Transcription-3 (STAT3) Is Constitutively Activated in Normal, Self-renewing B-1 Cells but Only Inducibly Expressed in Conventional B Lymphocytes. *J. Exp. Med.* **185**, 1035–1042 (1997).

146. O'garra, A. *et al.* Ly-1 B (B-1) cells are the main source of B cell-derived interleukin 10. *Eur. J. Immunol.* **22**, 711–717 (1992).

147. Moon, B., Takaki, S., Miyake, K. & Takatsu, K. The Role of IL-5 for Mature B-1 Cells in Homeostatic Proliferation, Cell Survival, and Ig Production. *J. Immunol.* **172**, 6020–6029 (2004).

148. Ansel, K. M., Harris, R. B. S. & Cyster, J. G. CXCL13 Is Required for B1 Cell Homing, Natural Antibody Production, and Body Cavity Immunity. *Immunity* **16**, 67–76 (2002).

149. Stoel, M. *et al.* Restricted IgA Repertoire in Both B-1 and B-2 Cell-Derived Gut Plasmablasts. *J. Immunol.* **174**, 1046–1054 (2005).